THE JOURNAL
OF
CHEMICAL PHYSICS

VOLUME 6 FEBRUARY, 1938 NUMBER 2

# The Ultraviolet Absorption of Simple Hydrocarbons

## IV. Unsaturated Cyclic Hydrocarbons in the Schumann Region

EMMA P. CARR AND HILDEGARD STÜCKLEN
*Department of Chemistry, Mount Holyoke College, South Hadley, Massachusetts*

(Received November 6, 1937)

The absorption spectra of cyclohexene, cyclopentene, 1–3 cyclohexadiene and benzene have been examined in vapor phase in the region $\lambda = 2300$–1600A. The electronic excitation responsible for the first group of bands in this region is practically independent of the cyclic structure of the molecule since the wave number of the first band agrees closely with that obtained for olefins having the same arrangement of hydrogen-atoms around the double bond. Characteristic vibrational frequencies and different electronic levels have been identified.

EARLIER papers in this series have reported absorption spectra measurements between $\lambda = 2300$A and 1600A for sixteen ethylenic hydrocarbons[1] and the present paper extends this investigation to include three cyclic hydrocarbons—cyclopentene, cyclohexene and 1–3-cyclohexadiene. The spectrum of benzene has been re-examined under conditions which give a better definition of the vibrational bands than was obtained in the earlier work and these results are used to compare with the measurements for the other cyclic hydrocarbons.

### EXPERIMENTAL

Cyclohexene was prepared by dehydration of cyclohexanol[2] according to the method outlined by Kistiakowsky and co-workers[3] and had a boiling point of 82.70°±.05 at 760 mm; an index of refraction, $n^{20}D$ 1.4465; a density, $d_4^{20}$ 0.8101. A part of the cyclohexene was converted into 1–3-cyclohexadiene as described by these authors. The diene used for the spectrographic work was a highly purified product obtained directly from the dibromide and its physical constants, b.p. 80.13°±0.05°, $n^{20}D$ 1.4742, $d_4^{20}$ 0.8413, were in satisfactory agreement with the cyclohexadiene of Kistiakowsky prepared by way of the cyclohexenyl ether.

Cyclopentene was prepared from cyclopentanone which in turn had been prepared from adipic acid according to the method used by Kistiakowsky and co-workers.[4] Cyclopentanone

[1] E. P. Carr and M. K. Walker, J. Chem. Phys. **4**, 751 (1936); E. P. Carr and H. Stücklen, Zeits. f. physik. Chemie **B25**, 57 (1934); J. Chem. Phys. **4**, 760 (1936).

[2] The preparation and purification of all the compounds used for spectrographic examination are under the direction of Professor Mary L. Sherrill of this laboratory. The purification of the cyclic hydrocarbons has been made by fractionations through a 35 cm Fenske column. The purity of the material is tested not only by the usual physical constants—boiling point, index of refraction and density but also by absorption spectrum measurements of the liquid hydrocarbon and its hexane solution with the quartz spectrograph. Cyclopentene was prepared by Elizabeth S. Matlack of this laboratory; cyclohexene and cyclohexadiene by Kate Wilkins. This latter work was done in partial fulfillment of the requirements for the M.A. degree at Mount Holyoke College.

[3] G. B. Kistiakowsky *et al.*, J. Am. Chem. Soc. **58**, 140 (1936).

[4] G. B. Kistiakowsky *et al.*, J. Am. Chem. Soc. **59**, 832 (1937).

TABLE I.

| CYCLOHEXENE | | |
|---|---|---|
| 1/λ | 1/λ | 1/λ |
| 47420 | 48560 | 49810 |
| 760 | 930 | 50110 |
| 48010 | 49245 | 430 |
| 260 | 510 | 730 |
| 51100 | 52240 | 53680 |
| 230 | 500 | 970 |
| 360 | 630 | 54305 |
| 465 | 860 | 630 |
| 580 | 965 | 55020 |
| 710 | 53215 | |
| 870 | 320 | |
| 52100 | 560 | |
| 55435 | 57820 | 59100 |
| 990 | 58220 | 270 |
| 56990 | 670 | 610 |
| 57350 | 970 | 60160 |
| | | 510 |

TABLE II.

| 1-3 CYCLOHEXADIENE | | |
|---|---|---|
| 1/λ | 1/λ | 1/λ |
| 47780–47975 | 48560 | 49000 |
| 48070–48210 | 680 | 100 |
| 48235–48365 | 790 | 200 |
| 48475 | 885 | 300 |
| 49400 | 49870 | 50410 |
| 480 | 970 | 525 |
| 580 | 50100 | 635 |
| 680 | 200 | 765 |
| 760 | 305 | |
| | | 53650 |
| | | 820 |
| 51185 | 52605 | 950 |
| 280 | 700 | 54355 |
| 380 | 810 | 440 |
| 500 | 900 | 540 |
| 615 | 53000 | 650 |
| 710 | 100 | 730 |
| 820 | 200 | 820 |
| 945 | 310 | 940 |
| 52050 | 430 | 55045 |
| 500 | 540 | |
| 57875 | 58125 | 58415 |
| 960 | 220 | 510 |
| 58035 | 315 | |

was reduced, using a copper-chromium oxide catalyst,[5] and the resulting cyclopentanol had a boiling point of 140–141° at 759 mm. The cyclopentanol was dehydrated by means of fused potassium acid sulphate, dried over lime and purified by distillation. The resulting cyclopentene had a boiling point of 44.02°±.02°, $n^{20}D$ 1.4420, $d_4^{20}$ 0.7716.

Benzene, Kahlbaum special for molecular weight determinations, was fractionated and the middle fraction boiling at 80.0–80.1° was used for spectrographic examination.

The apparatus and experimental procedure for the absorption spectra measurements have been described in detail.[6] For the earlier study of benzene a 12 cm absorption tube was used; all of the measurements reported in this paper were made with a 60 cm tube. The exposure time varied from 4 min. to 10 min. and all of the

TABLE III.

| BENZENE | | |
|---|---|---|
| 1/λ | 1/λ | 1/λ |
| 48800 | 50320 | 52480 |
| 49035 | 570 | 670 |
| 205 | 850 | 940 |
| 355 | 51030 | 53220 |
| 670 | 300 | 475 |
| 780 | 690 | 700 |
| 970 | 870 | 54040 |
| 50140 | 52030 | 430 |
| 55330 | 56740 | 57550 |
| 420 | 830 | 635 |
| 772 | 57020 | 735 |
| 860 | 095 | 840 |
| 56130 | 260 | 955 |
| 215 | 350 | 58120 |
| 505 | | 220 |
| 590 | | |
| 55420 | 56220 | 57115 |

TABLE IV.

| CYCLOPENTENE | | |
|---|---|---|
| 1/λ | 1/λ | 1/λ |
| 47603 | 48348 | 49168 |
| 720 | 490 | 285 |
| 815 | 645 | 400 |
| 935 | 772 | 520 |
| 48062 | 915 | 653 |
| 204 | 49040 | 788 |
| | | 900 |
| 50090 | 50870 | 51470 |
| 320 | 51200 | 645 |
| 405 | 260 | 825 |
| 700 | 310 | 52370 |
| | | 710 |
| 53140 | 54120 | 55610 |
| 685 | 660 | |

[5] This reduction was kindly carried out for us at the University of Wisconsin through the courtesy of Dr. Homer Adkins.

[6] E. P. Carr and H. Stücklen, reference 1.

bands which are given in the tables were photographed while the vapor was kept flowing through the absorption cell. When the vapor is stationary or flowing very slowly photochemical decomposition takes place and new absorption bands appear. With each compound a series of plates were taken after irradiation of the material from 10–45 min. in order to distinguish clearly between the bands of the original material and those due to the presence of disintegration products.

## Results

The spectra of the cyclic unsaturated hydrocarbons show the same general regions of absorption as were evident with the olefins and may be classified into regions *A–D* as was done in the earlier work. The present study is concerned primarily with the absorption between 2300 and 1650A which is the region previously discussed as region *C*, the long wave portion and *B*, the short wave. This subdivision is quite arbitrary and was made to simplify the discussion. Each of the cyclic hydrocarbons has been examined also in pure liquid and hexane solution phase with the quartz spectrograph, and these curves will be published in a separate paper in connection with a study of photochemical decomposition of these hydrocarbons.

The results of measurements with the fluorite vacuum spectrograph are presented in the form of tables and graphs. The most striking difference in the spectra of the aliphatic and cyclic hydrocarbons in this region is the presence of sharp, narrow bands in the latter, whereas, with the exception of cis- and transbutene-2 and isobutene all of the olefins show only diffuse bands. Tables I–IV give the wave numbers of the center of the absorption bands, which can be measured with an error of less than 10 $cm^{-1}$ for intense narrow bands. The values for each compound are subdivided into groups depending upon similarity in structure of the bands.

As in the previous work, the intensities of the bands as given in the curves are estimated from their appearance on the photographic plate since the Schumann plates do not admit of quantitative photometric measurement. The vapor pressure of the hydrocarbon in the absorption tube was varied from 40 mm to less than 0.1 mm.

The wave number at which absorption begins in the Schumann region was found for the olefins to be dependent upon the number of hydrogen atoms bound to the carbon atoms of the double bond. All of the cyclic compounds which have been studied, including benzene and diphenyl, have the grouping C−CH=CH−C and the analogous group for the olefins, R−CH=CH−R, was designated as II*a*. For this group the beginning of absorption for the olefins was between 48,200 and 49,200 $cm^{-1}$; for benzene this is at 48,800 $cm^{-1}$ and for the other cyclic hydrocarbons it is between 47,400 and 47,900 $cm^{-1}$. While there is a slight shift toward the visible of the first absorption band of all of the cyclic compounds except benzene in comparison with the olefins the close parallelism of the aliphatic and cyclic compounds is of interest. Evidently the energy of this electronic excitation which is common to all of the hydrocarbons containing the C=C linkage is not only independent of the nature of the alkyl substituent, as was shown previously, but it would seem also to be practically independent of whether the molecule has a cyclic or an open chain structure.

The variation in breadth of the narrow bands which are characteristic of these cyclic compounds is no doubt of significance but it seems premature to attempt any theoretical explanation. In the first group of bands of cyclohexene and cisbutene-2 the breadth of the bands is of the order of 100 $cm^{-1}$, while in transbutene-2, cyclopentene and cyclohexadiene it is from 40–50 $cm^{-1}$. In benzene these bands have broadened to such an extent that they overlap and give the effect of shallow diffuse bands and only in a narrow range of pressures are the single maxima sharp enough to be measured. In the short wave region benzene has a doublet band system in which the average width of a band is 40 $cm^{-1}$ and cyclohexene shows a comparable band system at somewhat longer wave-lengths.

## Discussion of Results

The first absorption bands in the Schumann region for ethylenic derivatives were ascribed to an electronic excitation corresponding to the transition $^1A_1 \rightarrow {}^1B_1$[7] which had been predicted

[7] E. P. Carr and H. Stücklen, J. Chem. Phys. **4**, 760 (1936).

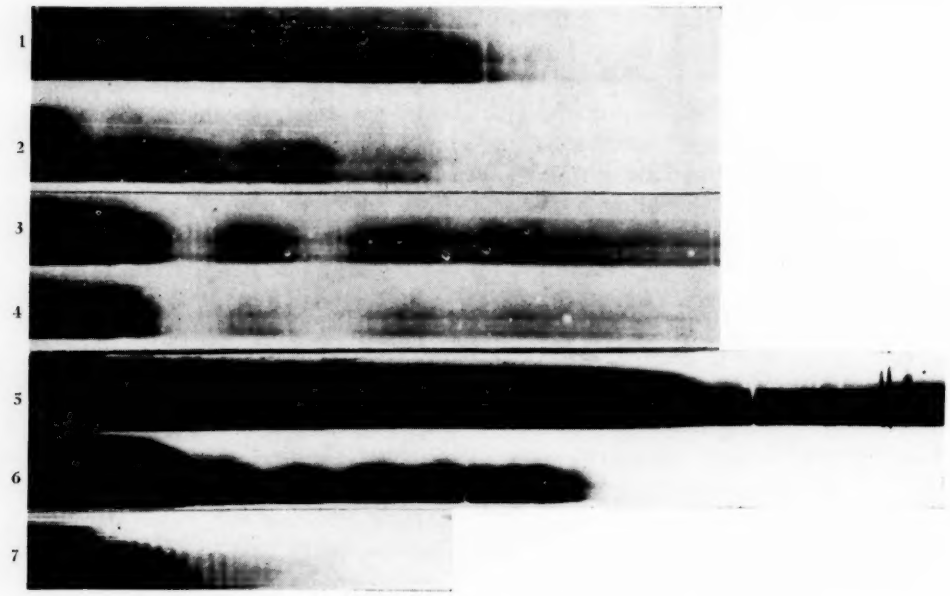


FIG. 1. 1,2, Cyclohexene; 3,4, cyclohexadiene; 5,6, benzene; 7, cyclopentene.

for the ethylene molecule.[8] Since the excitation involves an ($x$) orbital, localized in the region of the C=C bond, it would be reasonable to expect the vibrational bands which are characteristic of this linkage. Because of the breadth and diffuseness of the bands in the spectra of the higher olefins it was not possible to identify any of the vibrational bands with certainty but the appearance of fine structure in the butenes and in the cyclic compounds enables the measurement of band separations with an error of not more than 10 $cm^{-1}$. Vibrational frequencies of 1510 $cm^{-1}$ for the excited molecule of cisbutene-2, 1570 $cm^{-1}$ for transbutene-2, and 1485 $cm^{-1}$ for cyclohexene have already been pointed out[9] together with their relation to the Raman frequencies of 1658 and 1674 for cis- and transpentene-2 and 1646 $cm^{-1}$ for cyclohexene. The spectrum of cyclopentene in the Schumann region shows only a long series of equally spaced narrow bands of gradually increasing intensity with increasing wave number, whereas in the other cyclic compounds there are groups of bands with sharply marked maxima (Fig. 1). In cyclohexene and cyclohexadiene the separation between the most intense band in the first and second groups (Fig. 2) is of the order of that which is characteristic for this vibration in ethylenic compounds and seems, without question, to be related to the vibration along the axis of the C=C bond. In the spectrum of benzene (Fig. 2) the corresponding separation is 935 $cm^{-1}$ and this frequency must be ascribed to the C=C vibration which constitutes the so-called "breathing" frequency of the benzene molecule and corresponds to the 992 $cm^{-1}$ in the normal molecule.

In cyclohexene and cyclohexadiene there is a strong band, the separation of which from the strongest or 0−0 band of the first group is of

TABLE V.

| COMPOUND | 1/λ RAMAN* | 1/λ ULTRAVIOLET |
|---|---|---|
| Cyclohexene | 1646 $cm^{-1}$ | 1485 $cm^{-1}$ |
| | 2912 | 2670 |
| | 3024 | |
| 1-3-Cyclohexadiene | 1574 | 1360±50† |
| | 3042 | 2920 |
| Benzene | 992 | 935 |
| | 3060 | 2835 |

* K. W. Kohlrausch and R. Seka, Ber. **A68**, 528 (1935).
† There are two bands of almost equal intensity in the center of the second group. In measuring the separation of the maxima of different groups an error of ±50 $cm^{-1}$ is therefore possible.

[8] Mulliken, Phys. Rev. **41**, 751 (1932); J. Chem. Phys. **3**, 517 (1935).
[9] E. P. Carr and H. Stücklen, J. Am. Chem. Soc. (in publication).

the order of 2700–2900 $cm^{-1}$. This band is present in the benzene spectrum also where it is one of the intense bands in the fourth group and has been found in cisbutene-2 in the third group. A second member of the C=C vibrational series is clearly separated from it in all of the compounds except cyclohexadiene. This band could be ascribed to a C−H stretching vibration, the frequency of which for hydrocarbons in their normal state is known to be of the order of 3000 $cm^{-1}$. Considering intensities, this assignment would be allowed. The band is equal or stronger than the neighboring higher member of the C=C vibrational series, while this again is weaker than the preceding member of its series. A comparison of these vibration frequencies for the excited molecule with the corresponding ones for the normal molecule from the Raman spectra is given in Table V.

The absorption spectrum of cyclopentene (Fig. 3) is unique among the twenty-two hydrocarbons that have been examined in this laboratory. The beginning of absorption at 47,600 $cm^{-1}$ is in accord with that for the other cyclic hydrocarbons and the ethylenic derivatives of group II*a* but the spectrum in this region shows only a series of about twenty equally spaced narrow bands, the average separation of which is 130 $cm^{-1}$. The intensity of these bands increases gradually but there is no evidence in this electronic level of the discrete bands which have been ascribed to vibrations of the C=C bond in other molecules. It would seem as if an electronic excitation which is analogous to that found for the other unsaturated hydrocarbons is, in the case of cyclopentene, unaccompanied by the characteristic C=C vibration. It should be noted, however, that quite clearly marked band separations of 1520 and 2470 $cm^{-1}$ are shown in the higher electronic level which begins at about 53,000 $cm^{-1}$ although it has not been possible to identify corresponding vibrational bands in this electronic transition for other hydrocarbons except isobutene. A comparative table of Raman spectrum measurements for cyclopentene by various investigators is given by Reitz.[10] There is a strong Raman line at 1610 $cm^{-1}$ and a group of lines at 2846, 2902, 2947 and 3060 $cm^{-1}$, all of high intensity.

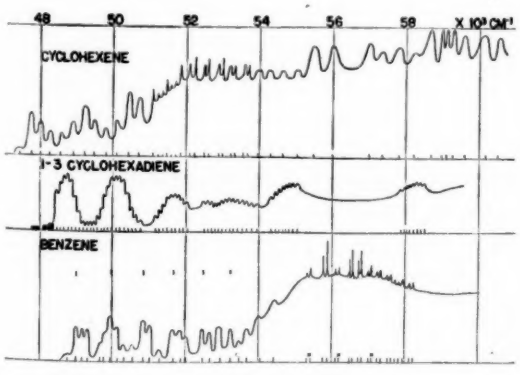


FIG. 2.

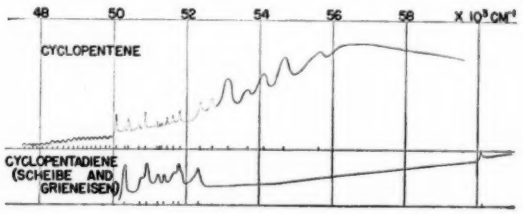


FIG. 3.

The doublet system in cyclopentene which appears at 50,000 $cm^{-1}$ is undoubtedly due to the presence of cyclopentadiene. This band system appears very faintly when the ordinary exposures of from 4 to 6 minutes are made but comes out very strongly on longer irradiation. The curve for cyclopentadiene given by Scheibe and Grieneisen[11] is reproduced below that for cyclopentene (Fig. 3) and shows quite clearly that this system in our measurements of cyclopentene must be due to the diene which has been formed by photochemical decomposition. Further discussion of the cyclopentene spectrum must be postponed until the spectrum of cyclopentane and cyclopentadiene can be examined.

From the general character of the bands in cyclohexene and their intensity relationships there would seem to be from 4–5 different electronic levels in the region between 47,000 and 61,000 $cm^{-1}$. The first excitation beginning at 47,750 $cm^{-1}$ seems to be completely analogous to that in the ethylenic derivatives which has been ascribed to a $^1A_1 \rightarrow {}^1B_1$ transition. The curves for cis- and transbutene-2 are given in

[10] A. W. Reitz, Zeits. f. physik. Chemie **B33**, 182 (1936).
[11] Scheibe and Grieneisen, Zeits. f. physik. Chemie **B25**, 52 (1934).

Fig. 4 in order to show the striking parallelism between the spectra of cisbutene-2 and cyclohexene in the region between 47,000 $cm^{-1}$ and 51,000 $cm^{-1}$. These results have served as a confirmatory test for the assignment of molecular configurations to the isomers of butene-2.[9] The

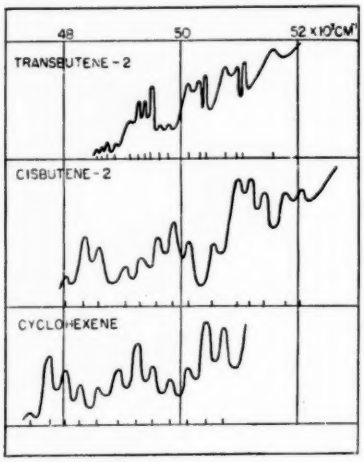


FIG. 4.

only other electronic excitation in this spectrum which shows a marked resemblance to anything which has been found in the spectra of other unsaturated hydrocarbons is the doublet system which begins about 52,000 $cm^{-1}$ and extends to 55,000 $cm^{-1}$, the last four groups not being resolved. This system is quite similar to that found in benzene between 55,500 and 58,500 $cm^{-1}$; in each case the short wave component of the doublet is much stronger than the other; the separation between the two bands in the doublet is of the order of 100 $cm^{-1}$ in benzene and 130 $cm^{-1}$ in cyclohexene. In both spectra the separation between successive doublets seems to remain fairly constant although the separation is somewhat larger in cyclohexene (350 $cm^{-1}$) than in benzene (250 $cm^{-1}$).

In cyclohexadiene a series of more than fifty narrow bands, with an average separation of 100 $cm^{-1}$ extends with but slight interruption from 48,500 to 55,000 $cm^{-1}$. Underlying this series of bands are the diffuse bands whose separations correspond to vibrational frequencies of the C=C and C−H bonds. The narrow band spectrum reappears again in another electronic level in the region of 58,000 $cm^{-1}$ but the separation here seems to be slightly less than in the longer wave region. It is not possible at this time to attempt any theoretical discussion of these narrow bands which seem to be so characteristic a part of the spectra of cyclopentene and 1–3-cyclohexadiene.

In the earlier discussion of the benzene spectrum[12] very little could be said about the region between 48,500 and 54,000 $cm^{-1}$ since the experimental conditions were not such that the narrow bands in this region were resolved and with the exception of the first two bands where some splitting was evident only the maxima of groups of diffuse bands were given. The results of the present investigation of the benzene spectrum show that the strongest bands of each of the first six groups, as indicated in Fig. 2, fit into a vibrational series of the form: $1/\lambda = 49035 + 960v - 25v^2$, the average deviation of $\pm 3$ $cm^{-1}$ being within the limits of experimental error. The lower intensity of the first, or 0−0 band, would be explained by the Franck-Condon principle; after the second the intensity decreases as must be expected for a vibrational series. In the case of cyclohexene and cyclohexadiene it is of interest to note that in each spectrum the first two bands have the same intensity.

The general characteristics of the spectra of benzene, cyclohexene, cyclohexadiene in the region beginning about 48,000 $cm^{-1}$ and their analogy to the spectra of the ethylenic derivatives point to the conclusion that the electronic transition involved is similar in all of the molecules. In the ethylenic hydrocarbons this transition was tentatively assigned to the transition $^1A_1 \rightarrow {}^1B_1$ and the much weaker absorption in the quartz region to a $^1A_1 \rightarrow {}^3B_1$ transition. The olefins show a step-out indicating a broad absorption band of very low intensity in the quartz region so that no study of fine structure is possible but the analogy to the benzene spectrum is shown by the fact that the absorption of the group II hydrocarbons in liquid and hexane solution is in precisely the same region as that of benzene solutions.[13] The sharp bands of

[12] E. P. Carr and H. Stücklen, Zeits. f. physik. Chemie **B25**, 57 (1934).

[13] E. P. Carr and G. F. Walter, J. Chem. Phys. **4**, 760 (1936); *International Critical Tables*, Vol. 5, p. 363.

the latter spectrum are well known and the vapor phase spectrum has been exhaustively investigated. If, therefore, the assumption that closely corresponding electronic transitions are involved in the excitation of all the molecules having the $-C-CH=CH-C-$ grouping is valid the absorption spectrum of benzene in the long wave region between 37,000 and 44,000 $cm^{-1}$ would be ascribed to a singlet-triplet transition. Some justification for this assumption is given by the recent interpretation of the fluorescence spectrum of benzene by Ingold and Wilson[14] in which a complete analysis of the spectrum was possible on the basis of transitions from three excited electron states to the zero level of the ground state.

[14] C. K. Ingold and C. L. Wilson, J. Chem. Soc. 941 (1936).

The vapor pressure of the benzene was too high and the absorption tube too short to resolve the benzene spectrum sufficiently to permit detailed analysis of the bands but the general characteristics of the spectrum between 48,800 and 54,400 $cm^{-1}$ and in the quartz region are sufficiently similar to indicate closely related electronic transitions. The probability of the singlet→triplet transition for ethylene was estimated by Mulliken to be of the order of $10^{-4}$ of that for the singlet→singlet transition and the ethylenic derivatives showed close agreement with that prediction. If the assumption of corresponding states for benzene is correct, comparison of the intensities in the two regions would show that the probability of the transition to the triplet state in benzene is about $10^{-2}$ of that for the singlet→singlet transition.

FEBRUARY, 1938 JOURNAL OF CHEMICAL PHYSICS VOLUME 6

# Infrared Absorption Studies

## IV. The Infrared Spectrum of Water in an Inert Solvent

L. B. Borst, A. M. Buswell and W. H. Rodebush
*University of Illinois, Urbana, Illinois*

(Received November 22, 1937)

The infrared absorption spectrum of $H_2O$, HDO and $D_2O$ in dilute solution in carbon tetrachloride and carbon bisulfide has been investigated with a grating of high resolving power, in the region 2.6–3.8$\mu$. Several bands have been identified as $\nu_3$ bands and the hitherto unobserved $\nu_1$ band for $H_2O$ is believed to have been found. The frequencies observed are compared with the same frequencies in the vapor and a displacement of frequency which is proportional to the frequency itself is observed in solution. A fine structure is observed in the case of $H_2O$ which may be ascribed to rotation unless some other explanation is found. The spectrum in carbon bisulfide appears to be identical with that in carbon tetrachloride.

THE infrared vibraton rotation spectrum of water vapor was investigated by Plyler and Sleator[1] and that of heavy water vapor has been recently studied by Barker and Sleator.[2] They have located the principal vibration frequencies for water and the two deuterium substituted molecules with the exception of $\nu_1$ which has not been observed in the symmetrical molecule and $\nu_3$ for HDO. $\nu_1$, however has been observed in the Raman spectrum for $H_2O$.[3] Studies of hydrogen chloride absorption in solution have been made by Plyler and Williams,[4] and West and Edwards.[5] Recently Kinsey and Ellis[6] have observed the infrared absorption spectrum of water in carbon bisulfide solution with a prism spectrograph.

[1] E. K. Plyler and W. W. Sleator, Phys. Rev. **37**, 1493 (1931).
[2] E. F. Barker and W. W. Sleator, J. Chem. Phys. **3**, 660 (1935).
[3] D. Bender, Phys. Rev. **47**, 252 (1935).
[4] E. K. Plyler and D. Williams, Phys. Rev. **49**, 215 (1936).
[5] W. West and R. T. Edwards, J. Chem. Phys. **5**, 14 (1937).
[6] E. L. Kinsey and J. W. Ellis, Phys. Rev. **51**, 1074 (1937).

It seemed desirable to the authors to investigate the spectrum of water in an inert solvent with a spectrograph of high resolving power in order to determine what differences were produced in the spectrum by the presence of the solvent and one for solution, was used. When the absorption of the vapor was measured, the cells were heated by circulating water from a thermostat. In representing the data, wave numbers are plotted as abscissa and log $I_0/I$ is plotted as ordinate, where $I_0$ is the galvanometer deflection through the pure solvent and $I$, the deflection when the solution is in the path.

The vapor absorption spectra of $H_2O$, HDO, and $D_2O$ were mapped for comparison and identification purposes with a prism spectrometer of low resolving power (Fig. 1).

When a survey was made of the solution with the same instrument there was observed a band at $2.7\mu$ due to $H_2O$ and three bands between 3.5 and $3.8\mu$ which were attributed to HDO and $D_2O$. These are shown in Fig. 2. The carbon

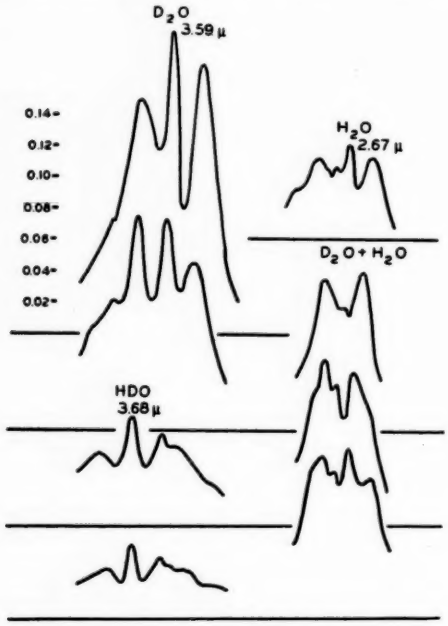


FIG. 1. Vapor absorption bands for mixtures of $H_2O$ and $D_2O$. Prism spectrometer.

solvent molecules. A grating spectrograph which was purchased from the University of Michigan was available for this purpose. This instrument has been described.[7] The grating was of the echelette type, 3600 lines to the inch, ruled on pure tin. It was constructed for us in the physics shop of the University of Michigan under the direction of Professor Barker. As a light source we used an ordinary street lighting bulb with a coiled tungsten filament of 6.6 amperes rating. The thin glass walls transmit very satisfactorily up to about $4\mu$ and this type of lamp is much superior to the Nernst glower. The utmost precautions were taken in purifying the solvents used in preparing the solutions. As a check on the calibration of the grating, the absorption spectrum of vapor was recorded. The results agreed within about 3 $cm^{-1}$ with those of Plyler and Sleator.

In measuring the absorption, a cell 7.5 cm in length with two compartments, one for pure

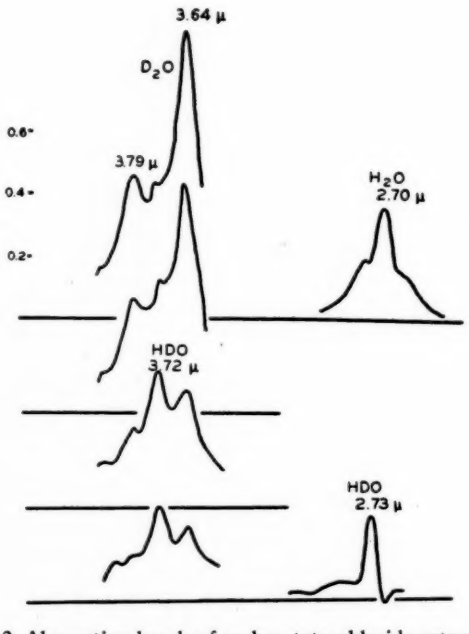


FIG. 2. Absorption bands of carbon tetrachloride saturated with a mixture of $H_2O$ and $D_2O$. Prism spectrometer.

tetrachloride was saturated with water containing varying percentages of $D_2O$. It is evident that there is no very close correspondence between the absorption in the vapor and in solution. The main absorption peaks are undoubtedly due to the antisymmetric vibration $\nu_3$. It is suggested that the additional small peaks in solution, which have no counterpart in the vapor, might be due to the symmetric vibration

[7] W. W. Sleator, Astrophys. J. **48**, 125 (1918).

$\nu_1$ which has not heretofore been observed in the infrared.

In Fig. 3 the absorption curves are given for $H_2O$ in carbon tetrachloride solution as obtained with the grating spectrometer. The upper curve is obtained from a 12.5 cm layer saturated with water. (The solubility of water in carbon tetrachloride is stated to be 0.0083 mole per liter.) The lower curve is obtained by diluting the solution to one-fourth of the original concentration. The fine structure obtained here is believed to be real as it was checked repeatedly. In order to eliminate the possibility of water vapor in the system, the curves shown in Fig. 4 were obtained. The upper curve is the absorption curve for water vapor and the lower curve is for 5 cm

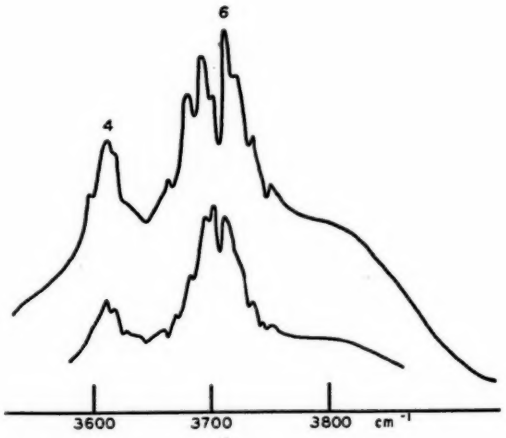


FIG. 3. $H_2O$ in carbon tetrachloride. Grating spectrometer.

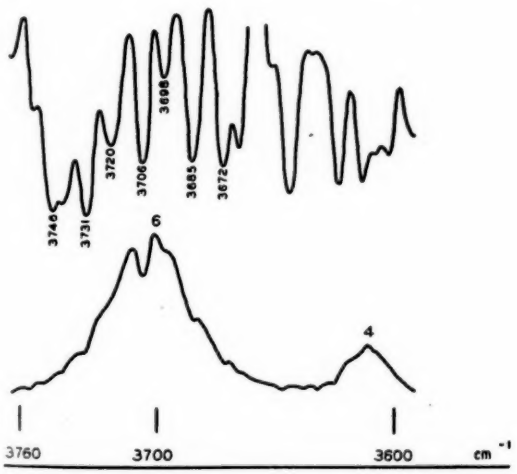


FIG. 4. Comparison of vapor and solution of $H_2O$. Grating spectrometer.

saturated carbon tetrachloride solution. There is no correlation observable.

Figure 5 is the absorption curve in the 2.7$\mu$ region for $D_2O$. The negative absorption simply indicates the presence of traces of water in the supposedly dry pure solvent. In spite of all precautions some water was present. In the cell to which $D_2O$ was added this water was effectively converted to HDO. The peak is therefore to be attributed to $\nu_3$ for HDO, the minima to the $H_2O$ in the solvent. There is evidence of fine structure.

In Fig. 6 are given the absorption curves for three concentrations of $D_2O$ in the region 3.4 to 3.9$\mu$. The upper curve (dotted line) was obtained from a sample saturated with 99.6 percent $D_2O$. The middle curve was for a solution saturated with 85 percent $D_2O$ and the lower curve was obtained upon diluting this solution one-half. The breaks in the lines are due to readjustment of the monochromator. These curves were obtained using the first order because of low intensity. The resolving power is therefore only one-half that used in obtaining the curves in Figs. 3, 4, and 5.

The identification of certain of the peaks seems obvious enough by comparison with the work of Sleator and colleagues. The frequency is shifted in solution to lower values, the shift being apparently roughly proportional to the frequency. Table I gives the principal absorption peaks. The number in the first column serves to locate the peak on the accompanying curves. The second column gives the frequency observed

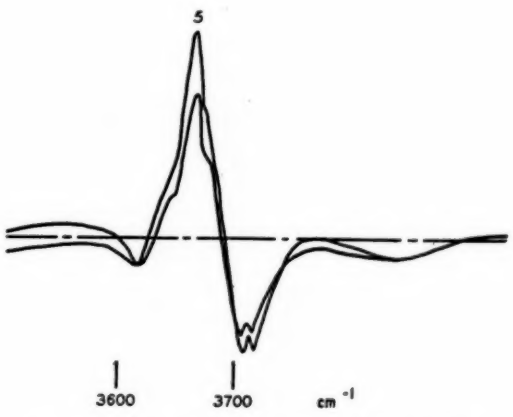


FIG. 5. Solution of $D_2O$ in carbon tetrachloride. Grating spectrometer.

by us in carbon tetrachloride solution. The third column gives the frequency as observed in the vapor either by infrared absorption or in the

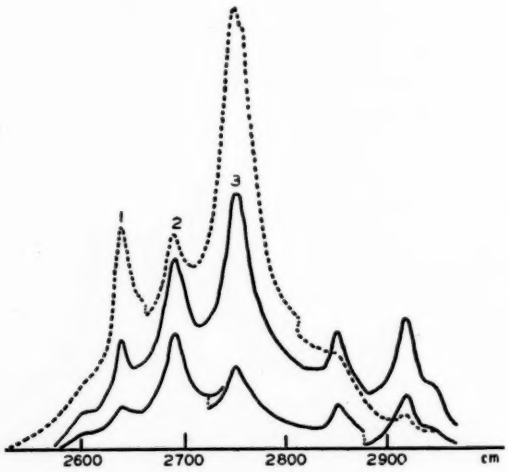


FIG. 6. Solution of $D_2O$ in carbon tetrachloride. Grating spectrometer.

Raman spectrum. The fourth column gives the difference between solution and vapor. This difference is seen to be roughly proportional to the frequency and this can be justified on theoretical grounds. $[\nu_1]$ is enclosed in brackets since this frequency has not been observed before in the infrared and the assignment is therefore necessarily tentative since there is no very obvious reason why it should be more active in solution than in the vapor state. $[\nu_3]$ has not been observed for HDO either in the Raman or infrared spectra and the calculated value for the vapor [3750] may be in error by 50 wave numbers.

TABLE I. *Frequencies ($cm^{-1}$) of the principal absorption peaks.*

| | SOLUTION | VAPOR | DIFFERENCE |
|---|---|---|---|
| 1 | 2640 $[\nu_1]$ $D_2O$ | 2666 | 26 |
| 2 | 2689 $[\nu_1]$ HDO | 2720 | 33 |
| 3 | 2748 $\nu_3$ $D_2O$ | 2784 | 36 |
| 4 | 3611 $[\nu_1]$ $H_2O$ | 3654 | 43 |
| 5 | 3659 $[\nu_3]$ HDO | [3750] | [91] |
| 6 | 3702 $\nu_3$ $H_2O$ | 3756 | 44 |

There seems to be no doubt as to the reality of the fine structure apparent in Fig. 3 and in the absence of other explanations it must be assumed to be due to some sort of submerged rotational structure. This fine structure was not observed in the deuterium substituted compounds for the reason that, assuming it to be a rotational structure, a higher resolving power would be required, whereas these spectra were observed in the first order with only half the resolving power used for ordinary water.

The absorption spectrum of water in solution in carbon bisulfide was observed but the curve is so nearly identical with those published here for the carbon tetrachloride solutions that there seems to be no reason for reproducing it.

The authors wish to acknowledge their indebtedness to Dr. J. G. Kirkwood and Dr. F. T. Wall for helpful discussions in regard to the interpretation of this work. They wish also to acknowledge their indebtedness to the Rockefeller Foundation for financial support.

# A Spectral Investigation of Glucose Glass

WILLI M. COHN
*Berkeley, California*

(Received November 12, 1937)

The spectral transmission of glucose glasses has been investigated over the wave-length region from 3600 to 8000A. Glasses of different thermal history were tested, ranging from white to dark brown in color. The glasses show different transmission values, and shifts of the transmission maximum and the absorption limit at small wave-lengths with increasing caramelization.

## I. INTRODUCTION

THE thermal properties of glucose glass have been investigated by Parks and co-workers.[1] The color of these glasses varies, depending on the thermal history, from white to dark brown indicating the formation of decomposition products during caramelization. (It is generally assumed that small amounts of colloidal carbon are finally liberated.) An investigation seemed of interest to determine the effect of caramelization on the spectral transmission of glucose glass.

[1] G. S. Parks and H. M. Huffman, J. Phys. Chem. **31**, 1842–55 (1927); G. S. Parks, H. M. Huffman and F. R. Cattoir, J. Phys. Chem. **32**, 1366–79 (1928); F. R. Cattoir and G. S. Parks, J. Phys. Chem. **33**, 879–882 (1929); G. S. Parks and W. A. Gilkey, J. Phys. Chem. **33**, 1428–37 (1929); G. S. Parks and S. B. Thomas, J. Am. Chem. Soc. **56**, 1423 (1934); G. S. Parks, L. E. Barton, M. E. Spaght and J. W. Richardson, Physics **5**, 193–199 (1934); G. S. Parks, L. J. Snyder and F. R. Cattoir, J. Chem. Phys. **2**, 595–598 (1934); J. C. Lyman and G. S. Parks, J. Chem. Phys. **4**, 218–219 (1936); G. S. Parks and J. D. Reagh, J. Chem. Phys. **5**, 364–367 (1937).

## II. METHOD

Spectra were obtained with my Hilger grating spectrograph, dispersion 49.4A/mm. The range from 3600 to 8000A was investigated using Wratten and Wainwright hypersensitive panchromatic plates and Eastman Kodak I-N plates. The first-order spectrum was used, the overlapping ultraviolet of the second order being eliminated by a No. 12 Wratten gelatin filter. A straight filament 8.5-volt lamp with rheostat control was used as a light source. A condenser lens projected the light on the slit. The slit width was 0.1 mm. A very fine neutral wedge from Hilger was placed in front of the slit. (A separate investigation showed that this wedge

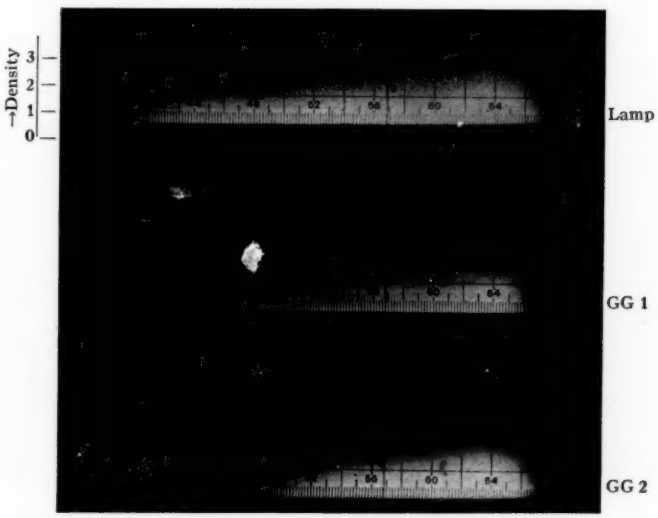


FIG. 1. Plate No. BL 401. Hyperpan plate. Wedge spectra for lamp alone, and glucose glasses GG 1 and GG 2. Time of exposure 2 minutes.

FIG. 2. Plate No. BL 410. I-N plate. Wedge spectra for lamp alone, and glucose glass GG 1. Time of exposure 10 minutes.

is neutral over the entire wave-length region investigated.) The density of the wedge was such that the light end transmits 10,000 times the light transmitted by the dark end.[2] A wave-length and density scale was printed on the plate, together with the spectrum. (The wave-length scale needs a slight correction which was determined from line spectra.)

The glucose glass samples were contained in metal cells of 23.5 mm inside diameter with silica glass windows, the length of cells GG 1 and 2 was 24.0 and that of all other cells was 25.0 mm. The samples were placed in front of the wedge. Several spectra were taken from each sample. The difference in density of the lamp and glass spectra on a plate was small enough to permit the photometric reduction.

The photometric reduction was carried out as follows: A wedge spectrum of the lamp alone was printed on each plate, together with one or two glucose glass spectra. All spectra on a plate were taken with the same time of exposure and the same voltage of the lamp. Fig. 1 shows the panchromatic plate BL 401 with wedge spectra of the lamp alone and glasses GG 1 and 2, and Fig. 2 shows the I-N plate BL 410 with wedge spectra of the lamp and glass GG 1.

The density of the glass and lamp spectra was measured every 20 mμ. A simple computation gave then the light transmission values. Considering the values for the lamp alone as unity the transmission of the glass could be computed in percent. The steep decrease in sensitivity of the panchromatic plates makes values around 660 mμ less accurate than the remaining values. (All values of less weight are given in parentheses in Table II.) The probable error of the measurements amounts to ±2 percent.

[2] C. E. K. Mees and S. H. Wratten, Brit. J. Phot. **54**, 384–385 (1907).

## III. SAMPLES

The samples were prepared by Dr. Parks and co-workers at different times, samples GG 1 and 2 were, approximately, four years old. These samples had been prepared from "C. P. Pfanstiehl" anhydrous glucose with a subsequent purification by the method of Hudson and Dale[3] with glacial acetic acid. The remaining samples were made directly from Pfanstiehl glucose without this special purification. The samples were, with the exception of GG 4 and 6, remarkably free of bubbles. No striae appeared in any glass. GG 4 and 7 showed the beginning of crystallization starting from the edge of one front end. GG 1 was practically colorless, the remaining samples extended from light yellow to dark brown in color, see Table I. This table presents also colorimetric values obtained by means of a Lovibond tintometer, series No. 52.[4] Glucose glasses GG 3 and 5, GG 4 and 6, and GG 7 and 8,

TABLE I. *Color and Lovibond values for glucose glasses.*

| GLASS NO. | COLOR | LOVIBOND VALUE |
|---|---|---|
| GG 1 | White | 3.0 |
| GG 2 | Light yellow | 11.0 |
| GG 7 | Yellow | 12.0 |
| GG 8 | Yellow | 10.7 |
| GG 9 | Yellow | 12.0 |
| GG 4 | Yellow-brown | 15.3 |
| GG 6 | Yellow-brown | 14.7 |
| GG 3 | Dark brown | 37.3 |
| GG 5 | Dark brown | 36.7 |

[3] C. S. Hudson and J. K. Dale, J. Am. Chem. Soc. **39**, 324–328 (1917).

[4] K. S. Gibson and F. K. Harris, Sci. Papers, Nat. Bur. Stand. No. 547, 1927.

respectively, show only small differences in color, each of these pairs having been prepared at about the same time.

## IV. Results

Table II contains the results of the individual measurements of the glucose glasses (reduced to a thickness of 25 mm). Fig. 3 shows the transmission curves including averages for glasses GG 3 and 5, GG 4 and 6, and GG 7 and 8. The difference in transmission values of GG 4 and 6 is due to the larger number of bubbles and the beginning of crystallization in GG 4. The following remarks refer to the results obtained.

(1) A careful study under varying conditions showed the absence of narrow absorption bands in the entire wave-length region investigated.

(2) The spectral energy distribution shows flat maxima for all glasses. The maxima occur in the range from 580 to 640 mμ. The maxima of transmission are shifted toward greater wave-lengths with increasing caramelization.

(3) The absorption limits at small wave-lengths are shifted toward the red with increasing caramelization. Table III gives the absorption limits for small wave-lengths.

(4) None of the glasses shows a limit of transmission toward great wave-lengths within the range investigated (up to 800 mμ). The transmission curves become, at great wave-lengths, approximately parallel to the abscissa for several glasses; a small increase in transmission is indicated for GG 8.

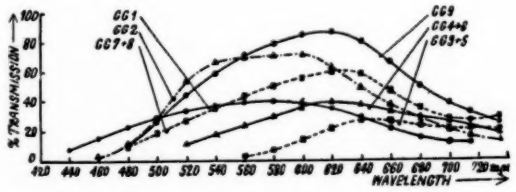


FIG. 3. Spectral transmission of glucose glasses.

(5) The transmission values of GG 1 are lower than those of the remaining glasses. This is probably due to the age of GG 1 as against the recent glass batches GG 3 to 9. It seems likely that crystallization has started already in GG 1 and 2, although it is not visible. Another cause of this difference may lie in the different purification process of the two groups of samples. A recrystallization would tend to decrease the transmission values over the entire spectrum.

TABLE II. *Transmission of glucose glasses in percent as a function of the wave-length; thickness of layer 25 mm.*

| Wave-length in mμ | GG 1 % | GG 2 % | GG 7 % | GG 8 % | GG 9 % | GG 4 % | GG 6 % | GG 3 % | GG 5 % |
|---|---|---|---|---|---|---|---|---|---|
| 440 | 8.4 | | | | | | | | |
| 460 | 15.2 | 2.1 | | | | | | | |
| 480 | 22.9 | 11.8 | 9.6 | 9.2 | 11.6 | | | | |
| 500 | 29.1 | 29.3 | 20.4 | 17.0 | 26.2 | | | | |
| 520 | 33.6 | 53.3 | 29.6 | 25.4 | 44.4 | 13.2 | 10.2 | | |
| 540 | 36.9 | 66.9 | 37.8 | 33.6 | 59.2 | 15.0 | 19.4 | | |
| 560 | 39.0 | 69.0 | 44.8 | 41.8 | 70.6 | 17.2 | 29.8 | 3.0 | (3.2) |
| 580 | 40.1 | 70.6 | 49.6 | 49.6 | 78.6 | 21.6 | 37.8 | 7.6 | 6.6 |
| 600 | 38.6 | 71.3 | 55.2 | 56.2 | 84.6 | 26.8 | 45.8 | 13.6 | 14.4 |
| 620 | 34.6 | 62.9 | 59.2 | 60.0 | 86.4 | 27.2 | 50.8 | 22.2 | 21.8 |
| 640 | 28.2 | 48.7 | 58.4 | 57.2 | 80.2 | 25.6 | 49.2 | 28.0 | 25.4 |
| 660 | (20.4) | (37.1) | (44.8) | (46.6) | (65.4) | (24.2) | (40.2) | (28.0) | (24.4) |
| 680 | 14.5 | 28.2 | | 34.6 | 49.6 | 23.4 | 36.8 | 27.0 | 19.4 |
| 700 | 11.0 | 20.7 | | 27.8 | 37.2 | 18.6 | 33.8 | 25.6 | 16.6 |
| 715 | 10.4 | 15.2 | | 27.0 | 31.2 | 13.3 | 31.2 | 24.8 | 16.9 |
| 735 | | 13.2 | | 28.3 | 24.6 | 11.6 | 26.9 | 24.7 | 15.7 |

TABLE III. *Absorption limits in mμ at short wave-lengths for glucose glasses.*

| Glass No. | GG1, mμ | GG2, mμ | GG7, mμ | GG8, mμ | GG9, mμ | GG4, mμ | GG6, mμ | GG3, mμ | GG5, mμ |
|---|---|---|---|---|---|---|---|---|---|
| Absorption Limit | 397 | 426 | 447 | 441 | 441 | 479 | 481 | 539 | 539 |

The results indicate that the spectral transmission of glucose glass depends on the thermal history of the glass, in a similar manner as do the thermal properties. A spectral investigation presents, if carried out under standardized conditions, a quick and sensitive method for a classification of samples, and a checking of the thermal history of the samples.

## V. Summary

The spectral transmission of glucose glasses of different thermal history has been investigated between 3600 and 8000A. All glasses show flat transmission maxima which are shifted toward greater wave-lengths with increasing caramelization. The absorption limits at small wave-lengths are shifted toward the red with increasing caramelization.

In conclusion I should like to express my thanks to Dr. George S. Parks of Stanford University for preparing the samples and for helpful discussions I have had with him.

# The Heat Capacity of Diamond from 70 to 300°K

KENNETH S. PITZER
*Department of Chemistry, University of California, Berkeley, California*
(Received November 20, 1937)

The specific heat of diamond has been measured over the temperature range 70 to 300°K, and is compared with the theoretical formula of Debye. Small but definite deviations are observed, which in both direction and order of magnitude are those to be expected when the approximations of the Debye formula are taken into consideration. The entropy of diamond at 298.1°K is 0.585±0.005 cal. per degree per mole.

THE temperature variation of the heat capacity of crystals received a satisfactory general explanation shortly after the development of quantum statistics. The papers of Einstein,[1] Born and v. Kármán,[2] and Debye[3] are particularly noteworthy, and it is the formula developed by the latter that has received most attention. Debye assumed that the frequencies of the normal modes of vibration of the crystal are distributed just as the vibration frequencies of a continuum, except that the spectrum is cut off at a certain maximum frequency ($\nu_D$) so chosen that there are exactly the proper total number of frequencies ($3N$ if $N$ be the total number of atoms).

TABLE I. *Molal heat capacity of diamond.*

| $T$, °K | $C_p$ (cal./deg.) | $(C_p/T^3)\times 10^{10}$ | $\theta_D$ (Debye) |
|---|---|---|---|
| 70.16 | 0.0224 | 650 | 1930 |
| 75.37 | .0296 | 692 | 1890 |
| 81.59 | .0362 | 667 | 1900 |
| 88.65 | .0452 | 650 | 1930 |
| 96.68 | .0592 | 655 | 1920 |
| 105.10 | .0785 | 677 | 1900 |
| 113.04 | .0991 | 686 | 1890 |
| 125.28 | .138 | 703 | 1874 |
| 134.29 | .174 | 719 | 1863 |
| 144.10 | .218 | 730 | 1851 |
| 153.71 | .267 | 736 | 1845 |
| 162.76 | .318 | 740 | 1840 |
| 173.33 | .386 | 743 | 1833 |
| 181.96 | .444 | 739 | 1832 |
| 191.44 | .518 | 740 | 1830 |
| 200.94 | .595 | 735 | 1818 |
| 211.84 | .685 | 722 | 1820 |
| 231.06 | .858 | 694 | 1817 |
| 241.09 | .918 | 653 | 1845 |
| 252.37 | 1.033 | 642 | 1840 |
| 264.31 | 1.137 | 616 | 1852 |
| 276.61 | 1.257 | 595 | 1855 |
| 287.96 | 1.355 | 568 | 1865 |

As seems likely in view of its derivation, the Debye formula only approximates the experimental data for most substances. Blackman[4] has discussed the nature of the deviations to be expected, and has shown that the specific heat curve for the vibrations of a given crystal will always approach the Debye formula at very low temperatures, but that it will be a rare and accidental occurrence if the Debye formula holds precisely over the entire temperature range.

It was the purpose of this investigation to consider the heat capacity curve for a particular substance in the light of these discussions. The choice of diamond as the subject was favored by the high symmetry of the crystal, the presence of only one kind of atom, the fact that the interatomic forces are reasonably well known and of short range, and the experimental consideration that, in a comparative sense, very low temperatures are easily attained.

## EXPERIMENTAL

About twenty grams of diamonds of a grade known as "bortz" were obtained for these experiments. The stones, while imperfect, were reasonably clear and were free from foreign matter. It is believed that their heat capacity was the same as that of perfect diamonds within the experimental errors of this investigation.

The calorimeter employed in this investigation was of similar character to that described by Latimer and Greensfelder[5] but was in size just large enough to contain the diamonds. The cryostat and other equipment were the same as has been used previously. The measurements

[1] Einstein, Ann. d. Physik **22**, 180, 800 (1907); **34**, 170, 590 (1911).
[2] Born and v. Kármán, Physik. Zeits. **13**, 297 (1912).
[3] Debye, Ann. d. Physik **39**, 789 (1912).
[4] Blackman, Proc. Roy. Soc. London **A148**, 365, 384 (1935); **A149**, 117, 126 (1935).
[5] Latimer and Greensfelder, J. Am. Chem. Soc. **50**, 2202 (1928).

were of similar accuracy except at the lowest temperatures where the heat capacity of the diamonds was only about one-tenth of the heat capacity of the empty calorimeter. The error in the results may be as large as 5 percent at the lowest temperatures but rapidly diminishes to about 0.2 percent at 150°K. At the highest temperatures the errors become somewhat larger due to the rapid heat exchange by radiation. The results are listed in Table I and are presented graphically in Fig. 1, together with those of other investigators.[6]

As can be seen from Fig. 1, the results of various investigations are in reasonably good agreement with the possible exception of the data of Nernst below 100°K. That these values may be in error seems not improbable when one considers that Nernst's results at even lower temperatures show a smaller heat capacity for the filled calorimeter than for the empty.

The entropy of diamond was calculated by a graphical integration of $C_p$ *vs.* log $T$, together with an extrapolation to the absolute zero based on the $T^3$ law. The results are summarized in Table II.

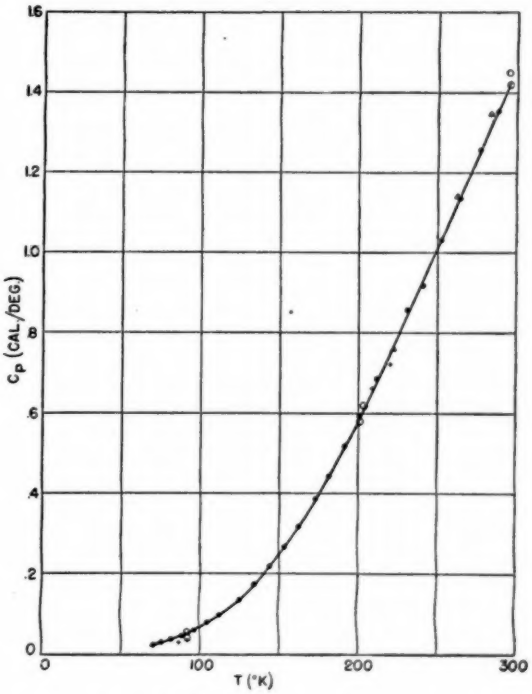


FIG. 1. The molal heat capacity of diamond in cal. per degree per mole. Solid circles, this research; crosses, Nernst; triangles, Weber; open circles, Robertson, Fox and Martin.

## DISCUSSION

Columns three and four of Table I give the values of $(C_p/T^3)$ and $\theta_D$ (Debye) respectively for the various temperatures. The heat capacity of diamond is found to be proportional to the third power of the temperature up to about 100°K, after which it rises faster than $T^3$ for about 75°. This increase of the heat capacity, faster even than $T^3$, is of course unexplainable by the Debye theory but is quite possible in view of Blackman's considerations of lattices. Similarly the values of $\theta_D$ are constant at about 1910 up to 100°K, then decrease gradually to about 1820 at 200°K, after which they appear again to rise slightly. This variation of about 5 percent is, of course, not very great but is entirely outside the experimental error.

TABLE II. *The molal entropy of diamond.*

| | | |
|---|---|---|
| 0 – 70.8°K | $T^3$ extrapolation | 0.0077 cal./deg. |
| 70.8–298.1° | Graphical from data | 0.5776 |
| | Entropy at 298.1°K = 0.585 ± .005 | |

Some rough calculations made by the writer indicate that this variation of $\theta_D$ is entirely reasonable. These calculations followed the general methods of Blackman[4] but were specifically set up for the diamond lattice. The only forces considered were central forces between adjacent atoms and forces tending to keep the bond angles those of a tetrahedron. The ratio between the two force constants was estimated from the normal vibration frequencies of propane. The results of this calculation deviate from the experimental values by about the same amount as the Debye theory, but the deviations are in the *opposite direction*. The true distribution of vibration frequencies is thus somewhere between that given by the rough lattice calculations and that of the Debye "continuum." It is now apparent that there is nothing anomalous about the specific heat of diamond, and that the assumption[7]

[6] Nernst, Ann. d. Physik **36**, 395 (1911); Weber, Phil. Mag. **49**, 161 (1875); Robertson, Fox and Martin, Proc. Roy. Soc. London **A157**, 579 (1936).

[7] Simon, Sitzber. preuss. Akad. Wiss., Physik. Math. Klasse **33**, 477 (1926).

of "thermal quantum jumps" is quite unnecessary.

In conclusion it may be said that there is agreement between experimental and theoretical specific heats of crystals, within the uncertainty in the latter. This uncertainty is, nevertheless, quite large, and it is hoped that in the near future the experimental data presented above can be compared with a more precise theory.

The writer wishes to thank Professor W. M. Latimer for his assistance in obtaining the sample of diamonds and for his interest and advice throughout the investigation.

---

FEBRUARY, 1938 JOURNAL OF CHEMICAL PHYSICS VOLUME 6

# Order and Disorder in Binary Solid Solutions*

JOHN G. KIRKWOOD
*University of Chicago, Chicago, Illinois and*
*Cornell University, Ithaca, New York*

(Received November 12, 1937)

A theory of order and disorder in solid solutions, based upon a direct evaluation of the crystalline partition function, is described. As in the theory of Bethe, the fluctuation in energy within states of a fixed degree of order, is taken into account. The method promises to be of use in the study of other cooperative phenomena.

## I

IT has been found that the atoms of certain solid solutions, although distributed at random among the lattice sites of the crystal at high temperatures, tend to arrange themselves into an ordered structure or superlattice at low temperatures. Moreover, there exists a critical temperature, analogous to the Curie temperature in ferromagnetism, below which the ordering process first begins to set in. Experimental evidence for the existence of order in such alloys as Cu-Au and Cu-Zn is provided by x-ray analysis of their crystal structure, and by the observation of discontinuities in certain of their physical constants or in their derivatives, which occur at the critical temperature.

Bragg and Williams[1] have treated the problem of order and disorder from the theoretical standpoint. Their theory accounts for the existence of a critical temperature and provides an approximate description of the influence of order on the thermodynamic functions of binary solid solutions. In the development of the theory they assume that the energy of the crystal is determined by its degree of long range order. It was pointed out by Bethe[2] that a given degree of order includes many crystalline configurations of different energy. Bethe developed a more elaborate theory in which the fluctuations in energy were taken into account. His theory, later extensively applied by Peierls,[3] yields results which are more nearly in accord with experiment than does the theory of Bragg and Williams.

We shall describe here an alternative theory of order and disorder, essentially equivalent to Bethe's in its degree of approximation, but somewhat less unwieldy in form. It is based upon a straightforward evaluation of the partition function of the crystal by the methods of statistical mechanics. The method of calculation bears a certain resemblance to that of the Heisenberg theory of ferromagnetism. However, the convergence difficulties, encountered by the ferromagnetism theory at low temperatures, do not arise, at least for solid solutions of rational composition. We believe that the theory may prove useful not only in the study of order and disorder in solids, but also in the treatment of cooperative phenomena in general.

## II

We consider a binary solid solution containing equal numbers, $N$, of atoms of the components

* The outlines of the present theory were sketched by the author at the Symposium on the Structure of Metallic Phases, held by the department of physics of Cornell University, July 1, 1937.

[1] Bragg and Williams, Proc. Roy. Soc. London **A145**, 699 (1934); **151**, 540 (1935); **152**, 231 (1935).

[2] Bethe, Proc. Roy. Soc. London **A150**, 552 (1935).

[3] Peierls, Proc. Roy. Soc. London **A154**, 207 (1936).

We suppose that the crystal is built up of two interpenetrating simple lattices, $a$ and $b$, as for example, a body-centered cubic structure. Each lattice point of $a$ has $z$ nearest neighbor sites on lattice $b$, and each point of $b$ has an equal number of nearest neighbor sites on $a$. In enumerating the microscopic states of the crystal we must consider the possible distributions of the $N$ atoms of type 1 and the $N$ atoms of type 2 among the sites of the two lattices, $a$ and $b$. We shall refer to each such distribution as a configuration of the crystal. We shall make the assumption that the partition function associated with lattice vibrations is the same for all configurations of the crystal. With this simplification the partition function may be expressed as the product of two factors, one arising from configuration and the other from lattice vibrations. Correspondingly, the thermodynamic functions split up into a configurational term and a lattice vibrational term. The latter may be calculated in the usual manner by the methods of Debye and of Born and Kármán.[4] We shall be interested here only in the configurational contributions.

The various configurations of the crystal may be partially characterized by a parameter, $s$, called the long range order, which is defined as follows.

$$s=(N_1^{(a)}-N_1^{(b)})/N, \tag{1}$$

where $N_1^{(a)}$ is the number of atoms of type 1 situated on lattice $a$, and $N_1^{(b)}$ the number on lattice $b$. We remark that $N_1^{(a)}$ is equal to $N_2^{(b)}$, the number of atoms of type 2 on lattice $b$, and that $N_1^{(b)}$ is equal to $N_2^{(a)}$, the number of type 2 on $a$. Further, since $N_1^{(a)}+N_1^{(b)}=N$, we may write

$$\begin{aligned} N_1^{(a)}&=N_2^{(b)}=N(1+s)/2,\\ N_1^{(b)}&=N_2^{(a)}=N(1-s)/2. \end{aligned} \tag{2}$$

We notice that when $s$ has the values, $\pm 1$, the crystal is in a completely ordered state with all atoms of type 1 on one of the lattices and all atoms of type 2 on the other lattice. On the other hand, when $s$ is zero, each type of atom is randomly distributed between the two lattices.

In the theory of Bragg and Williams the energy of the crystal was assumed to be determined by the long range order, $s$. As was pointed out by Bethe, this assumption is equivalent to ignoring the influence of configurational fluctuations on the value of the partition function. If the interaction of pairs of atoms which are not nearest neighbors can be neglected, the energy may be expressed as a linear function of a parameter, $p$, which is a measure of the local order of the crystal.

$$\begin{aligned} E&=E_0-2N\alpha kT(1-p),\\ \alpha&=zV_0/2kT,\\ V_0&=(V_{11}+V_{22})/2-V_{12}, \end{aligned} \tag{3}$$

where $V_{11}$, $V_{22}$, and $V_{12}$ are the mutual energies of the indicated types of nearest neighbor pair, and $p$ is given by,

$$p=(2/Nz)\sum_{a=1}^{N}\nu_a n_a, \tag{4}$$

where $\nu_a$ is the number of atoms of type 1 occupying lattice point $a$, either zero or unity, and $n_a$ is the number of sites of lattice $b$, neighboring site $a$, which are occupied by atoms of type 1, a number ranging from zero to $z$. The parameter, $p$, may be alternatively expressed in the form,

$$p=(1/Nz)\sum_{a,\,b}{}^{(n)}\nu_a\nu_b, \tag{5}$$

where $\nu_b$ is the number of atoms of type 1 occupying site $b$, and the sum extends over all pairs of $a$ and $b$ sites which are neighbors. The constant, $E_0$, is the energy of the two pure crystals, 1 and 2, before mixing, provided there is no change in the lattice parameters on mixing. We remark that Bethe's local order parameter, $\sigma$, is equal to $1-2p$. It is immaterial whether we work with the variable $\sigma$ or $p$. The parameter, $\sigma$, has the intuitive advantage of vanishing when the average environment of any lattice point is randomly distributed between atoms of the two types. Specification of a pair of values, $(s, p)$ does not of course completely characterize the configuration of the crystal. We shall designate by $\omega(s, p)$ the number of different configurations corresponding to the pair of values of the order parameters $(s, p)$.

By statistical mechanics, the free energy, $F$, of the crystal is related to the partition function, $f(\beta)$, in the following manner.

$$F=-(1/\beta)\log f(\beta), \tag{6}$$

[4] See R. H. Fowler, *Statistical Mechanics*, Chap. IV (Cambridge University Press, 1936).

where $\beta$ is equal to $1/kT$. We shall find it convenient to calculate the configurational partition function for a fixed value of the long range order, $s$, and then to minimize the free energy with respect to $s$. The configurational partition function for a fixed $s$ may be written as follows.

$$f(\beta, s)=\sum_{p=0}^{1-s}\omega(s, p)e^{-2N\alpha(p-1)}, \tag{7}$$

where the sum extends from 0 to $1-s$, the maximum value of $p$. The total number of configurations included by a fixed $s$ for all values of $p$ is readily seen to be the product of the number of ways the $N$ sites of lattice $a$ may be distributed among $N_1^{(a)}$ atoms of type 1 and $N_2^{(a)}$ atoms of type 2, by the number of ways the $N$ sites of lattice $b$ may be distributed among $N_1^{(b)}$ atoms 1 and $N_2^{(b)}$ atoms 2. We distribute the sites among the atoms rather than the atoms among the sites in order to avoid distinguishing between configurations which differ only by the interchange of atoms of the same type. We may therefore write,

$$\sum_{p=0}^{1-s}\omega(s, p)=\left[\frac{N!}{N_1^{(a)}!N_2^{(a)}!}\right]\left[\frac{N!}{N_1^{(b)}!N_2^{(b)}!}\right]. \tag{8}$$

It is convenient to define a distribution function, $\varphi(p)$, which is normalized to unity.

$$\sum_{p=0}^{1-s}\varphi(p)=1;$$

$$\varphi(p)=\frac{N_1^{(a)}!N_2^{(a)}!N_1^{(b)}!N_2^{(b)}!}{N!^2}\omega(s, p). \tag{9}$$

Making use of Eqs. (2) and (9), we may write (7) in the following form.

$$e^{-2N\alpha}f(\beta, s)=\left[\frac{N!}{[N(1+s)/2]![N(1-s)/2]!}\right]^2 \times\sum_{p=0}^{1-s}e^{-2N\alpha p}\varphi(p). \tag{10}$$

The sum in (10) may be expressed in terms of the semi-invariants of Thiele,[5] which are conveniently used to characterize a distribution function by its moments. The semi-invariants are defined as follows,

$$\exp\left[\sum_{n=1}^{\infty}(\lambda_n/n!)x^n\right]=\sum_{n=0}^{\infty}(M_n/n!)x^n,$$

$$M_n=\sum_{p=0}^{1-s}p^n\varphi(p). \tag{11}$$

By logarithmic differentiation the $\lambda_n$ may be shown to satisfy the following set of linear equations, in which the moments $M_n$ of the distribution function appear as coefficients.

$$\sum_{m=1}^{n}\binom{n-1}{m-1}\lambda_m M_{n-m}=M_n;\quad n=1, 2, \cdots. \tag{12}$$

Solution of these equations for the first three $\lambda_n$ yields,

$$\begin{aligned}\lambda_1&=M_1,\\ \lambda_2&=M_2-M_1^2,\\ \lambda_3&=M_3-3M_1M_2+2M_1^3.\end{aligned} \tag{13}$$

By expansion in series and comparison with Eq. (11), it is readily verified that the sum in (10) may be expressed in the form,

$$\sum_{p=0}^{1-s}e^{-2N\alpha p}\varphi(p)=\exp\left[\sum_{n=1}^{\infty}((-2N\alpha)^n/n!)\lambda_n\right]. \tag{14}$$

Using Eqs. (6), (10), and (14), and approximating the factorials of large numbers by Stirling's formula, we obtain the following expression for the configurational free energy of the crystal,

$$\begin{aligned}-F(s)/kT=N[&2\log 2-(1+s)\log(1+s)\\ &-(1-s)\log(1-s)]+\sum_{n=1}^{\infty}((-2N\alpha)^n/n!)\lambda_n\\ &+2N\alpha.\end{aligned} \tag{15}$$

The equilibrium value of the long range order corresponds to a minimum in the free energy, $F(s)$, and is to be determined by the condition:

$$\partial F(s)/\partial s=0. \tag{16}$$

Before proceeding to the calculation of the moments of the distribution function, we remark the retention of only the term involving $\lambda_1$ amounts to assuming $\varphi(p)$ to have the form of a delta function, $\delta(p-\lambda_1)$. This leads to the Bragg and Williams approximation. Retention of the first two terms, involving $\lambda_1$ and $\lambda_2$ is equivalent to assuming that $(p-\lambda_1)/\lambda_2^{\frac{1}{2}}$ has a continuous

[5] See A. Fisher, *Mathematical Theory of Probability*, Vol. I, second edition (Macmillan, 1922).

range of values between $-\infty$ and $+\infty$, and that $\varphi(p)$ is Gaussian in form.

$$\varphi(p)=(1/(\pi\lambda_2)^{\frac{1}{2}})e^{-(p-\lambda_1)^2/2\lambda_2}. \quad (17)$$

Since we shall find by calculation that $1/\lambda_2^{\frac{1}{2}}$ is of the order, $N^{\frac{1}{2}}$, the error involved in assuming the infinite interval for $(p-\lambda_1)/\lambda_2^{\frac{1}{2}}$ is of negligible order. The Gaussian form for $\varphi(p)$proves itself to be a rather good approximation, and, as we shall show, leads to results in substantial agreement with those obtained by the more complicated method of Bethe.

For the calculation of the moments of the distribution function we make use of the following relations.

$$\sum_{a=1}^{N}\nu_a=N_1^{(a)};\quad \sum_{b=1}^{N}\nu_b=N_1^{(b)};\quad \sum_{a=1}^{N}n_a=zN_1^{(b)}. \quad (18)$$

A calculation, the details of which are given in the appendix, leads to the result,

$$\begin{aligned}\lambda_1&=(1-s^2)/2,\\ \lambda_2&=(1-s^2)^2/4Nz,\\ \lambda_3&=s^2(1-s^2)^2/2N^2z^2.\end{aligned} \quad (19)$$

In the expressions for the thermodynamic functions of the crystal we shall retain only the terms in $\lambda_1$ and $\lambda_2$. The reader may ascertain with a little calculation that the term in $\lambda_3$ makes only very small contributions. We obtain for the free energy,

$$\begin{aligned}-F(s)/NkT=&\,2\log 2-(1+s)\log(1+s)\\ &-(1-s)\log(1-s)+\alpha(1+s^2)\\ &+\alpha^2(1-s^2)^2/2z+\cdots.\end{aligned} \quad (20)$$

The equilibrium value of the long range order, $s$, corresponding to a minimum in the free energy at constant temperature, $(\partial F/\partial s)_\alpha=0$, is found to satisfy the following trancendental equation,

$$\begin{aligned}s&=\tanh\gamma s\\ \gamma&=\alpha-\alpha^2(1-s^2)/z.\end{aligned} \quad (21)$$

The Bragg and Williams approximation is obtained if the terms in $\alpha/z$ are neglected in Eqs. (20) and (21). We note first of all that Eq. (21) has solutions other than $s=0$, only if $\alpha$ is positive, which we shall see corresponds to a negative energy of mixing. If $\alpha$ is negative there will be a critical solution temperature and separation into two phases. However, treatment of this case requires the discussion of solutions of arbitrary composition. When $\alpha$ is positive, Eq. (21) has a solution other than $s=0$, only below a certain critical temperature, $T_c$, corresponding to a value of $\alpha_c$, satisfying the following equation.

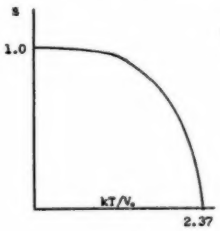


FIG. 1.

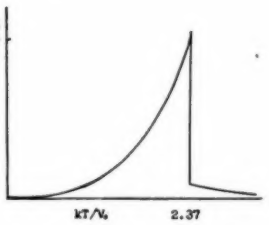


FIG. 2.

$$\begin{aligned}&\alpha_c^2-z\alpha_c+z=0,\\ &\alpha_c=(z/2)[1-(1-4/z)^{\frac{1}{2}}],\\ &T_c=zV_0/2k\alpha_c.\end{aligned} \quad (22)$$

For the simple cubic structure, $z=6$, we find $T_c$ equal to 2.366 $V_0/k$, a value which differs only slightly from that of Bethe, 2.372 $V_0/k$. In Fig. 1, $s$ is plotted as a function of $kT/V_0$ for $z=6$. The average or thermodynamic energy, $\bar{E}=\partial(F/T)/\partial(1/T)$ and the entropy, $S=(\bar{E}-F)/T$, may be written in the form,

$$\begin{aligned}\bar{E}/NkT&=-\alpha(1+s^2)-\alpha^2(1-s^2)^2/z,\\ S/Nk&=2\log 2-(1+s)\log(1+s)\\ &\quad-(1-s)\log(1-s)-\alpha^2(1-s^2)^2/2z.\end{aligned} \quad (23)$$

The configurational heat capacity per atom, equal to $(1/2N)(\partial\bar{E}/\partial T)_v$ has the form,

$$\frac{c_v}{k}=\alpha^2\left[\frac{s^2[1-(2\alpha/z)(1-s^2)]^2}{\cosh^2\gamma s-\gamma-2\alpha^2s^2/z}+\frac{1}{2z}(1-s^2)^2\right]. \quad (24)$$

The configurational heat capacity is plotted as a function of $kT/V_0$ for $z=6$ in Fig. 2. It undergoes a jump at the critical temperature, $c_v/k$ having the value, 4.23 just below $T_c$, and the value 0.134 just above. The peak of $c_v/k$ is thus higher than Bethe's value, 2.14. The inclusion of the term in $\lambda_3$ would lower our value somewhat. The configurational heat capacity does not vanish above the critical temperature, because a certain average degree of local order persists even after the long range order vanishes, and its gradual destruction with increasing temperature contributes to the heat capacity. Since $s$ is a continuous function of the temperature, $\bar{E}$ is also a

continuous function of the temperature. Thus there is no heat of transition, and we have to do with a phase change of the second kind at the critical temperature. In contrast with a phase change of the first kind, there is only one equilibrium phase present at the transition temperature.

It is possible to apply the present theory to face-centered crystals with an atomic ratio, 1 : 3, a case considered by Bragg and Williams and by Peierls, with satisfactory results. The theory may be readily generalized for a crystal constructed of two interpenetrating lattices with any composition instead of the special 1 : 1 atomic ratio considered here. However, when $\alpha$ is positive, certain difficulties are encountered at very low temperatures. They arise from the failure of the series in $\lambda_n$ to converge rapidly. If the Gaussian approximation, involving only $\lambda_1$ and $\lambda_2$ is used, the transcendental equation for $s$ fails to have a nonvanishing solution near the absolute zero, except for the atomic ratio, 1 : 1, treated in the present article. This is analogous to the difficulty encountered in the Heisenberg theory of ferromagnetism, according to which the spontaneous magnetization would vanish at low temperatures. In our case the difficulty may be removed for a region of composition in the neighborhood of the atomic ratio, 1 : 1, by including the term in $\lambda_3$. Outside this region, terms in the $\lambda_n$ of still higher order are required. The extension of the theory to solid solutions of arbitrary compositions will be discussed in detail at a later time. Its limiting form for vanishing long range order promises to be of use in the theory of liquid solutions.

In conclusion, the writer wishes to express his thanks to Professor H. Bethe of Cornell University and to Professor F. Bitter of the Massachusetts Institute of Technology for many helpful discussions.

## Appendix

### Calculation of the moments

From Eq. (4) we observe that the moment, $M_m$, of the distribution function, $\varphi(p)$, may be written in the form,

$$M_m=(2/Nz)^m\langle(\sum_{a=1}^{N}\nu_a n_a)^m\rangle_{Av}, \tag{25}$$

where $_{Av}$ denotes an *a priori* average over all crystalline configurations. Since the *a priori* distributions on the two different lattices $a$ and $b$ are independent, an average of the form, $\langle(f_1(\nu_1\cdots\nu_N)f_2(n_1\cdots n_N)\rangle_{Av}$, may be written as $\langle f_1(\nu_1\cdots\nu_N)\rangle_{Av}\langle f_2(n_1\cdots n_N)\rangle_{Av}$, inasmuch as the $\nu_a$ refer to atoms on lattice $a$ and the $n_a$ to atoms on lattice $b$. To avoid confusion, we remark that this is true since we are concerned only with *a priori* averages. It would not be true of statistical-mechanical averages, where the Boltzmann factors, of course, introduce correlation between the distributions on the separate lattices. We shall employ the following sum relations in the subsequent calculations,

$$\sum_{a=1}^{N}\nu_a{}^m=rN;\quad \sum_{a=1}^{N}n_a=zwN,$$

$$r=N_1{}^{(a)}/N=(1+s)/2,\quad w=N_1{}^{(b)}/N=(1-s)/2. \tag{26}$$

These relations follow from Eqs. (2) and (18), and from the fact that $\nu_a{}^m=\nu_a$ when $m$ is not zero, since the $\nu_a$ are either zero or unity.

Since the average values of $\langle\nu_a{}^m\rangle_{Av}$ and $\langle n_a\rangle_{Av}$ are of course the same for all lattice sites, we obtain by averaging both sides of Eqs. (26),

$$\langle\nu^m\rangle_{Av}=r,\quad \langle n\rangle_{Av}=zw, \tag{27}$$

where $\langle\nu^m\rangle_{Av}$ and $\langle n\rangle_{Av}$ refer to any lattice site. Similarly, $\langle\nu_a\nu_{a'}\rangle_{Av}$ has the same value, $\langle\nu\nu'\rangle_{Av}$, for any pair of sites (not true of $\langle n_a n_{a'}\rangle_{Av}$). Thus we have from Eq. (26),

$$r^2N^2=\langle(\sum_{a=1}^{N}\nu_a)^2\rangle_{Av}=N\langle\nu\rangle_{Av}+N(N-1)\langle\nu\nu'\rangle_{Av}, \tag{28}$$

$$\langle\nu\nu'\rangle_{Av}=\frac{r(rN-1)}{N-1}=r^2-\frac{rw}{N}+O\left(\frac{1}{N^2}\right).$$

We shall also require the value of $\langle n^m\rangle_{Av}$, the average of $n_a{}^m$ for any site $a$. The number of ways in which a set of $z$ sites of lattice $b$ may be assigned to $n$ atoms of type 1 and the remaining $N-z$ sites to $N_1{}^{(b)}-n$ atoms of type 1 and $N_2{}^{(b)}-z+n$ atoms of type 2 is evidently equal to $\binom{N}{N_1{}^{(b)}-n}\binom{z}{n}$, while the total number of configurations of lattice $b$ is $\binom{N}{N_1{}^{(b)}}$. Thus we may write for the normalized probability, $P_z(n)$, of configurations in which the $z$ neighbors of a site of lattice $a$ include $n$ atoms of type 1,

$$P_z(n)=\binom{N}{N_1{}^{(b)}}^{-1}\binom{N}{N_1{}^{(b)}-n}\binom{z}{n}$$
$$=\binom{z}{n}r^{z-n}w^n+O\left(\frac{1}{N}\right). \tag{29}$$

The average value $\langle n^m\rangle_{Av}$ may then be expressed as follows,

$$\langle n^m\rangle_{Av}=\sum_{n=0}^{z}n^mP_z(n)$$
$$=[(\partial^m/\partial x^m)(we^x+r)^z]_{x=0}. \tag{30}$$

The relations stated above suffice for the calculation of $M_1$ and $M_2$. For the higher moments others of a similar nature would be needed.

We may calculate $M_1$ at once, using Eqs. (25) and (27), and obtain the result,

$$M_1=\frac{2}{NZ}\sum_{a=1}^{N}\langle\nu_a\rangle_{Av}\langle n_a\rangle_{Av}=\frac{2\langle\nu\rangle_{Av}\langle n\rangle_{Av}}{z}=(1-s^2)/2. \quad (31)$$

For the moment, $M_2$, we may write, by virtue of the independence of averages on the separate lattices,

$$M_2=\frac{4}{N^2Z^2}[N(\langle\nu^2\rangle_{Av}-\langle\nu\nu'\rangle_{Av})\langle n^2\rangle_{Av}+\langle\nu\nu'\rangle_{Av}\langle(\sum_{a=1}^{N}n_a)^2\rangle_{Av}]. \quad (32)$$

From Eq. (30) we find that $n$ is equal to $z^2r^2+zrw$. This result together with Eqs. (27), (28), and (32) yields,

$$M_2=M_1^2+(4/NZ)r^2w^2+O(1/N^2) \quad (33)$$
$$=M_1^2+(1-s^2)^2/4Nz+O(1/N^2).$$

The third moment, $M_3$, may be obtained in a similar fashion, although the calculation is somewhat more tedious. When substituted in Eqs. (13), the moments so obtained yield Eqs. (19).

The moments may be calculated in another way if $p$ is expressed in the form of Eq. (5). A method analogous to that employed by Van Vleck[6] in his treatment of the Heisenberg theory of ferromagnetism may then be employed. This method, though somewhat simpler to state, involves about the same amount of computational labor as the one described above.

[6] J. H. Van Vleck, *Electric and Magnetic Susceptibilities*, Vol. 12, § 78 (Clarendon Press, Oxford, 1932).

FEBRUARY, 1938 JOURNAL OF CHEMICAL PHYSICS VOLUME 6

# The Electron Diffraction Investigation of the Molecular Structures of Ketene and Thiophosphoryl Chloride[1]

J. Y. Beach[2] and D. P. Stevenson
*Frick Chemical Laboratory, Princeton University, Princeton, N. J.*

(Received November 23, 1937)

The structures of the gas molecules of ketene and thiophosphoryl chloride have been determined by the diffraction of 57 kilovolt electrons. The interpretation of the photographs was made by the visual method in conjunction with the radial distribution method. The results for ketene are: carbon-carbon distance 1.35±0.02A., and carbon-oxygen distance 1.17±0.02A. The carbon-hydrogen distance was assumed to be 1.07A. The results for thiophosphoryl chloride are: phosphorus-chlorine distance 2.01±0.02A, phosphorus-sulphur distance 1.94±0.03A, and the Cl−P−Cl angle 107±3°. The results are discussed in terms of covalent radii and the resonance of molecules among several electronic structures.

THE apparatus used in this investigation is closely similar to the one described by Brockway[3] and used by Pauling, Brockway *et al.* for determining the structures of gas molecules. The electrons were accelerated by a potential of roughly 57 kilovolts. The wave-length of the electrons was 0.0515A. This wave-length was found accurately by taking transmission pictures of gold foil, the structure of which is known. In interpreting the photographs we have used the visual method and the radial distribution method. Both of these procedures have been described by Pauling and Brockway.[4] Bauer[5] has developed an analytic method, based on visual measurement, for interpreting photographs. The method consists of differentiating the theoretical scattering curve and setting the derivative equal to zero at each of the measured maxima and minima. The interatomic distances are then obtained by solving a set of simultaneous equations.

The formula used in the visual method for calculating the intensity of the scattered elec-

[1] Presented before the American Chemical Society, Rochester, September, 1937.

[2] National Research Fellow in chemistry.

[3] For a general review of the experimental procedure and a summary of electron diffraction results see L. O. Brockway, Rev. Mod. Phys. **8**, 231 (1936).

[4] The visual method of interpretation, originally developed by R. Wierl, Ann. d. Physik **8**, 531 (1931) and **13**, 453 (1932), has been tested and discussed by L. Pauling and L. O. Brockway, J. Chem. Phys. **2**, 867 (1934). The radial distribution method was developed, tested and applied to a large number of compounds by L. Pauling and L. O. Brockway, J. Am. Chem. Soc. **57**, 2684 (1935).

[5] S. H. Bauer, J. Chem. Phys. **4**, 406 (1936).

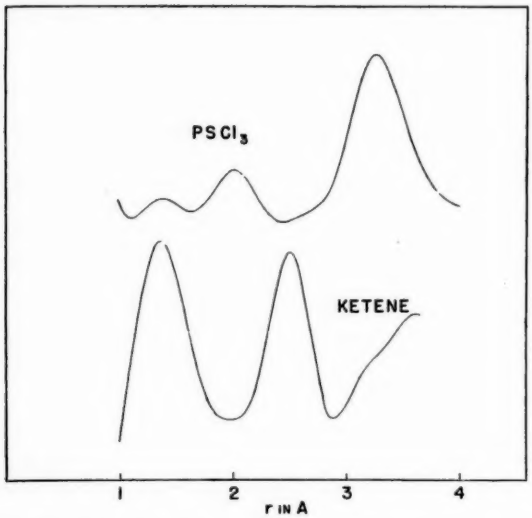


FIG. 1. Radial distribution curves for ketene and thiophosphoryl chloride.

trons as a function of the scattering angle is

$$I=\Sigma_i\Sigma_j Z_i Z_j(\sin sr_{ij}/sr_{ij}), \qquad (1)$$

where $Z_i$ and $Z_j$ are the atomic numbers of the $i$th and $j$th atoms, $r_{ij}$ is the distance between the $i$th and $j$th atoms, and $s$ is

$$(4\pi \sin \Theta/2)/\lambda.$$

Both summations are taken over every atom in the molecule. $\lambda$ is the wave-length of the electrons and $\Theta$ is the angle through which the electrons are scattered. To evaluate Eq. (1) a model for the molecule is assumed, the $r_{ij}$'s are calculated from the geometry of the model and put into the formula. The intensity, in arbitrary units, is calculated and plotted in terms of $s$. This procedure is repeated for a number of molecular models, the number depending on the complexity of the molecule and on the pre-existent ideas regarding its structure. The shape of the intensity curve, that is the relative heights and spacings of the maxima and minima, is dependent only on the shape assumed for the molecule and not on the assumed size. The size assumed affects only a scale factor which is automatically corrected when the ring diameters of the maxima and minima on the films are compared quantitatively with the positions of the maxima and minima on the theoretical curve. In general many of the models for the molecule can be eliminated from a qualitative comparison of the photographs with the calculated curves. By qualitative comparison is meant a comparison of the relative heights and spacings of maxima and minima between photographs and curves without resorting to measurement of the photographs. The final results are obtained from a quantitative comparison of the photographs with the qualitatively acceptible calculated curves.

The radial distribution method consists of inverting the intensity formula. Instead of calculating the intensity of scattering as a function of the structure, the density of atoms in the molecule is calculated in terms of the observed scattering. This distribution function is obtained directly from measurements on the photographs, no assumption of molecular model being involved. These functions for ketene and thiophosphoryl chloride are shown in Fig. 1.

## KETENE

The ketene used in this investigation was prepared by Dr. W. E. Vaughn, Dr. Elgene A. Smith and Mr. M. A. Dolliver of Harvard University. From the time the preparation was made until the photographs were taken it was kept in an evacuated vessel at the temperature of solid carbon dioxide and alcohol. During all of the time the ketene was kept cold it remained a clear colorless liquid. Just before it was discarded the dimer began to deposit as a colorless solid on the bottom of the container. The polymer remained colorless until allowed to warm up to room temperature in the presence of air, at which time it turned brown. The presence of some of the dimer at the time the last pictures were taken could not influence the photographs because of the low vapor pressure of the dimer at low temperatures. The boiling point of the dimer is about 128°C. The pictures were taken with the sample at −75°C.

Visual inspection of the photographs shows five maxima. In addition, on some of the photographs, there is a spurious maximum close to the intense central image. When this occurs it is easy to detect as its position is well inside the possible position of diffraction maxima and is quite variable. The first maximum is very intense. The second appears to be a small

maximum or shelf on the outside of the first. The third maximum is sharp. The fourth is less sharp and is close to the third. The fifth is sharp but is very faint and is farther from the fourth than the fourth is from the third. The visually estimated intensities along with the measured values of $s$ are given in the third and fourth columns on Table I.

TABLE I. *Ketene.*

| MAX. | MIN. | $I$ | $s_{obs}$ | $s_{calc}$ | C−CA |
|---|---|---|---|---|---|
| 1 | | 20 | 5.657 | 5.93 | 1.442 |
| 2 (shelf) | | 7 | 8.193 | | |
| | 3 | | 9.578 | 8.96 | 1.291 |
| 3 | | 10 | 10.53 | 10.43 | 1.367 |
| | 4 | | 12.04 | 11.42 | 1.308 |
| 4 | | 4 | 12.91 | 12.30 | 1.315 |
| 5 | | 1 | 15.45 | 15.35 | 1.371 |
| | | | | Ave. | 1.349 |

Results: C−C 1.35±0.02A
C−O 1.17±0.02A
C−H 1.07A (assumed) H−C−H angle 109° 28′ (assumed)

The five term radial distribution function is shown in Fig. 1. It possesses maxima at 1.37A and at 2.51A. The first peak represents the carbon-carbon and the short carbon-oxygen distances unresolved. The second peak gives the long carbon-oxygen distance.

To calculate the theoretical scattering curves it is necessary to evaluate Eq. (1) for several models. No attempt is made to determine the position of the hydrogen atoms. In calculating intensities it was assumed that the carbon-hydrogen distance is 1.07A, which is intermediate between the carbon-hydrogen distance in acetylene (1.06A) and the carbon-hydrogen distance in methane (1.09A). The angle between the carbon-hydrogen bonds was assumed to be tetrahedral. The scattering from the hydrogen atoms is such a small part of the total scattering that the assumptions regarding their position cannot affect the results obtained. There are two distances to be determined: the carbon-carbon distance and the carbon-oxygen distance. The scattering curve, except for a scale factor, is determined entirely by the shape of the molecule, in this case the ratio of the carbon-carbon distance to the carbon-oxygen distance. Accordingly several intensity curves are calculated for ratios of the carbon-carbon distance to the carbon-oxygen distance varying from 1.38/1.13 to 1.38/1.36. These curves are shown in Fig. 2. From a qualitative comparison of the curves with photographs it is found that the most satisfactory curve is the one for which the ratio is 1.38/1.20. The fifth maximum, counting the shelf on the first maximum as a separate maximum, on the 1.38/1.16 curve is too low, while the second maximum (or shelf) on the 1.38/1.24 curve is too low. Quantitative comparison of the photographs with the 1.38/1.20 curve is given in Table I. The final values are: for the carbon-carbon distance, 1.35±0.02A and for the carbon-oxygen distance 1.17±0.02A.

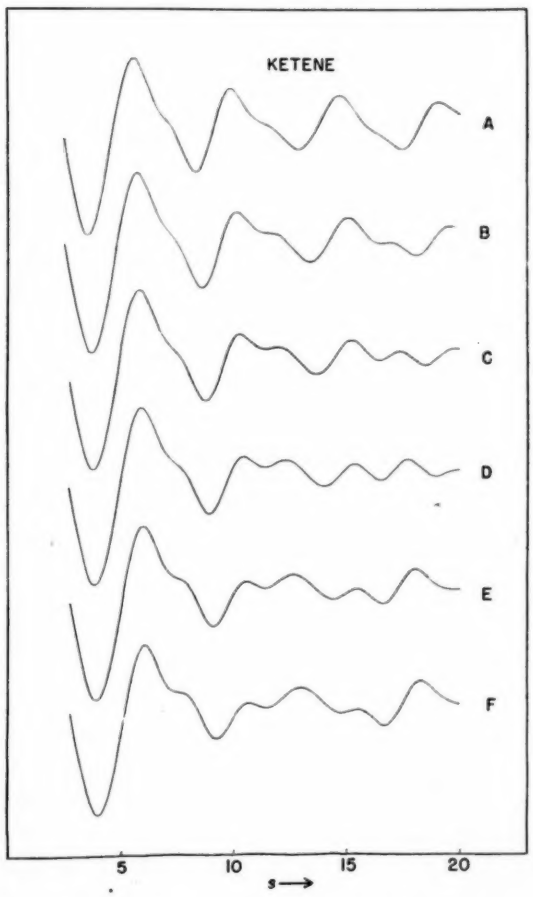


FIG. 2. Theoretical intensity curves for ketene. The ratios of the carbon-carbon distance to the carbon-oxygen distance are: curve *A*, 138/132; curve *B*, 138/1.28; curve *C*, 1.38/1.24; curve *D*, 1.38/1.20; curve *E*, 1.38/1.16; curve *F*, 1.38/1.13.

### Thiophosphoryl Chloride

The thiophosphoryl chloride used in this investigation was an Eastman product purified by repeated fractional distillation in vacuo by Mr. F. B. Jennings. The photographs, taken with the sample at 50°C, show six rings. The first three are sharp, the second being the most intense. The fourth maximum is less intense than the third and is close to the third. The fifth is intense and sharp. The sixth is weak and is difficult to measure. The visually estimated intensities are given in Table II.

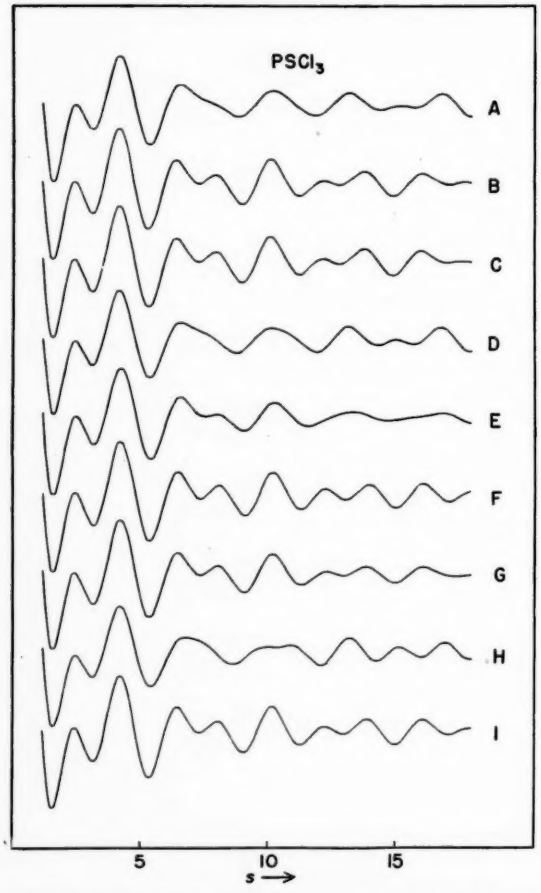


FIG. 3. Theoretical intensity curves for thiophosphoryl chloride. Denoting the Cl−P−Cl angle by $\alpha$ and the ratio of the phosphorus-chlorine distance to the phosphorus-sulfur distance by $\rho$, the curves are for the following models: curve *A*, $\alpha=100°$ and $\rho=2.02/1.93$; curve *B*, $\alpha=105°$ and $\rho=2.02/1.93$; curve *C*, $\alpha=109°\ 28'$ and $\rho=2.02/1.93$; curve *D*, $\alpha=115°$ and $\rho=202/1.93$; curve *E*, $\alpha=100°$ and $\rho=2.02/1.85$; curve *F*, $\alpha=105°$ and $\rho=2.02/1.85$; curve *G*, $\alpha=109°\ 28'$ and $\rho=2.02/1.85$; curve *H*, $\alpha=115°$ and $\rho=202/1.85$; curve *I*, $\alpha=105°$ and $\rho=2.02/1.89$.

TABLE II. *Thiophosphoryl chloride.*

| MAX. | MIN. | *I* | $s_{obs}$ | $s_{calc}$ | P−Cl*A* |
|---|---|---|---|---|---|
| | 1 | | 1.691 | 1.59 | 1.899 |
| 1 | | 14 | 2.442 | 2.43 | 2.010 |
| | 2 | | 3.388 | 3.17 | 1.890 |
| 2 | | 25 | 4.238 | 4.18 | 1.992 |
| | 3 | | 5.449 | 5.33 | 1.976 |
| 3 | | 17 | 6.290 | 6.42 | 2.062 |
| | 4 | | 7.326 | 7.29 | 2.010 |
| 4 | | 7 | 8.036 | 7.98 | 2.006 |
| | 5 | | 9.132 | 8.98 | 1.986 |
| 5 | | 12 | 10.12 | 10.11 | 2.017 |
| | 6 | | 11.83 | | |
| 6 | | 2 | 13.19 | | |
| | | | | Ave. | 2.007 |

(1st max. and 1st and 2nd min. omitted)

Results: P−Cl $2.01\pm0.02$A
P−S $1.94\pm0.03$A
Cl−P−Cl angle $107°\pm3°$.

The five term radial distribution function is shown in Fig. 1. In calculating the radial distribution function the sixth maximum was omitted because of the difficulty in measuring it. The peak at 2.02A represents the phosphorus-chlorine and the phosphorus-sulfur distances unresolved. The peak at 3.27A represents the chlorine-chlorine and the sulfur-chlorine distances unresolved. The small peak at 1.38A is without significance.

In calculating theoretical intensity curves the only models considered were those having the symmetry $C_{3v}$. Having made this assumption—that the three chlorine atoms are equivalent—two parameters are necessary to specify the shape of the molecule. These parameters are taken to be the angle between two phosphorus-chlorine bonds, $\alpha$, and the ratio of the phosphorus-chlorine distance to the phosphorus-sulfur distance, $\rho$. Theoretical intensity curves were calculated for models having values of $\alpha$ ranging from 100° to 115° and $\rho$ ranging from 2.02/2.10 to 2.02/1.77. Sixteen curves were calculated. Nine of these are shown in Fig. 3. The top four show the effect of changing $\alpha$ from 100° to 115° keeping $\rho$ constant at 2.02/1.93. The next four show the effect of varying $\alpha$ with $\rho$ constant at 2.02/1.85. Curve I is one of the qualitatively acceptable curves. From the curves shown and other curves it is seen that values of $\alpha$ of 100° or less and 115° or greater are unsatisfactory because of the prominence of the fourth maximum

on the photographs. The 105° models are unsatisfactory when $\rho$ is greater than 2.02/2.02 for the same reason. The tetrahedral models are unsatisfactory when $\rho$ is greater than 2.02/2.10 because the average of the chlorine-chlorine and sulfur-chlorine distances is greater than the 3.27A required by the radial distribution curve. The tetrahedral and 105° curves are unsatisfactory when $\rho$ is less than 2.02/1.77 because the average of the chlorine-chlorine and sulfur-chlorine distances is less than the 3.27A required by the radial distribution curve. All the curves within these limits are qualitatively acceptable. As the most probably correct model we have chosen the one for which $\alpha$ is 107° and $\rho$ is 2.02/1.95. This curve is not shown in Fig. 3 but is practically identical in appearance with curve I. Quantitative comparison of the photographs with the 107°, 2.02/1.95 curve is shown in Table II. The final values are: for the phosphorus-chlorine distance 2.01±0.02A, for the phosphorus-sulfur distance 1.94±0.03A and for the Cl−P−Cl angle 107°±3°.

## Discussion

The distances found in ketene are not those that would be expected if ketene has the electronic structure

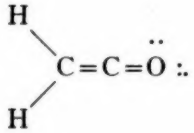

The expected distances for this structure, from Pauling and Brockway's[6] recent revision of the covalent radius table of Pauling and Huggins,[7] are 1.34A for the carbon-carbon bond and 1.24A for the carbon-oxygen bond. It is seen that the carbon-carbon distance is greater and the carbon-oxygen distance is less than expected. This is immediately accounted for by resonance of the molecule between the above structure and the structure

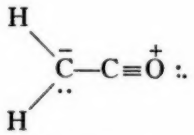

It is possible to estimate the extent of the resonance by using the relation between bond type and bond distance given by Pauling, Brockway and Beach[8] and revised by Pauling and Brockway.[6] This procedure leads to the result that the structure is three quarters double-bond, double-bond and one quarter single-bond, triple-bond.

The P−Cl distance in $PSCl_3$ (2.01A) is about the same as the P−Cl distance in $PCl_3$ (2.00A) obtained by Brockway and Wall[9] and Pauling and Brockway.[10] The sum of the single covalent radii for phosphorus and chlorine is 2.09A. The shortening of the bond is ascribed by Brockway and Jenkins[11] to partial double bond character due to resonance of the molecule to structures of the type

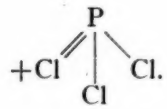

Structures of the type

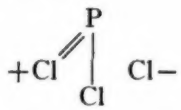

may also contribute, as suggested by Gregg, Hampson, Jenkins, Jones and Sutton.[12] The possibility that the shortening is due to ionic character of the bonds was eliminated by Brockway and Jenkins by a study of several metal methyls. In these compounds, the atoms of which have greater relative electronegativities than phosphorus and chlorine, the distances are normal. Here, double bond formation cannot occur because of the necessity for observing the octet rule on carbon. It was therefore concluded that the shortening in $PCl_3$ (and other similar compounds) is due to partial double bond character and not to ionic character. In our discussion of $PSCl_3$ we shall accordingly assume that ionic character cannot affect the length of the bonds.

[6] L. Pauling and L. O. Brockway, J. Am. Chem. Soc. **59**, 1223 (1937).

[7] L. Pauling and M. L. Huggins, Zeits. f. Krist. **A87**, 205 (1934).

[8] L. Pauling, L. O. Brockway and J. Y. Beach, J. Am. Chem. Soc. **56**, 2706 (1935).

[9] L. Brockway, and F. T. Wall, J. Am. Chem. Soc. **56**, 2373 (1934).

[10] L. Pauling and L. O. Brockway, J. Am. Chem. Soc. **57**, 2684 (1935).

[11] L. O. Brockway and H. O. Jenkins, J. Am. Chem. Soc. **58**, 2036 (1936).

[12] A. H. Gregg, G. C. Hampson, G. I. Jenkins, P. F. L. Jones and L. E. Sutton, Trans. Faraday Soc. **33**, 852 (1937).

To a first approximation the structure of $PSCl_3$ is

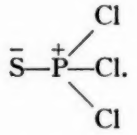

(I)

The contributing structures which will tend to shorten the P−Cl bond are of the following type:

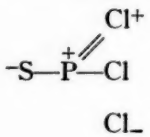

(II)

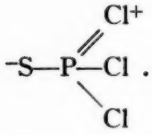

(III)

Structure (II) will not contribute, however, because of the adjacent charge rule.[12a] Probably a more important (lower energy) structure, tending to shorten the P−S bond, is

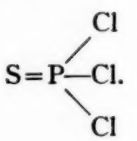

(IV)

The structure

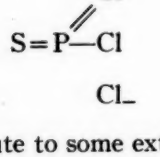

(V)

may also contribute to some extent.

In these last three structures the octet rule is not observed for phosphorus. However, violation of the octet rule in atoms in other than the first row of the periodic table is permissible; for example $PF_5$, etc. The structures that shorten the P−Cl bond in $PSCl_3$ are less numerous and probably less important than the ones for $PCl_3$. It is therefore surprising that the P−Cl distance in $PSCl_3$ is not substantially greater than in $PCl_3$. The answer to this question is found in the discussion of the short N−O distance in nitrate ion given by Elliott.[13] The short distance is attributed to the resultant positive charge on the nitrogen atom. In the most important structure for $PSCl_3$ there is a resultant charge of plus one on the phosphorus atom which by analogy with the small radius for nitrogen in nitrate ion leads one to expect a short P−Cl distance in $PSCl_3$. This effect apparently just offsets the lack of suitable contributing double P−Cl bond structures mentioned above, leaving the P−Cl distance in $PSCl_3$ the same as in $PCl_3$.

If the electronic structure of $PSCl_3$ is simply structure (I) written above, the P−S bond being a single bond between oppositely charged atoms; the considerations of Elliott would predict that the bond distance is the single bond distance. The increase in the single bond radius of the negative sulfur atom would be offset by the decrease in the radius of the positive phosphorus atom. That this prediction leads to correct results is seen in the case of a large number of tetrahedral crystals. In these crystals the most important electronic structure, responsible for the tetrahedral orientation of bonds, is one in which bonded atoms have equal and opposite formal charges. In these cases the interatomic distances are observed to be just the interatomic distances for normal valence bonds for which there are no resultant charges on bonded atoms. The observed P−S distance in $PSCl_3$ is 1.94A, nearly the same as the double bond distance for this bond (1.95A). Having ruled out any effect of ionic character and formal charges on the length of this bond, the shortening below the single bond distance must be due to a considerable (about one-half) contribution of structure (III). It is difficult to see how the P−S distance can be less than the double bond distance. This effect is also observed in the case of sulfate and phosphate crystals. In the cases investigated the distance between the central atom of the anion and the oxygen atom is found to be roughly the double bond distance.

We wish to express our appreciation to Professor C. P. Smyth for suggesting that the apparatus be built and for his continued interest in the research.

[12a] L. Pauling and L. O. Brockway, J. Am. Chem. Soc. **59**, 13 (1937).

[13] Norman Elliott, J. Am. Chem. Soc. **59**, 1380 (1937).

# On the Adiabatic Demagnetization of Caesium Titanium Alum

J. H. Van Vleck
*Harvard University,* Cambridge, Massachusetts*
(Received December 13, 1937)

Titanium salts should behave more simply than most materials under magnetic cooling, since the ground level of the paramagnetic ion is here inherently doubly degenerate and so unaffected by crystalline fields. De Haas and Wiersma show that as long as the magnetic moment remains constant during adiabatic demagnetization, the temperature is a linear function of a field strength, a most valuable fact since it permits the establishment of a thermodynamic temperature scale. The present paper computes when deviation of the moment from constancy should commence because of the perturbing effect of second-order terms (the first nonvanishing order) in the dipole-dipole coupling energy. The calculated moment does not remain constant to as low field strengths as reported experimentally. The discrepancy cannot be ascribed to a counterbalancing effect of exchange coupling but may be due to the neglect of third and higher order dipole terms. Because of these large dipole perturbations, the status of the experimental temperature scale in titanium alum becomes rather uncertain. The present stage of the theory may be tested more accurately by using much lower initial fields than in the existing Leiden experiments.

## Introduction

THE production of very low temperatures by the method of adiabatic demagnetization is a subject already classic. However, the great difficulty is the determination of the thermodynamic temperature. This is usually estimated by assuming Curie's law. The latter, however, cannot be accurate, as it would require zero specific heat in the absence of an applied magnetic field, and so allows no heat capacity to prevent the substance from cooling clear down to the absolute zero!

A neat way out of the difficulty, though of somewhat limited applicability, has been proposed by de Haas and Wiersma,[1] who suggest and try the following procedure. As the field is diminished adiabatically from the high value which produced the initial decrease of entropy at helium temperatures, there is a certain interval during which the moment retains the same value as at the original temperature and field strength. It is purely a matter of thermodynamics to show, as they do, that as long as this is the case, the thermodynamic temperature is a linear function of field strength, so that

$$T=aH+b. \tag{1}$$

The constants $a$ and $b$ in general involve the intensity of magnetization $M$ as a parameter, and can be determined by finding two known pairs of values of $H$, $T$ in the helium range which yield the same given value of $M$. Once $a$ and $b$ have been fixed, (1) can be used to yield $T$ in terms of $H$ at low temperatures where $T$ cannot be measured by ordinary means. If the field is reduced below a certain critical point, however, the moment deviates from its original value, in general decreasing. Below this point, Eq. (1) ceases to apply.

To illustrate, de Haas and Wiersma find that caesium titanium alum has the same moment when demagnetized to 105 gauss as under the initial conditions of 1.20°K and 24,075 gauss. They thus conclude that the temperature associated with 105 gauss is $1.20\times(105/24{,}075)$ or 0.0052°K. Below 105 gauss the moment decreases rapidly, and at 1.05 gauss has less than 1/50 of its initial value.

In selecting a material to be measured, it is important to find one which comes as close as possible to an "ideal" behavior, i.e., to zero specific heat when $H=0$. When $H\neq 0$ there is a finite, socalled magnetic specific heat even for an ideal substance. It is when $H$ is reduced so far that the heat capacity due to other causes begins to be comparable with this magnetic specific heat that (1) starts to lose validity.

De Haas and Wiersma's choice of caesium titanium alum was an exceedingly wise one. In the first place it is magnetically dilute. Secondly, it has a spin of $S=\frac{1}{2}$ and susceptibility measurements show that it is in a nondegenerate orbital state, at least below hydrogen temperatures or

* At present, visiting professor, Princeton University.
[1] W. J. de Haas and E. C. Wiersma, Physica **3**, 491 (1936).

so. On superposing both spin and orbit, one thus sees that the $Ti^{+++}$ ion is in a doubly degenerate state. Now a fundamental theorem of Kramers[2] tells us that no crystalline field whatsoever is capable of separating the levels in a doubly degenerate state with an odd number of electrons. Hence there is no Stark splitting to create deviations from Curie's law. The only apparent cause of deviation from an ideal behavior is therefore the magnetic dipole-dipole coupling, and possibly a little exchange interaction, between the widely spaced paramagnetic ions. In the present paper we calculate when these effects should begin to enter.

The computation of the influence of the dipole-dipole coupling involves no unknown constants, as the lattice spacing is known. We find that when terms of the second order (the first non-vanishing order) in this coupling are included, the moment at 105 gauss should be about 18 percent lower than the value associated with the initial field 24,000 gauss. Experimentally, the moments are the same at these two field strengths to within the experimental error, estimated by de Haas and Wiersma as five percent. Conceivably the discrepancy arises from the neglect of third and higher order dipole terms, but in any event the existence of such large dipole perturbations casts serious doubts on the propriety of using (1), without further investigation, to determine temperatures as low as 0.0052°K, the value yielded by (1) at 105 gauss. Quite irrespective of quantitative estimates, simple qualitative considerations show that one should expect ideal conditions probably not to persist down to 0.0052°K. Namely, the dipole-dipole perturbations should be appreciable when the temperature ceases to be high compared with the characteristic temperature[3] $\tau=3N\beta^2/k$ associated with dipole-dipole interaction. Here $N$ is the number of atoms/cc, and $\beta$ is the Bohr magneton $he/4\pi mc$. Now caesium titanium alum has $\tau=0.0038$°K and so one would *a priori* expect the dipole corrections to be appreciable at temperatures considerably above 0.0052°K.

## Mathematical Details

It is necessary to have formulas for the entropy and magnetic moment of an ensemble of coupled atoms. Practically all the requisite calculations have been made in a previous paper by the writer,[4] henceforth called l.c., in which the partition function was computed in Eqs. (21), (23), (27) to the second approximation in the coupling parameters, with arbitrarily large external applied fields. As the demagnetization measurements are made on a powder, the anisotropic term proportional to $\Omega_4$ in Eq. (21) of l.c. can be omitted, since it averages to zero. The effective field $H$ is now to be taken as identical with the applied field, rather than as primarily an inner Weiss field such as was used in the previous application of the calculations to ferromagnetism.

Once the partition function $Z$ has thus been determined, it is a matter of simple differentiation to find the entropy $S$ and magnetic moment $M$, *viz.*,

$$S=-\partial F/\partial T, \quad M=-\partial F/\partial H, \quad F=-kT\log Z.$$

Thus it is found that

$$S/kN=\log 2+\log\cosh(g\beta H/2kT)-(g\beta H/2kT)\tanh(g\beta H/2kT) +(\tau/T)f_S'+(\tau/T)^2(f_S''+F_S+G_S), \quad (2)$$

$$M/g\beta N=B_1+(\tau/T)f_M'+(\tau/T)^2(f_M''+F_M+G_M), \quad (3)$$

where $B_1, f_S\cdots G_M$ are functions only of the argument $x=g\beta H/2kT$ and are defined as follows:

[2] H. A. Kramers, Proc. Amsterdam Acad. **33**, 959 (1930).
[3] Cf. J. H. Van Vleck, J. Chem. Phys. **5**, 320 (1937); M. H. Hebb and E. M. Purcell, ibid., p. 338.
[4] J. H. Van Vleck, Phys. Rev. **52**, 1189 (1937). The following errata may be noted in this paper. In the first line of Eq. (21), read 4 in place of $y$. In the third relation of Eq. (27), $Q$ should read $Q_0$ and in the formula for $z'v$ on the first line of p. 1193, $N$ should read $N^{-1}$. Because we are usually dealing with measuring fields large enough to produce saturation, it is necessary to use the calculations of this article rather than the treatment appropriate to weak final fields given in reference 3. Hebb and Purcell (reference 3) have already discussed calorimetric measurements on the field-free specific heat of caesium titanium alum.

$B_1=\frac{1}{2}\tanh(g\beta H/2kT)$, $f_S'=\frac{1}{3}(\Phi-vz')(-g\beta H/kT)(1-4B_1^2)B_1$,
$9f_S''=(\Phi-vz')^2[8B_1^4-2B_1^2-(g\beta H/kT)(1-4B_1^2)(B_1-8B_1^3)]$,
$9F_S=-(z''v^2)[4B_1^4+\frac{3}{2}-4B_1^2+(g\beta H/kT)(4B_1^3-2B_1)(1-4B_1^2)]$,
$9G_S=-Q_0[\frac{1}{4}-B_1^2][3-16B_1^2+\frac{1}{5}(g\beta H/kT)(10B_1-32B_1^3)]$.
$f_M'=\frac{1}{3}(\Phi-z'v)(1-4B_1^2)B_1$, $9f_M''=(\Phi-z'v)^2(1-4B_1^2)(B_1-8B_1^3)$, $9F_M=z''v^2(1-4B_1^2)(4B_1^3-2B_1)$,
$9G_M=Q_0[\frac{1}{5}(kT/g\beta H)^2(24B_1^3-12B_1)]+Q_0(4-16B_1^2)[-\frac{1}{8}B_1+\frac{2}{5}B_1^3+\frac{3}{5}(kT/g\beta H)(\frac{1}{4}-\frac{3}{2}B_1^2)]$.

Here
$$g=2,\quad Q_0=14.4,\quad z=12,\quad \tau=3N\beta^2/k=0.0038°\mathrm{K}, \tag{4}$$

$$\beta=he/4\pi mc,\quad v=-2\sqrt{2}J/g^2\beta^2N,\quad z'=6\sqrt{2},\quad z''=r^{-6}N^{-2}z=6, \tag{5}$$

where $J$ is the usual exchange integral between adjacent atoms. Exchange coupling between the atoms is included as a possibility in order to examine whether this can sometimes fortuitously neutralize the perturbing effect of the dipole-dipole forces. In (4), (5) we give the values of various expressions appropriate to caesium titanium alum, i.e., a face-centered lattice with practically all the magnetism arising from spin. For increased generality in connection with possible future uses, we mention that (2), (3) still apply to other types of cubic lattices provided the definitions (4), (5) of the symbols are replaced by more general ones given in l.c.[3, 4]

The $G$ terms in (2) and (3) are the perturbations due to dipole-dipole interaction, which enter only in the second order ($\tau^2$). The terms $f'$ and $f''+F$ give respectively the first and second-order effect of the exchange ($v$) as well as demagnetization ($\Phi$) corrections. The significance of the demagnetization plus Lorentz factor $\Phi$ is explained in l.c. and earlier papers,[3, 4] and need not be elaborated here. Anyway, $\Phi$ vanishes for a sphere, the shape of the test body used in the Leiden experiments.

If we omit all the correction terms of the various types $f$, $F$, $G$, Eqs. (2), (3) reduce to

$$M/g\beta N=\tfrac{1}{2}\tanh x, \tag{6}$$

$$S/kN=\log 2+\log\cosh x-x\tanh x, \tag{7}$$

where $x=g\beta H/2kT$. Then (1) clearly applies with $b=0$. We show below in fine print that (6), (7) are also valid when the $f$ terms are retained, provided the argument is taken as

$$x=g\beta[H+(\Phi-z'v)M]/2kT. \tag{8}$$

In this case (1) is still correct, with now

$$b/a=(\Phi-z'v)M. \tag{9}$$

One way to prove (6), (7), (8) is to expand (6), (7) as Taylor's series in $(\Phi-z'v)$, using successively more accurate values of $M$ on the right side. Then (2), (3) and (6), (7) agree to terms in $(\Phi-v'z)^2$ inclusive, provided $F=G=0$. Another way of establishing the result is to utilize the well-known fact that the demagnetization plus Lorentz or $\Phi$ corrections are equivalent to use of an effective local field $H+\Phi M$ in the formula for the moment. If the $v$ as well as $\Phi$ terms are included, it is clear that the effective field is $H+(\Phi-z'v)M$, since $\Phi$ and $-z'v$ enter in a simple additive fashion in $f$. One immediately suspects that as far as the entropy is concerned, the $f$ terms are also incorporated by employing a field of this character. An analytical proof that (6, 8) imply (7), except for an easily determined function of $T$ alone, is furnished by the thermodynamic relation

$$(\partial M/\partial T)_H=(\partial S/\partial H)_T$$

inasmuch as by (6) and (8)

$$(\partial x/\partial T)_H/(\partial x/\partial H)_T=-(\partial H/\partial T)_x$$
$$=-(\partial H/\partial T)_M=-2kx/g\beta.$$

In view of the foregoing, we can drop the $f$ terms in (2), (3), as they do not affect the constancy of the moment, or the validity of (1). We henceforth interpret $H$ not as the applied field $H_a$ but rather as the local field $H_a+(\Phi-z'v)M$. Our proof of the equivalence of the $f$ terms to this effective field ceases to apply with complete rigor when the $F$ and $G$ corrections are superposed, but the resulting error is unimportant for our purposes, as to a sufficient approximation the various contributions may be considered additive.

Since $S$ is constant under adiabatic conditions, Eq. (2) determines $T$ as a function of $H$. The procedure is to solve (2) for $T$ in terms of $H$, or more simply, for $T$ in terms of $x=g\beta H/2kT$. The resulting pairs of values of $T$, $H$ (or $T$, $x$) are then substituted in (3) and in this way the course of the moment during the adiabatic demagnetization can be calculated.

In computing the influence of the $F$ and $G$ terms, it is often possible to make one of two simplifications appropriate to different limiting conditions.

TABLE I.

| | | | | |
|---|---|---|---|---|
| $H_0=24{,}000$ gauss, $T_0=1.17°$K ($x_0=1.37$) | | | | |
| $H$ | 430 | 250 | 105 | 1.05 |
| $(T/\tau)_{calc}$ | 5.50 | 3.15 | 1.20 | 1.61 |
| $(x_0/x)_{calc}$ | .993 | .972 | .89 | 120 |
| $(M/M_0)_{calc}$ | .99 | .97 | .82 | .001 |
| $(M/M_0)_{obs}$ | | | 1.00 | .016 |
| $H_0=12{,}000$ gauss, $T_0=1.25°$ ($x_0=0.64$) | | | | |
| $H$ | 200 | 115 | 64 | 5.23 |
| $(T/\tau)_{calc}$ | 5.7 | 3.60 | 2.81 | 2.68 |
| $(x_0/x)_{calc}$ | 1.04 | 1.14 | 1.60 | 18.8 |
| $(M/M_0)_{calc}$ | .93 | .79 | .51 | .040 |
| $(M/M_0)_{obs}$ | | | | .050 |
| $H_0=7000$ gauss, $T_0=1.17°$ ($x_0=0.4$) | | | | |
| $H$ | 145 | 95 | 50 | 5.23 |
| $(T/\tau)_{calc}$ | 7.20 | 5.5 | 4.4 | 4.02 |
| $(x_0/x)_{calc}$ | 1.14 | 1.33 | 2.00 | 17.4 |
| $(M/M_0)_{calc}$ | .85 | .71 | .47 | .052 |

Down to fields of about 200 gauss one can usually with fair approximation assume that the argument of the $F$ and $G$ terms, which are perturbations, has the same value $x_0$ as at the initial helium temperature, while the leading terms in $S$ and $M$, i.e. those of structure (6), (7) can be developed as a Taylor's series in $x-x_0$, and only terms through the first order retained. On remembering that $S$ remains constant, it is thus found that

$$x-x_0=[(F_S{}^0+G_S{}^0)/x_0(1-4B_1{}^{02})](\tau/T_0)^2(H_0/H)^2 \quad (10)$$

$$M-M^0=g\beta N[\tfrac{1}{2}(F_S{}^0+G_S{}^0)x_0{}^{-1}+F_M{}^0+G_M{}^0](\tau/T_0)^2(H_0/H)^2 \quad (11)$$

where $H_0$, $T$ are the original helium values of $H$, $T$, and where $F^0$ means that $F$ is to be evaluated with the argument $x=x_0$, etc.

At very low field strengths ($x$ about 0.3 or lower), a Taylor's development in ascending powers of $H$ can be made, *viz.*

$$S/kN=\log 2-\tfrac{1}{2}x^2-\tfrac{1}{3}(\tau/2T)^2(Q_0+z''v^2)+\tfrac{1}{3}(\tau/2T)^2x^2(3Q_0+4z''v^2), \quad (12)$$

$$M/g\beta N=\tfrac{1}{2}x-(\tau/3T)^2x(\tfrac{3}{4}Q_0+z''v^2)-\tfrac{1}{6}x^3+x^3Q_0(97\tau^2/675T^2)+x^3z''v^2(11\tau^2/54T^2). \quad (13)$$

Eq. (12) is readily solved for $(\tau/T)^2$, and the result substituted in (13).

## EFFECT OF EXCHANGE COUPLING

The $F$ terms in (10), (11), or $v$ terms in (12), (13) represent the part of the exchange corrections which cannot be incorporated by the artifice of a local field proportional to $M$. The expression $\frac{1}{2}F_S{}^0x^{-1}+F_M{}^0$ in (11) is easily seen to be always negative. Hence exchange effects tend to decrease the moment in adiabatic demagnetization, regardless of the sign of $v$, i.e., of the exchange integral. The constancy of the moment reported in the Leiden experiments thus cannot be attributed to a fortuitous cancelation of exchange and dipole-dipole corrections, a hypothesis which looked hopeful before the requisite mathematical calculations were made. We henceforth omit the exchange terms $F$, as they do not help matters any. It is, of course, reasonable that the exchange integrals should be very small, because of the large spacing between paramagnetic ions. The most important effect of any possible exchange coupling is to give rise to a nonvanishing constant $b$ in (1), since $b$ is by (9) of the first rather than second order in the exchange integral. Such a $b$ term, of course, does not affect the constancy of the moment, but might prove troublesome in calculating the temperature, inasmuch as $b$ is negligible compared with $aH$ at helium temperatures and so cannot be detected by calibration experiments made there, but may be appreciable at the final low temperatures, where $aH$ is small.

## EFFECT OF DIPOLE-DIPOLE COUPLING

Table I illustrates the effect of dipole-dipole forces as calculated from Eqs. (2), (3). The values of $H$ given in the table often are not round numbers because $x_0/x_0$ rather than $H$ is conveniently taken as the independent variable in numerical solution. The ratio $x_0/x=(TH_0/HT_0)$ is the same as the factor by which the temperature deviates from the "ideal" value (1).

One immediately speculates as to the cause of the rather glaring discrepancy between the observed and calculated behavior in the case of the demagnetization from 24,000 gauss. As far as we can see, the only possibility is to attribute it to neglect of third and higher powers of the dipole-dipole interaction, as Eqs. (2), (3) are correct only to the second power, the first nonvanishing order, in this coupling. The effect of each successive power is dimensionally of the order $\tau/T$ compared with the preceding. Unfortunately the ratio $\tau/T$ is not very small, and so the convergence of the development of the partition function is notoriously bad in problems of the present sort.

The ultimate inadequacy of Eqs. (2), (3) can be seen in a particularly striking way by the graphical construction given in Fig. 1. If we plot $S$ against $1/H^2$, Eq. (2) shows that the curves of constant $x=g\beta H/2kT$ are straight lines of slope $\tau(k^2x^2/\beta^2)G_S$, as illustrated in Fig. 1. Since the entropy retains a constant value $S_0$ during demagnetization, the magnitude of $x$ and hence of the temperature appropriate to the final field strength $H$ can be found by locating the point in Fig. 1 whose ordinate is $S_0$ and whose abscissa is $1/H^2$, and then finding which line passes through this point. Fig. 1 shows that often the lines cross, so that many points yield more than one value of $x$. Such a situation is impossible, as it would require that the temperature be a two-valued function of the field strength, an absurdity. Also, if the curves crossed, to the right of the crossing we would have higher $S$ correlated with higher $x$, and hence $(\partial S/\partial T)_H<0$, i.e., a negative specific heat, something obviously impossible physically, and also impossible mathematically because of the exponential character of the partition function. Hence the lines of large $x$ which start with positive slope doubtless ultimately tend to curve downwards when the neglected higher powers of the dipole-dipole interaction are included, as we have indicated schematically by the dashed lines in Fig. 1, whose exact position is, of course, only conjectural. The lines corresponding to small $x$ are reliable further to the right than those of large $x$ because the former correspond to smaller values of $\tau/T$ for given $H$.

To the extreme left of Fig. 1, the effect of the neglected higher members is unimportant and the lines are reliable. Consequently Fig. 1 shows that for $x_0$ greater than about 0.9, the ratio of temperature to field strength actually decreases for a while during adiabatic demagnetization. (This is reflected by some values of $x_0/x$ being less than unity in the table for $x=1.37$.) In the vicinity of $x=.9$, there is a line of zero initial slope, and for this particular field strength, Eq. (1) is valid even when second order terms in the dipole-dipole interaction are included.

The table for $x=1.37$ shows actually a lower temperature for $H=105$ gauss than for $H=1.05$. This absurd situation is because $x$ has been determined from a rising line for $H=105$, the only choice available here (as $S_0/kN=0.22$), while a descending line has been employed for $H=1.05$. The values of $\tau/T$ are here so high that obviously no quantitative significance can be attached to our calculations with straight lines.

Of course the mere fact that Fig. 1, or general considerations, show that third and higher order dipole terms cannot really be neglected, by no means makes it clear that the neglected members will just cancel the included second-order effects, so that the moment has the same value at 105 and 24,000 gauss. Indeed, the substitution of the dashed curves for the solid lines in Fig. 1 raises the temperature, and so accentuates the falling off of the moment, unless there is a counterbalancing upward bending of the curves of constant $x$ in the $M-(1/H^2)$ plane. (According to (3) these curves are straight lines with downward slope for all $x$.) If there is an actual near equality of moments at these two field strengths, the question immediately arises as to whether the moment remains constant at intervening fields, or instead passes through a maximum somewhere between 105 and 24,000 gauss. It would obviously be desirable to have measurements at intermediate fields. Unfortunately such measurements are not available and do not appear very feasible with de Haas and Wiersma's apparatus since at low temperatures, a weak solenoid capable of producing only low "measuring fields" is employed, while the very large magnet used at helium temperatures is only fit for high fields. So the gap in data apparently cannot be closed. However, even a small increase in the measuring field above 105 gauss would be illuminating. If there is an intervening maximum, which we rather doubt, Eq. (1) obviously cannot be used to determine the thermodynamic temperature, since its derivation requires that the moment remain constant over an interval rather than be merely fortuitously equal at two field strengths. If, however, the high temperature

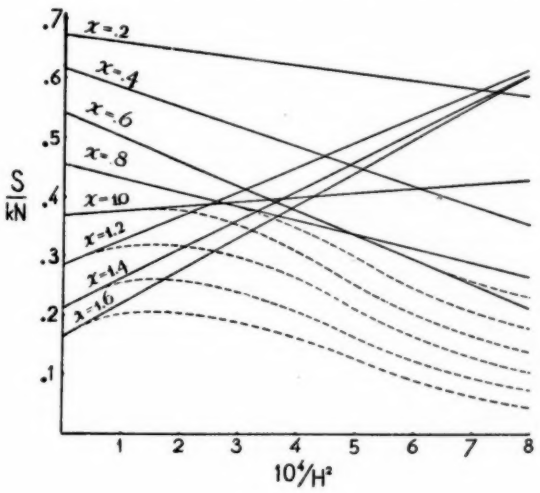


FIG. 1.

value of the moment is being approached asymptotically, (1) might be approximately correct. In this event, $M$ would needs be slightly lower at 105 than at 24,000 gauss, but the deviation might conceivably be so much lower

than our estimate of 18 percent as to escape detection. Two other causes besides the neglected higher order members which might reduce the apparent discrepancy are (a) a $g$ factor slightly less than 2, inasmuch as the second-order dipole perturbation is proportional to $g^4$, and (b) experimental errors in the relative calibrations of the magnets used at high and low temperatures. The error due to the latter cause might amount to 5 percent or so.

It is clear that additional theoretical and experimental work is much to be desired, because of the light it will shed on the mooted question of how far dipole-dipole interaction can be represented by an inner field of the Lorentz type. If the Lorentz hypothesis were strictly correct, then Eqs. (6), (7), (8) would always be fulfilled, and (1) would be valid at all temperatures. The latter is, of course, impossible, but the Lorentz assumption is to a certain extent the equivalent of the simplest form of the Heisenberg theory of magnetism, in which the constant of proportionality in the Weiss molecular field is independent of temperature, but which works much better than a second-order (so-called "Gaussian") perturbation calculation. All the same, it is impossible to have a power series in $\tau/T$ with nonvanishing coefficients always summing to zero, but this situation is what would be required if the perturbations of various orders are to neutralize each other so as to restore the accurate validity of (1).

It seemed worth while to publish the calculations in their present form, inclusive only of second order dipole effects, not merely because a third order computation would be quite long, but primarily because an experimental test of the second order corrections is possible by using much lower initial demagnetizing fields than 24,000 gauss. The lower this initial field $H_0$, the smaller the final value of $\tau/T$ and so by decreasing $H_0$ the ambiguity due to the neglected members becomes asymptotically small. Table I shows that the order of magnitude of the critical field strength $H_c$ at which appreciable deviations of $M/M_0$ from unity first appear is not greatly influenced by the size of the initial field, so that experiments with lower $H_0$ remain feasible. The advantage is that $H_c$ can be computed with increasing certainty, the smaller $H_0$. Unfortunately the only published measurement with $H_0=12{,}000$ gauss is for a very weak final field, 5.23 gauss. The discrepancy of about 25 percent between the observed and calculated value of $M$ at this field is far from excessive for a possible influence of higher order members, since $\tau/T$ is still not small enough to make the series converge at all adequately,[5] and, after all, a deviation of 25 percent is small compared with the total reduction in moment by a factor 20. It would be of interest if measurements were available with still smaller initial fields, say 2000 to 7000 gauss.

It may be noted that in his most interesting experiments on paramagnetic relaxation, Gorter[6] finds that in caesium titanium alum the absorption per titanic ion does not increase greatly on dilution with nonmagnetic ingredients. This he interprets as showing that some other factor than coupling between paramagnetic ions interferes with the free orientation of the spin. Because of Kramers' theorem on double degeneracy,[2] and because no adequate disturbing nuclear moments can be invoked, it is hard to see what this mysterious factor can be. If it really exists, it perhaps modifies the present calculations for extremely low temperatures, in some unknown way.

The writer is much indebted to Dr. C. J. Gorter for valuable discussion.

---

[5] That our neglected higher order terms are very important even in demagnetization from 12,000 gauss can be seen by integrating Hebb and Purcell's (reference 3) specific heat formula (13) so as to obtain an expression for the entropy. This formula is more special than our (2) in that it applies only to very weak fields, but it does include third and fourth as well as second order terms in the dipole interaction. The inclusion of these two extra orders makes the value of $(T/\tau)$ appropriate to zero field strength imaginary, an absurdity, rather than 2.68 as given in the table. The situation is reminiscent of that in the Heisenberg theory of ferromagnetism, where Opechowski shows that an imaginary Curie point is obtained if extra terms are included in place of stopping with the usual approximations (Physica **4**, 181 (1937)).

[6] Cf. C. J. Gorter and R. de L. Kronig, Physica **3**, 1018 (1936).

# Statistical Mechanics of Condensing Systems. III*

JOSEPH E. MAYER AND S. F. HARRISON
*Johns Hopkins University, Baltimore, Maryland*

(Received November 20, 1937)

A general development of the Gibbs phase integral for a system of chemically saturated molecules gives equations for the thermodynamic properties of the system. The equations predict the usual condensation phenomenon of the gas to form a condensed phase with a surface tension at temperatures below a characteristic temperature $T_m$. At $T_m$ the surface tension of the condensed phase is zero, and this phase undergoes a discontinuous change without heat of transition. Between $T_m$ and the true critical temperature $T_c$, there exists a finite volume interval for which $P$ and the Gibbs free energy $F$ is independent of the volume. Above $T_c$ the usual $P-V$ diagram predicted above the critical point is found, with no volume for which $(\partial P/\partial V)_T$ is zero.

## THE GENERAL METHOD

IN a preceding paper[1] one of the authors has shown that the method commonly used in statistical mechanics to obtain the second virial coefficient, if followed through more completely, leads to equations predicting the existence of a condensed phase. In this paper we propose to develop a more concise method of handling the equations, and to show that the equations also predict the existence of some unexpected phenomena at the critical point. The method is a development, without arbitrary physical or mathematical assumptions, of the equations for the thermodynamic properties in terms of several series of integrals. In the temperature pressure range for which the liquid is stable the integral playing the predominant role cannot be numerically evaluated.

The system with which we wish to work must be limited to have certain properties if the development is to be applicable.

Three of these limitations are absolutely essential. They are: first, that the masses of the particles making up the system are large enough so that the classical laws of mechanics are applicable at the temperatures and volumes we wish to investigate; second, that the mutual potential between particle pairs falls off with the fourth or higher power of the distance between the pairs; and third, that the total potential energy of the system is representable as the sum of the potentials between pairs of particles which depend only on the differences of the coordinates of the pairs. The last limitation is equivalent to restricting the system to one composed of chemically saturated molecules incapable of forming true valence bonds with each other. It does not mean, of course, that we neglect higher than two-body collisions: on the contrary, we specifically treat multiple interactions, but we regard these as being made up of the sum of the interactions between all conceivable pairs of molecules.

Certain other unessential limitations are imposed on the system, limitations which are not necessary for the applicability of the general method, and which could be eliminated one by one at the cost of more complicated equations and a more complicated terminology and notation. These limitations are: that the system consist of $N$ identical molecules; that $N$ is large enough so that terms of the order of $N^{-1}$ or smaller can be neglected compared to unity; and that the individual molecules have three translational degrees of freedom only. This latter limitation means that internal degrees of freedom are absent or neglected, and that the mutual potential of a pair of molecules depends on their distance apart only, and not on mutual orientation angles.

The problem is attacked by means of the normalized phase integral, which is $1/N!\,h^{3N}$ times the integral (over the $3N$ momenta and $3N$ coordinates of $N$ particles), of the exponent of minus the Hamiltonian divided by $kT$. The integration over the momentum space can be performed immediately if Cartesian coordinates are used. There remains the integration over the coordinate or configuration space. The integrand

* Contribution from the chemical laboratory of the Johns Hopkins University.

[1] Joseph E. Mayer, J. Chem. Phys. 5, 67 (1937).

is the exponent of the negative of the potential energy divided by $kT$. Since this potential energy is the sum of the potential energies of the $N(N-1)/2$ possible pairs, the integrand can be written as the product of this number of terms. As in the usual method of obtaining the second virial coefficient, a function of the distance $r_{ij}$ between molecules $i$ and $j$, the quantity $f(r_{ij})+1$ (which defines the function $f$), is substituted for each exponential. The product is then expanded. The steps are indicated by the following equations.

$$Q=\frac{1}{N!h^{3N}}\int\int\cdots\int e^{-H(p,\ q)/kT}dp_1\cdots dq_N$$

$$=\left(\frac{2\pi mkT}{h^2}\right)^{3N/2}\frac{Q_\tau}{N!}, \quad (1)$$

$$Q_\tau=\int\int\cdots\int e^{-V(q)/kT}d\tau_1\cdots d\tau_N$$

$$=\int\int\cdots\int\prod_{N\geq i>j\geq 1}e^{-v(r_{ij})/kT}d\tau_1\cdots d\tau_N$$

$$=\int\int\cdots\int\prod_{N\geq i>j\geq 1}[1+f(r_{ij})]d\tau_1\cdots d\tau_N \quad (2)$$

$$=\int\int\cdots\int[1+\sum_{i>j}f_{ij}+\sum f_{ij}f_{i'j'}+\cdots]$$

$$\times d\tau_1\cdots d\tau_N,$$

with $$d\tau_1=dx_idy_idz_i, \quad (3)$$

$$f_{ij}=f(r_{ij})=(e^{-v(r_{ij})/kT}-1). \quad (4)$$

A plot of $f(r)$ for $A/r^6$ law of attraction and $B/r^{12}$ repulsion potential at a temperature corresponding to the stable existence of a liquid is shown in Fig. 1. Since $f$ drops rapidly to zero as the value of its argument $r$ increases, the value of any term in the sum of Eq. (2) which involves a certain $f_{ij}$, is zero if the distance $r_{ij}$ between the two molecules $i$ and $j$ is large. This term contributes to the total phase integral only in that part of configuration space for which the two molecules $i$ and $j$ are close together. For this reason we shall refer to the two molecules $i$ and $j$ as being "bound" to each other in any term containing the function $f_{ij}$. If, in any particular term, a molecule $i$ is not bound to any other molecule (i.e., its index does not occur anywhere as a subscript in the product) we shall refer to it as a free molecule, or as being in a cluster consisting of one molecule. If, in a given term, the molecule $i$ is bound to $j$, and neither $i$ nor $j$ is bound to any other molecule, we shall say that $i$ and $j$ are in a cluster of two molecules. If $i$ is bound to $j$ and $j$ bound to $k$, whether or not $i$ is bound to $k$ we shall say $i$, $j$, $k$ form a cluster of three, etc. Or in general, if $l$ molecules are bound directly or indirectly to each other, but none of them is bound to any molecule not occurring in the group we shall say that they form a cluster of $l$ molecules in that particular term.

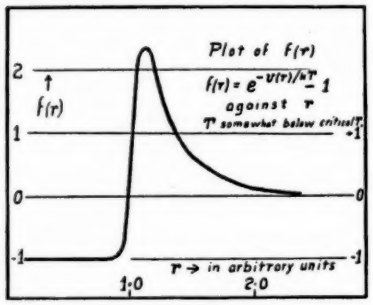


FIG. 1.

We now propose to collect together all terms characterized by having the same number, $m_1$, of clusters of one molecule (free molecules), $m_2$ clusters of two molecules, . . ., $m_l$ clusters of $l$ molecules each. This method of collecting terms is purely arbitrary and by no means the only logical method of procedure from this point; it appears, however, to be justified, *a posteriori*, by the simplicity with which important results can be deduced from the procedure. Other equally logical procedures have failed so far to lead to interpretable results.

The physical significance of this particular grouping of terms is the following. All terms characterized by the same set of numbers, $m_l$, of clusters of size $l$, have in common the property that they contribute to the total phase integral $Q$ only in that part of the configuration space where $m_2$ pairs of molecules are spatially close to their mates, . . ., $m_l$ clusters of $l$ molecules each are close to the other molecules of the clusters, etc., whereas the contribution to the integral is independent of the coordinates of the $m_1$ free molecules.

The quantity $b_l$, the integral over a cluster of size $l$, is defined by the following equation:

$$b_l=\frac{1}{Vl!}\int\int\cdots\int\sum_{l\geq i>j\geq 1}\prod f_{ij}d\tau_1\cdots d\tau_l \qquad (5)$$

(all products consistent with a single cluster).

The normalization factor $1/l!$ is merely for convenience. The integration is extended over the configuration volumes of all of the particles. The integrand is the sum of all possible products of the $f$'s which are consistent with the existence of a single cluster. For small values of $l$, and for volumes of macroscopic dimensions, $b_l$ is independent of the volume, due to the property of $f$ that $f(\infty)=0$. For values of $l$ of the order of the number of particles in the system, the volume below which $b_l$ becomes (significantly) volume dependent we shall later see is the volume of the condensed phase. It can be seen that in any term, the integration over the last particle, the $l$'th particle, in every cluster yields the volume, $V$, as a factor in the term, which is the reason we have defined $b_l$ with $V$ in the denominator. If $b_1$ is taken by definition to be unity this is also true of the $m_1$ clusters of single molecules.

It is then easily seen that the expression for $Q_\tau/N!$ becomes

$$\frac{Q_\tau}{N!}=\sum_{\substack{m_l\\ \Sigma lm_l=N}}\prod_l\frac{(Vb_l)^{m_l}}{m_l!}=\sum_{\substack{m_l\\ \Sigma lm_l=N}}\prod_l\frac{(Nvb_l)^{m_l}}{m_l!}, \qquad (6)$$

with $$v=\frac{V}{N}\ \text{(the volume per molecule)}. \qquad (7)$$

## The General Equations

The logarithm of the sum $Q_\tau/N!$ of Eq. (6) may be approximated with sufficient accuracy by the logarithm of the largest term,[1] giving Eq. (9). This method is only valid if all the $b_l$'s are positive. Professor Born has pointed out to the authors that the function $Q_\tau/N!$, which can be seen to be the coefficient of $Z^N$ in the expansion of the exponent $\sum vb_lZ^l$, can be expressed as a Cauchy integral and evaluated by means of the well-known method of steepest descents, leading also to Eq. (9). We believe that Professor Born will publish this proof shortly along with several other comments on the method of the present article. Another method of obtaining the asymptotic Eq. (9) is discussed in the appendix of this article.

If a function $Z(vb_1, vb_2, \cdots, vb_l, \cdots)$ is defined as the lowest positive real root of the equation ((A4) of the appendix),

$$G_1(vb_l)\equiv\sum_{l\geq 1}lvb_lZ^l=1, \qquad (8)$$

and the functions $G_j$ are defined as

$$G_j(vb_l)=\sum_{l\geq 1}l^jvb_lZ^l, \qquad (9)$$

so that $G_1=1$, then we find that, (Eq. (A57) of the appendix),

$$\frac{1}{N}\ln\frac{Q_\tau}{N!}=G_0(vb)-\ln Z, \qquad (10)$$

plus terms of order of magnitude $1/N$, as long as $Q_\tau$ is positive and real for all large values of $N$, a condition which it obviously always fulfills.

The Helmholtz free energy $A$, the free energy at constant volume, or the work function of Lewis and Randall, is derived immediately from the phase integral as

$$A=-kT\ln Q$$

and from (1),

$$A=RT\left[\ln\left(\frac{h^2}{2\pi mkT}\right)^{\frac{1}{2}}-\frac{1}{N}\ln\frac{Q_\tau}{N!}\right],$$

which, with (10) becomes

$$A=RT[\ln(h^2/2\pi mkT)^{\frac{1}{2}}-G_0(vb_l)+\ln Z]. \qquad (11)$$

The negative of the derivative of this with respect to the volume gives the pressure

$$\begin{aligned}P&=-(\partial A/\partial V)_T=kT(\partial/\partial v)[G_0(vb_l)-\ln Z]\\&=(RT/V)[G_0(vb_l)+G_{0v}(vb_l)],\end{aligned} \qquad (12)$$

where

$$G_{jv}(vb_l)=\sum_{l\geq 1}l^jvb_lZ^l(\partial\ln b_l/\partial\ln v). \qquad (13)$$

(the details of the differentiation are given in the appendix, preceding Eq. (A18)). The free energy at constant pressure, $F$, the Gibbs, and Lewis

and Randall, free energy, is given by

$$F=A+PV$$
$$=RT[\ln (h^2/2\pi mkT)^{\frac{3}{2}}+\ln Z+G_{0v}]. \tag{14}$$

We shall defer a more detailed discussion of the nature of these equations until the properties of the arguments $b_l$ have been discussed more fully. However, one interpretation will be introduced at this point. The original Eq. (6) for $Q_\tau$ can be handled more simply than by the method of the appendix if all the $b_l$'s are positive. In this case the logarithm of the total sum of $Q_\tau/N!$ can be shown to become asymptotically equal to the logarithm of the largest term as $N$ increases indefinitely. Now the largest term is characterized by the set of numbers $m_l^*$, the number of clusters of size $l$, with $lm_l^*$ the number of molecules in clusters of size $l$, and $lm_l^*/N$ the fraction of material in clusters of size $l$. $lm_l^*/N$ can be shown to be equal to $lvb_lZ^l$ so that the $l$'th term in the sum $G_1$ of Eq. (8) is the (most probable) fraction of material in clusters of $l$ molecules. The $l$'th term in $G_0$ is the number of clusters of $l$ molecules each, divided by the total number of molecules, and from the Eq. (12) for the pressure it can be seen that each cluster contributes exactly as much to the pressure as a single molecule, (if $G_{0v}$ is zero). For large values of $v$, $\partial \ln b_l/\partial \ln v$ is zero and $G_{0v}$ must be zero. The volume below which $G_{0v}$ differs from zero will be called $v_f$ and later be shown to be that of the condensed phase.

## Evaluation of the $b_l$'s

We shall now investigate the integrals over the clusters, the $b_l$'s of Eq. (5). It can be shown[1] that normalized irreducible integrals $\beta_k$ can be so defined that the cluster integral $b_l$ is the sum of coefficients times products of the $\beta_k$'s raised to various powers.

The first three normalized irreducible integrals are

$$\beta_1=(1/V)\int f_{21}d\tau_1d\tau_2=\int_0^\infty 4\pi r^2f(r)dr, \tag{15}$$

$$\beta_2=(1/V2!)\int\int f_{32}f_{31}f_{21}d\tau_1d\tau_2d\tau_3, \tag{16}$$

$$\beta_3=(1/V3!)\int\int\int[3f_{43}f_{32}f_{21}f_{41}+6f_{43}f_{32}f_{21}f_{41}f_{42}$$
$$+f_{43}f_{32}f_{21}f_{41}f_{42}f_{31}]d\tau_1d\tau_2d\tau_3d\tau_4. \tag{17}$$

The coefficients 3 and 6 in $\beta_3$ occur because permutation of the indices gives, respectively, 3 and 6 different products leading to the same integrals. The general $k$'th irreducible integral is an integral over the configuration space of $k+1$ particles. The integrand is the sum of all products of $f$ between $k+1$ particles which connect every particle to every other particle by more than a single path,

$$\beta_k=(1/Vk!)\int\int\cdots\int\sum_{k+1\geq i>j\geq 1}\prod f_{ij}d\tau_1\cdots d\tau_{k+1}. \tag{18}$$

Products having all particles more than singly connected.

If $n_k$ is the power to which $\beta_k$ is raised in a certain term in $b_l$ we have the condition that

$$\sum_k kn_k=l-1.$$

The coefficient with which a term, defined by the powers $n_k$, occurs in $b_l$ is very simple, namely

$$l^{-2}\prod_k l^{n_k}/n_k!.$$

The proof that this is the correct coefficient caused the authors a great deal of difficulty. They are greatly indebted to Dr. Goeppert Mayer for the final completion of the proof. An indication of the general method of this proof is given in the second part of the appendix. Due to its complicated nature the proof is not given in detail.

The equation for $l^2b_l$ becomes

$$l^2b_l=\sum_{\substack{n_k\\ \Sigma kn_k=l-1}}\prod_k(l\beta_k)^{n_k}/n_k!. \tag{19}$$

Comparison with (6) shows that it is similar in form to the equation for $Q_\tau/N!$, indeed it is identical in form with the Eqs. (A58) and (A36) of the appendix defining the function $F_1(M, x)$. We may use Eq. (A59) of the appendix which, with the arbitrary introduction of the function $p(l, \beta)$, is also an exact equation for $b_l$,

$$b_l=\frac{[b_0(\beta)]^l\rho(\beta)}{(2\pi G_2(\beta))^{\frac{1}{2}}l^{5/2}}\frac{1}{p(l,\beta)}, \tag{20}$$

where $p(l, \beta)$ is a function which takes erratic values for small values of $l$ but which becomes asymptotically equal to unity as $l$ becomes large. For $b_0(\beta)$ the equation, (A42),

$$\ln b_0(\beta) = G_0(\beta) - \ln \rho \tag{21}$$

is obtained. $\rho$ is determined by the $\beta_k$'s in the same way that $Z$ is determined by the $vb_l$'s (Eq. 8), i.e.,

$$\sum_{k\geq 1} k\beta_k \rho^k = 1, \tag{22}$$

and

$$G_0(\beta) = \sum_{k\geq 1} \beta_k \rho^k. \tag{23}$$

For small values of $l$ it is more convenient to use Eq. (19) to determine $b_l$, for large values of $l$ the form (20) is of course preferable. The condition for Eq. (20) to be valid is that Eq. (22) has a real positive root of $\rho$, the lowest real positive root being the correct one to use.

### Developments for the Gas

Returning now to Eq. (8), we see that at infinite volumes, since $b_1$ is unity, $Z = 1/v$, and $G_0 = 1$. Using these values in (11), (12) and (14) the equations of a perfect gas are obtained, remembering that $G_{0v}$ is zero for large volumes.

As long as the sum $G_1$ is absolutely convergent, (see the discussion in the appendix), $Z$ can be developed as a power series in $1/v$. Use of such a power series in (8) enables one to equate coefficients, and if $b_l$ is expressed by (19), one obtains

$$\begin{aligned} Z = (1/v)\{1 - \beta_1 v^{-1} - [\beta_2 - (\beta_1^2/2)]v^{-2} \\ - [\beta_3 - \beta_1\beta_2 + (\beta_1^3/6)]v^{-3} \cdots\} \\ = v^{-1} e^{-\sum \beta_k v^{-k}}. \end{aligned} \tag{24}$$

This may, in turn, be used in (9) to calculate $G_0(vb_l)$ as a power series in descending powers of $v$. The following simple equations are obtained:

$$G_0(vb_l) = \frac{PV}{RT} = 1 - \sum_k \frac{k}{k+1} \beta_k v^{-k}, \tag{25}$$

$$A = RT\left[\ln\left(\frac{h^2}{2\pi mkT}\right)^{\frac{3}{2}} \frac{1}{ev} - \sum_k \frac{1}{k+1} \beta_k v^{-k}\right], \tag{26}$$

$$F = RT\left[\ln\left(\frac{h^2}{2\pi mkT}\right)^{\frac{3}{2}} \frac{1}{v} - \sum_k \beta_k v^{-k}\right]. \tag{27}$$

It is seen that $-k\beta_k/(k+1)$ is the $(k+1)$th virial coefficient.

The developments were first made by algebraic evaluation of the first few terms. They can however be proved by inserting the solution of Eq. (24) for $Z$ in Eq. (8), and by manipulation of the sum obtained on expanding the exponential it can be shown that the coefficients of all powers of $1/v$ except the zeroth power are equal to zero. Professor Max Born has written to the authors that there exists a still simpler proof of the equations. The developments are, however, only valid if the sum $G_1(vb_l)$ converges absolutely, so that the last terms are negligible in their effect on the determination of $Z$.

From (25) we may evaluate $(\partial P/\partial V)_T$ as

$$(\partial P/\partial V)_T = -(RT/V^2)[1 - \sum k\beta_k v^{-k}], \tag{28}$$

and if we define $\rho$ as the reciprocal of the largest volume for which this becomes zero, it becomes the smallest positive root of the equation $g_1(\beta, \rho) - 1 = 0$, identically the Eq. (22) by which $\rho$ was previously defined. We see, then, that the quantity $\rho$ has the physical significance of being the reciprocal of the largest volume, $v_s$, for which $(\partial P/\partial V)_T = 0$,

$$v_s = 1/\rho \tag{29}$$

From Eq. (24) for $Z$ when $v = v_s = 1/\rho$, and (21) for $b_0$, we see that

$$Z_s = b_0^{-1}, \quad v = v_s = \rho^{-1}. \tag{30}$$

By differentiating the logarithm of $Z$ in (24) with respect to the logarithm of the volume, one obtains

$$\partial \ln Z/\partial \ln v = \sum k\beta_k v^{-k} - 1, \tag{31}$$

which, in view of the definition of $v_s$ as the largest root of this equation, is zero at $v = v_s$, and negative at all higher volumes. It follows that for $v > v_s$, $b_0 Z < 1$, and the sums $G_j(vb_l)$ converge absolutely (see the discussion of the second section of the appendix). In the range of volumes, $v_s \leqslant v \leqslant \infty$, then, the equations (24) to (31) are valid.

The quantity $Z$ has the dimensions of the reciprocal of a volume. From the equation for $F$, (14), it can be seen that for large volumes when $G_{0v}$ is zero, $Z^{-1}$ is the volume per molecule of a perfect gas having the same free energy $F$ as the

real gas in question. The quantity $(vZ)=\gamma_c$ may be called the concentration activity coefficient of the gas. It is the dimensionless quantity by which the concentration of the gas must be multiplied to obtain the concentration of an ideal gas having the same free energy $F$. From (24) this is seen to have the value

$$\gamma_c=vZ=e^{-\Sigma\beta_k v^{-k}}. \tag{32}$$

## Condensation

For volumes lower than $v_s$ the sums $G_j(vb_l)$ are not absolutely convergent, (see the discussion in the second section of the appendix), and the equations (24) to (32) will no longer be valid. In this range we may use (20) for $b_l$, which, inserted in (8) leads to the equation for the determination of $Z$,

$$\frac{v}{(2\pi)^{\frac{1}{2}}}\sum_{l\geq 1}\frac{(b_0Z)^l\rho(\beta)}{l^{\frac{3}{2}}(G_2(\beta))^{\frac{1}{2}}p(l,\beta)}=1. \tag{33}$$[2]

Since $p(l,\beta)$ becomes asymptotically unity for large values of $l$, it can be readily seen that $b_0Z$ cannot become more than infinitesimally greater than unity. For values of the volume $v$ equal to, or less than $v_s$, we can, to within terms of the order of magnitude of $1/N$, write

$$Z=1/b_0, \quad \partial \ln Z/\partial v=0, \quad v\leqslant v_s. \tag{34}$$

By taking the derivative of $G_0(vb_l)/v$ with respect to $v$ one obtains

$$\frac{\partial}{\partial v}\left[\frac{G_0(vb_l)}{v}\right]=\frac{1}{v}\left[\frac{\partial \ln Z}{\partial v}+G_{0v}(vb_l)\right]. \tag{35}$$

If now $v_f$ is defined as the volume above which $G_{0v}$ is essentially zero, and since $v_s$ is the volume below which $\partial \ln Z/\partial v$ is zero, in the volume range $v_f\leqslant v\leqslant v_s$ we find that $G_0/v$ is a constant. From (12) for $P$ we see that the pressure is a constant in this volume range. Since $Z$ is independent of $v$, and $G_{0v}$ zero in this volume range, we see from (14) that the free energy, $F$, is also independent of the volume. This constancy of $P$ and $F$ for $v_f\leqslant v\leqslant v_s$ may be considered to be the thermodynamic criterion of a change of phase. $v_f$ is seen to be the volume per molecule of the condensed phase, and $v_s$ the volume per molecule of the saturated vapor.

The decrease of volume from $v_s$ to $v_f$ is accompanied by an increase of the fraction of material in the very large clusters, $lvb_lZ^l$, from zero to almost unity,[3] since the sum becomes divergent in this range (see the discussion in the appendix), but there is no corresponding increase in the fraction of material in the moderately large clusters; this remains essentially zero during the whole process. The fraction of material in the small clusters decreases proportionally with $v$ in this range. Even at $v_f$ the density of the small clusters, the number per unit volume, $b_lZ^l$, is the same as in the saturated vapor at $v_s$. Insofar as the clusters have a physical meaning this states that the number of free molecules in the liquid per unit volume is equal to the number per unit volume in the vapor in equilibrium with the liquid. This same relationship of equal densities in liquid and saturated vapor holds for all the small clusters.

With the knowledge that the volume of the saturated vapor per molecule is $v_s=1/\rho$, and that Eq. (25) holds down to exactly this volume we may write the equation for the vapor pressure over the condensed phase as

$$P_s=kT\rho[1-\sum_k(k/k+1)\beta_k\rho^k], \qquad (v_f\leqslant v\leqslant v_s). \tag{36}$$

Since $Z=b_0^{-1}$ for the range $v_f\leqslant v\leqslant v_s$, and $G_{0v}(vb_l)$ is zero, we may write from (14), for the free energy $F$ of the saturated vapor, and of the

[2] We have written $G_2(\beta)$ as though it were independent of $l$. In the case (A26) of the appendix for which the sums $G_j(\beta)$ are not absolutely convergent $G_2(\beta)$ will depend on $l$. For this reason we have written $G_2(\beta)$ under the summation sign.

Since we have previously found that $Zb_0=1$ at $v=1/\rho$ it follows that $\sum 1/l^{3/2}(G_2(\beta))^{\frac{1}{2}}p(l,\beta)=(2\pi)^{\frac{1}{2}}$, an equation which we should be able to verify independently, but have been unable to do. Essentially this equation, however, has been carefully checked numerically for a wide variety of different values of the $\beta_k$'s.

[3] The treatment of $F_0(M,x)$ in the appendix is not fully valid without further discussion if $G_1(x)$ diverges. The method of steepest descents is also invalid in this case. An extension of the method of the appendix shows that the equations used in the article are correct, in this case, to the degree of accuracy to which they are used. The method of using the logarithm of the largest term shows the difficulty most clearly. In the previous treatment the numbers $m_l$ are treated as continuous, although they are obviously integers. If this simplification is not made, it becomes apparent that in the range of volumes $v_f\geq v\geq v_s$ for which condensation takes place, only one of the large clusters is present for which $l=N(v_s-v)/v_s$. The equations as used in this article are in no way affected.

liquid under its own vapor pressure,

$$F_s = RT[\ln (h^2/2\pi mkT)^{\frac{3}{2}} - \ln b_0]$$
$$= RT[\ln (h^2/2\pi mkT)^{\frac{3}{2}} - G_0(\beta) + \ln \rho], \quad (v_f \leqslant v \leqslant v_s). \quad (37)$$

### The Critical Point

The $\beta_k$'s are all positive at very low temperatures. As the temperature increases the $\beta_k$'s of higher $k$ values tend to become negative. As discussed in the appendix, above a certain temperature, $T_c$, there exists no real root of equation (22) for $\rho$. Above this temperature Eq. (20) for $b_l$ is invalid, and the complete argument that predicts the condensation phenomenon breaks down. One is immediately tempted to identify $T_c$ with the critical temperature. This identification is made complete when we observe that $\rho$ has also been defined as the reciprocal of the volume for which $(\partial P/\partial V)_T$, as given by Eq. (28), becomes zero. Above $T_c$, where no real root for $\rho$ in Eq. (22) exists, there is no positive volume for which $(\partial P/\partial V)_T$ is equal to zero.

From Eq. (28) we may calculate $(\partial^2 P/\partial V^2)_T$, and find

$$(\partial^2 P/\partial V^2)_T = (RT/V^3)[2 - 2\sum k\beta_k v^{-k} - \sum k^2\beta_k v^{-k}], \quad (v \geqslant v_s). \quad (38)$$

At $v_s = 1/\rho$ this becomes, since $G_1(\beta) = 1$,

$$(\partial^2 P/\partial V^2)_{T,\ v=v_s} = -(RT/V^3)G_2(\beta), \quad (v = v_s). \quad (39)$$

As is shown (Eq. (A 60)), in the appendix $G_2(\beta)$ is zero at $T = T_c$.

### Continuity or Discontinuity at the Condensation Point

For the sake of completeness we may return to the general Eq. (12) for the pressure $P$, and, limiting ourselves to $v \geqslant v_f$, for which $G_{0v}$ is zero, calculate $(\partial P/\partial V)_T$ and $(\partial^2 P/\partial V^2)_T$ as

$$\left(\frac{\partial P}{\partial V}\right)_T = \frac{\partial}{\partial V}\frac{RT}{V}G_0(vb_l) = -\frac{RT}{V^2}\frac{1}{G_2(vb_l)}, \quad (v \geqslant v_f), \quad (40)$$

$$\left(\frac{\partial^2 P}{\partial V^2}\right)_T = -\frac{RT}{V^3}\frac{G_3(vb_l) - 3G_2(vb_l)}{[G_2(vb_l)]^3}, \quad (v \geqslant v_f). \quad (41)$$

If $v > v_s$ all the sums in these expressions are finite, and the expressions are more readily calculated by the equivalent equations (28) and (38). For $v < v_s$, however, the sums diverge (in the sense discussed in the second section of the appendix) and $G_2(vb_l)$ becomes of order of magnitude $N$, and $G_3(vb_l)$ of order $N^2$; both $(\partial P/\partial V)_T$ and $(\partial^2 P/\partial V^2)_T$ are seen to be zero.

It is more difficult to ascertain from Eq. (42) whether $(\partial^2 P/\partial V^2)_T$ becomes "infinite" (i.e., of order of magnitude $N$), or not, as the volume $v_s$ is crossed. Eq. (39), however, answers this question. If the sums $G_1(\beta)$ and $G_2(\beta)$ converge, $(\partial^2 P/\partial V^2)_T$ is seen to be finite at $v = v_s$; whereas if they diverge, this function becomes "infinite" as the volume crosses $v_s$.

It appears then that the question of whether $(\partial P/\partial V)_T$ goes continuously or discontinuously to zero at $v = v_s$ is determined by whether the sums $G_1(\beta)$ and $G_2(\beta)$ converge or diverge. If the sums are convergent $(\partial P/\partial V)_T$ goes continuously to zero as $v$ decreases through $v_s$, and we must assume that the vapor cannot be supersaturated in the sense that a higher pressure than $P_s$ could be observed. If, however, the sums are divergent, there is a sudden break in the shape of the $P$–$V$ curve at $v_s$, and supersaturation of the vapor would be expected.

### Surface Tension and the Temperature $T_m$

For large values of $k$ we have been unable to find a method of calculating the $\beta_k$'s numerically. It is, however, fairly obvious that they must obey the relationship

$$(\lim k \to \infty) \ln \beta_k = k \ln \beta_0, \quad (42)$$

in which $\beta_0$, of the dimensions of a volume, represents the contribution as a factor to $\beta_k$ of the integration over an average particle. It is also fairly obvious that in the important terms of the products of $f_{ij}$'s of Eq. (18) a number of molecules proportional to $k^{\frac{1}{2}}$ must have fewer "bonds" to neighbors than the average particles. These are the particles which are physically on the surface of the mechanical frame which may be associated to each product of $f$'s. We may now amend (42) to

$$\ln \beta_k = k \ln \beta_0 - \gamma k^{\frac{1}{2}} + \ln \alpha(k, \beta_0) - n \ln k, \quad (43)$$
$$\beta_k = \beta_0{}^k e^{-\gamma k^{\frac{1}{2}}} \alpha(k, \beta_0)/k^n, \quad (44)$$

where $\beta_0$ is a positive quantity with the dimensions of volume, the dimensionless $\gamma$ may be positive or negative, $\alpha(k, \beta_0)$ is presumed to be independent of $k$ for large values of $k$, (a property which we shall not really use), and $k^{-n}$ is introduced merely because it seems rather probable that some such term should be present. The only portions of (44) which are of importance are the already justified $\beta_0$ and $\gamma$.

Now for low values of the temperature, $T$, $\gamma$ must be positive, the contribution of the "surface" molecules to $\beta_k$ must be less than the contribution of the "inner" molecules, and we must expect that $d\gamma/dT<0$. Let us assume $\gamma>0$ for $T<T_m$, $d\gamma/dT<0$, and $\gamma=0$ at $T=T_m$. We now propose to show that, for $T<T_m$, $kT\gamma/(36\pi v_f^2)^{\frac{1}{3}}$ is the surface tension, $S$, or surface free energy of the condensed phase.

The case (44) is the same as the case II discussed in the appendix under the title "Convergence of the Auxiliary Functions." Below $T_m$ with $\gamma$ positive the sums $G_1(\beta)$ and $G_2(\beta)$ diverge in the sense used in that section. For temperatures above $T_m$ the sums converge.[4] We have already seen in the preceding section that the cases of divergent and convergent $G_2(\beta)$ correspond respectively to discontinuous and continuous transitions of $(\partial P/\partial V)_T$ to zero at the volume $v_s$ of the saturated vapor. The existence of a positive surface tension below $T_m$ assures the instability of the small clusters; so an arbitrary restriction to integration over that region of phase space where no large numbers of molecules are close together (corresponding to the arbitrary assumption that the $b_l$'s of large $l$ values are zero or small) would result in a $P$–$V$ curve showing higher values of $P$ than $P_s$ for $v<v_s$.

The proof that $kT\gamma/(36\pi v_f^2)^{\frac{1}{3}}$ is the surface tension is as follows. In the appendix it is shown that $\rho$, (the same as $z$ of Eq. (A25II)) depends on $l$, the upper limit of summation, if the sums are divergent, and indeed, (A29II),

$$\rho=\beta_0^{-1}e^{\gamma/l^{\frac{1}{3}}}. \tag{45}$$

If this value of $\rho$ is inserted in Eq. (20) for $b_l$, with (21) for $b_0$, we find a multiplicative factor $e^{-\gamma l^{\frac{1}{3}}}$ in $b_l$. Now consider the chemical reaction in which clusters of size $l$ dissociate to form clusters of size $l/n$. The concentration of clusters of size $l$ is given by $c_l=b_lZ^l$, since $vb_lZ^l$ gives the number of such clusters divided by $N$. The concentration of clusters of size $l/n$ is $b_{l/n}Z^{l/n}$. Inserting these values in the reaction constant $K=c_{l/n}{}^n/c_l$, and using the relationship $\Delta F^0=-kT\ln K$ we find, upon neglecting lower order terms that

$$\Delta F^\circ=-kT\gamma l^{\frac{1}{3}}(1-n^{\frac{1}{3}}), \tag{46}$$

where $\Delta F^\circ$ is the difference in free energy (at hypothetical unit concentration) between $n$ clusters of size $l/n$ and one cluster of size $l$. This difference in free energy must be the product of the surface tension $S$ multiplied by the increase of surface in the reaction. The area of the surface of a (spherical) drop of $l$ molecules will be $(36\pi)^{\frac{1}{3}}(v_fl)^{\frac{2}{3}}$, since $v_f$ is the volume per molecule of the condensed phase. The area increase is then seen to be $(36\pi v_f^2l^2)^{\frac{1}{3}}(n^{\frac{2}{3}}-1)$ and one obtains with (46) the equation for the surface tension in terms of $\gamma$,

$$S=kT\gamma/(36\pi v_f^2)^{\frac{1}{3}}. \tag{47}$$

In this section we have inserted the quantity $\gamma$ into the equation for $\beta_k$ as a reasonable assumption and have shown that its reality is in agreement with the experimental observation of the existence of a surface tension. For our equations to have a physical meaning, however, it is important that the quantity $\alpha(k, \beta_0)$ be positive for all large values of $k$, as long as $\gamma$ is positive. In this case $G_2(\beta)$ must be very large and positive. At $T_m$ the quantity $\gamma$ is zero, and although it may and presumably does become negative for higher temperatures, because of the necessary convergence of the sums $G_1(\beta)$ and $G_2(\beta)$ above $T_m$, the quantity $\rho$ does not depend on the upper limit of summation $l$, and $\ln b_l$ will contain no term proportional to $l^{\frac{1}{3}}$. Therefore, the surface tension $S$ is zero for $T>T_m$. How-

[4] Actually, although the sums certainly converge if $\gamma$ is negative, it is not necessarily true that they diverge for all positive values of $\gamma$, and they would not if $\sum\alpha(k, \beta_0)k^{-n}$ were greater than unity. We should define $T_m$ as the temperature at which the sums change from divergent to convergent, which could be at a finite positive value of $\gamma$. This would change nothing in the subsequent argument except that the surface tension $S$ would extrapolate to a finite value at $T_m$ and would become discontinuously zero at this temperature. This appears not to be the case experimentally.

ever, $G_2(\beta)$ is positive at $T=T_m$, and so the temperature $T_c$, the true critical temperature, at which $G_2(\beta)=0$, must lie higher than $T_m$, $T_m<T_c$.

Thus $T_m$, the temperature at which the surface tension of the condensed phase becomes zero, and where the meniscus between liquid and gas disappears, is not identical with, but is lower than the true critical temperature $T_c$, the temperature at which the $P$–$V$ curve has a horizontal tangent for only one volume. The two temperatures have been hitherto regarded as identical by most theoretical workers.

To recapitulate: we are forced to the conclusion that there exist two characteristic temperatures, $T_c$ and $T_m$, with $T_c>T_m$. Above $T_c$ the $P$–$V$ curve is nowhere horizontal and there exists no difference between gas and liquid. Below $T_m$ the condensed phase has a surface tension and the $P$–$V$ curve shows (at least) one discontinuity in slope at the volume $v_s$, below which it is horizontal. Between $T_m$ and $T_c$ there is a finite temperature range in which the $P$–$V$ curve is horizontal over a finite volume interval, but has no discontinuous change in slope. Between $T_m$ and $T_c$, and of course also above $T_c$, there exists no surface tension.

### Temperature Derivatives

In order to obtain equations for the thermodynamic quantities $S$, $E$, $H$, and $(\partial P/\partial T)_V$, etc., it will be necessary to express the functions $\beta_k$ as functions of $T$ and to differentiate them. Although this might be done formally without any special assumption as to the form of $\beta_k$ for large values of $k$, certain relationships become more obvious if Eqs. (43) and (44) are used for $\beta_k$. Using the definitions

$$-d\ln\beta_0/d\ln T=B_0, \tag{48}$$

$$-d\gamma/d\ln T=C_0, \tag{49}$$

$$d\ln\alpha(k,\beta_0)/d\ln T=B_k, \tag{50}$$

we may write

$$d\ln\beta_k/d\ln T=-kB_0+k^{\frac{1}{3}}C_0+B_k. \tag{51}$$

By the use of (51) in Eq. (26) for $A$ with $v\geqslant v_s$ one obtains

$$\left(\frac{\partial A}{\partial T}\right)_V=-S=\frac{A}{T}-\tfrac{3}{2}R+R\Big[B_0\sum_k\frac{k}{k+1}\beta_k v^{-k}-C_0\sum_k\frac{k^{\frac{1}{3}}}{k+1}\beta_k v^{-k}-\sum_k\frac{B_k\beta_k}{k+1}v^{-k}\Big], \tag{52}$$

or

$$S=R\Big[\ln\left(\frac{2\pi mkTe}{h^2}\right)^{\frac{3}{2}}ev+\sum_k\frac{\beta_k}{k+1}v^{-k}-B_0\sum_k\frac{k\beta_k}{k+1}v^{-k}+C_0\sum_k\frac{k^{\frac{1}{3}}\beta_k}{k+1}v^{-k}+\sum_k\frac{B_k\beta_k}{k+1}v^{-k}\Big]. \tag{53}$$

Using $E=A+TS=A-T(\partial A/\partial T)_V$, and $H=E+PV$, with (25) for $PV$ one obtains

$$E=RT\Big[\frac{3}{2}-B_0\sum_k\frac{k\beta_k}{k+1}v^{-k}+C_0\sum_k\frac{k^{\frac{1}{3}}\beta_k}{k+1}v^{-k}+\sum_k\frac{B_k\beta_k}{k+1}v^{-k}\Big], \tag{54}$$

$$H=RT\Big[\frac{5}{2}-(B_0+1)\sum_k\frac{k\beta_k}{k+1}v^{-k}+C_0\sum_k\frac{k^{\frac{1}{3}}\beta_k}{k+1}v^{-k}+\sum_k\frac{B_k\beta_k}{k+1}v^{-k}\Big]. \tag{55}$$

Similarly (25), if differentiated, yields

$$\left(\frac{\partial P}{\partial T}\right)_V=\frac{R}{V}\Big[1-\sum_k\frac{k\beta_k}{k+1}v^{-k}+B_0\sum_k\frac{k^2\beta_k}{k+1}v^{-k}-C_0\sum_k\frac{k^{5/3}\beta_k}{k+1}v^{-k}-\sum_k\frac{kB_k\beta_k}{k+1}v^{-k}\Big]. \tag{56}$$

For $dP_s/dT$ we may use

$$dP_s/dT=(\partial P/\partial T)_{v=v_s}+(\partial P/\partial V)_{T,\,v=v_s}(\partial V_s/\partial T)$$

but since $(\partial P/\partial V)_{T,\,v=v_s}$ is zero, we find that $dP_s/dT$ is equal to $(\partial P/\partial T)_V$ when $v=v_s$.[5]

[5] This apparently high-handed neglect of the "infinite" value of $(\partial^2P/\partial V^2)_T$ when the sum $G_2(\beta)$ diverges is justified by the fact that $G_2(\beta)$, and hence $(\partial^2P/\partial V^2)_T$, is actually finite in a mathematical sense, although very large. We have used the expression "discontinuous" for $(\partial P/\partial V)_T$ at $v=v_s$ in the physical sense since magnitudes of order $N$ are pretty big. This is, of course, mathematically unjustifiable, and all our equations are strictly speaking continuous. The equation (56) for $(\partial P/\partial T)_V$ and (57) for $dP_s/dT$ lead to different values for these two quantities if $v$ is infinitesimally greater than $v_s$. We shall discuss the values of the thermodynamic properties of the super-saturated vapor in the neighborhood of $v=v_s$ in the following section.

Using the condition that $G_1(\beta)=1$ at $v=v_s=\rho^{-1}$, and that $k^2/(k+1)=k-k/(k+1)$ we obtain

$$\frac{dP_s}{dT}=\frac{R}{V_s}\Big[(1+B_0)\Big(1-\sum_k \frac{k\beta_k}{k+1}\rho^k\Big) - C_0\sum_k \frac{k^{5/3}\beta_k}{k+1}\rho^k-\sum_k \frac{kB_k\beta_k}{k+1}\rho^k\Big]. \quad (57)$$

Finally, by noting that $G_1(\beta)=1$ at $v=v_s=\rho^{-1}$ so that $dG_1/dT=0$, we obtain for $d\ln v_s/d\ln T$,

$$d\ln v_s/d\ln T=-B_0+[G_2(\beta)]^{-1} \times[C_0\sum k^{5/3}\beta_k\rho^k+\sum kB_k\beta_k\rho^k], \quad (58)$$

or, since $G_2(\beta)$ is "infinite" when $T<T_m$

$$d\ln v_s/d\ln T=-B_0, \quad (T<T_m). \quad (59)$$

It is seen from Eq. (58) for $d\ln v_s/d\ln T$ that this quantity increases discontinuously as $T$ is increased through the value $T=T_m$. $dP_s/dT$ is, however, seen to be continuous at $T=T_m$. Further differentiation shows that $d^2P_s/dT^2$ is discontinuous at $T_m$. Since $dP_s/dT$ is continuous at $T_m$ there is no discontinuous change in the heat content of the condensed phase at this temperature; therefore no true change of phase occurs at $T_m$.

At $T=T_c$ since $G_2(\beta)$ is zero it is seen from (58) that $d\ln v_s/d\ln T$ is infinity. Numerical calculations of the $\beta_k$'s at this temperature have shown that the derivative approaches infinity from the negative side as is to be expected.

## Equations of the Supersaturated Vapor

Equation (28) for $(\partial P/\partial V)_T$ and (56) for $(\partial P/\partial T)_V$ show discontinuities at $v=v_s$ if $T<T_m$ and the sums $G_1(\beta)$ and $G_2(\beta)$ are divergent. The point $v=\beta_0^{-1}$, $\beta_0/v=1$ lies on the circle of convergence of the sum $G_1(\beta)$ if that sum is regarded as having an infinite upper limit of summation. The value of $v_s$ is infinitesimally smaller than $\beta_0$ so that $\beta_0/v_s$ is actually larger than unity by a very small amount. If we set $\beta_0/v$ exactly equal to unity (a value which it has when $v$ is negligibly larger than $v_s$) we obtain a value of $G_j(\beta)$ which may be used in (28) and (56) for the supersaturated vapor in the neighborhood of the volume $v_s$. Using (44) for $\beta_k$, this leads to

$$g_j(\beta,v^{-1})=\sum_{k,\ \beta_0/v=1} k^j\beta_k v^{-k} =\sum_k \alpha(k,\beta_0)e^{-\gamma k^{\frac{1}{3}}}k^{j-n}=G_j^0(\beta). \quad (60)$$

The symbol $G_j^0(\beta)$ has been used to indicate the sum $g_j(\beta,v^{-1})$ when $\beta_0/v=1$, $G_j(\beta)$ being the value when $G_1=1$ which for divergent sums, $T<T_m$, gives $\beta_0/v=1+\epsilon$. It is obvious that $G_0(\beta)=G_0^0(\beta)$ always, but $G_1^0(\beta)<1$ if $T<T_m$. Since $\partial\ln g_j(\beta,v^{-1})/\partial\ln v=-g_{j+1}(\beta,v^{-1})$ we may develop $g_j(\beta,v^{-1})$ in terms of a semi-convergent Taylor's series as

$$g_j(\beta,v^{-1})=\sum_{\nu\geq 0}[\ln v-\ln v_s]^\nu \times(\partial^\nu/\partial\ln v^\nu)g_j(\beta,v^{-1})_{v=v_s} =\sum_{\nu\geq 0}[(-\ln v\rho)^\nu G^0_{j+\nu}(\beta)]/\nu!. \quad (61)$$

This equation could be used for values of $v<v_s=\rho^{-1}$ with any of the equations (25) to (32) or (52) to (59) to calculate the thermodynamic functions of the supersaturated vapor. We shall not carry out the obvious operations.

It is interesting to note that the sum $g_1(\beta,v^{-1})$ is itself semi-convergent for values of $v$ smaller than $v_s$, that is the first terms of $g_1(\beta,v^{-1})$ converge, and it is only after a comparatively large value of the index of summation of $k$ has been reached that the terms commence to grow larger again. Using (44) for $\beta_k$ and differentiating $\beta_k(v_s/v)^k$ with respect to $k$, we find that the term of minimum value is given by the equation

$$\frac{1}{k}\frac{\partial\ln\alpha(\beta_0,k)}{\partial\ln k}-\frac{n}{k}-\frac{2}{3}\frac{\gamma}{k^{\frac{1}{3}}}+\ln\frac{v_s}{v}=0. \quad (62)$$

For large values of $k$ this is approximately

$$k=\frac{8}{27}\frac{\gamma^3}{[\ln(v_s/v)]^3}, \quad (63)$$

which should give approximately the size of droplet which forms least easily at a volume $v<v_s$. After a droplet of this size has once been formed in a supersaturated vapor of volume $v$, the drop should increase rapidly in size until the pressure attains the value $P_s$.

## Conclusion

Except for Eq. (44) assuming a special form for $\beta_k$ no assumptions have been introduced into the general deductions other than those listed in the third and fourth paragraphs of the introduction. The assumption in (44) that $\ln \beta_k$ varies linearly with $k$ for large $k$ values can scarcely be questioned. The addition of a term proportional to $k^{\frac{1}{3}}$ appears, *a priori*, to be reasonable, and is later justified by its appearance in the final equations as the surface free energy.

We conclude that a liquid-saturated vapor system has two characteristic temperatures, $T_m$ and $T_c$, instead of one critical temperature as usually assumed. Above $T_c$ and below $T_m$ the properties correspond to those predicted classically above and below the critical point, but between $T_m$ and $T_c$ for a certain volume range we predict properties which are not given by any classical description of the critical phenomenon. The authors will show in a subsequent paper that published experimental results amply confirm this conclusion.

Numerical evaluation of the first few $\beta_k$'s shows that the experimental properties of the critical point, especially its relative position with respect to the temperature for which the second virial coefficient is zero (the Boyle point), and the value of $PV/RT$, are in agreement with the assumption that only $\beta_1$ and $\beta_2$ play a role at these temperatures and pressures. It is probable that a calculation of $\beta_1$, $\beta_2$ and $\beta_3$, which is not impracticable, would suffice to cover the range above $T_m$. As yet no theoretical calculation of $\beta_0$ appears to be practicable. Until this is accomplished, no numerical values below $T_m$ can be theoretically calculated.

It is possible, by means of the formal introduction of new quantities, to extend the equations to volumes below $v_f$. This appears to be unfruitful at the present time.

## Appendix

### The auxiliary functions

We shall first investigate the properties of a set of functions which occur repeatedly in the article. The functions $g_j$ of the variables $x_1, x_2, \cdots, x_\nu \cdots, q$ will be defined as

$$g_j(x_1, \cdots, x_\nu, \cdots, q) = \sum_{\nu \geq 1} \nu^j x_\nu q^\nu, \tag{A1}$$

so that

$$q \partial g_j/\partial q = g_{j+1}. \tag{A2}$$

If the value of the lowest real root of the equation for $q$, $g_1 = 1$, be designated as $z$, then this $z$ is a function of the arguments $x_\nu$; and if this $z$ replaces $q$ in the functions $g_j$ they then become new functions $G_j$ of the arguments $x_\nu$ alone.

$$G_j(x) = \sum_{\nu \geq 1} \nu^j x_\nu z^\nu, \tag{A3}$$

$$G_1(x) = \sum_{\nu \geq 1} \nu x_\nu z^\nu = 1 \quad \text{defines } z, \tag{A4}$$

where the symbol $x$ is used to represent all the $x_\nu$'s together.

Now

$$\partial G_j/\partial x_\nu = \partial g_j/\partial x_\nu + (\partial \ln z/\partial x_\nu) \cdot q(\partial g_j/\partial q)_{q=z}, \tag{A5}$$
$$= \nu^j z^\nu + G_{j+1}(\partial \ln z/\partial x_\nu).$$

Since

$$\partial G_1/\partial x_\nu = 0 = \nu z^\nu + G_2 \partial \ln z/\partial x_\nu, \tag{A6}$$

it follows that

$$\partial \ln z/\partial x_\nu = -\nu z^\nu/G_2, \tag{A7}$$

and from (A5) that

$$\partial G_j/\partial x_\nu = \nu z^\nu(\nu^{j-1} - G_{j+1}/G_2), \tag{A8}$$

$$\partial^2 \ln z/\partial x_\nu^2 = (\nu z^\nu)^2(2\nu G_2 - G_3)/G_2^3. \tag{A9}$$

Also

$$\partial(G_0 - \ln z)/\partial x_\nu = z^\nu, \tag{A10}$$

$$\partial^2(G_0 - \ln z)/\partial x_\nu^2 = -(\nu z^\nu)^2/G_2. \tag{A11}$$

If the $x_\nu$'s are all functions of one variable $y$, $x_\nu = x_\nu(y)$ from (A8)

$$\partial G_j/\partial y = \sum_\nu x_\nu \partial G_j/\partial x_\nu (\partial \ln x_\nu/\partial y)$$
$$= \sum \nu^j x_\nu z^\nu (\partial \ln x_\nu/\partial y) - (G_{j+1}/G_2) \sum_\nu \nu x_\nu z^\nu (\partial \ln x_\nu/\partial y), \tag{A12}$$

$$\partial \ln z/\partial y = -[\sum_\nu \nu x_\nu z^\nu (\partial \ln x_\nu/\partial y)]/G_2. \tag{A13}$$

It is seen from (A12) that $\partial G_1/\partial y$ is identically zero.

We shall have use for the special case that the $x_\nu$'s are explicitly written in the form $x_\nu = v b_\nu$, but the $b_\nu$'s may also be functions of $v$. If $x_\nu = v b_\nu$,

$$\partial \ln x_\nu/\partial \ln v = 1 + \partial \ln b_\nu/\partial \ln v, \tag{A14}$$

and we define

$$G_{jv} = \sum_\nu \nu^j v b_\nu z^\nu (\partial \ln b_\nu/\partial \ln v), \tag{A15}$$

then from (A12) and (A13)

$$\partial G_j/\partial \ln v = G_j - G_{j+1}/G_2 + G_{jv} - G_{j+1}/G_2 G_{1v}, \tag{A16}$$

$$\partial \ln z/\partial \ln v = -(1 + G_{1v})/G_2, \tag{A17}$$

$$\partial(G_0 - \ln z)/\partial \ln v = G_0 + G_{0v}. \tag{A18}$$

In the special case that all $x_\nu$'s are proportionatl to $u$, i.e., if

$$\partial \ln x_\nu/\partial \ln u=1 \tag{A19}$$

$$\partial G_j/\partial \ln u=G_j-G_{j+1}/G_2, \tag{A20}$$

$$\partial \ln z/\partial \ln u=-1/G_2. \tag{A21}$$

These functions play a role in handling the properties of the function $F_0(M, x)$ which will be defined later.

**Convergence of the auxiliary functions**

In the definitions (A3) and (A4) of $G_j$ and $z$, the sums were written as if $\nu$ varied from unity to infinity. We shall, however, be interested in cases in which the summation is explicitly limited to $1 \leqq \nu \leqq M$ with $M$ an extremely large number, although the $x_\nu$'s are defined to $\nu=\infty$. Actually we shall only be interested in cases for which

$$\left(\lim_{\nu\to\infty}\right) \ln x_\nu=\nu \ln x_0, \tag{A22}$$

and in two different modifications of this dependence of $x_\nu$ on $\nu$, namely

$$x_\nu=\alpha(x_0, \nu)x_0{}^\nu/\nu^n, \tag{A23I}$$

and

$$x_\nu=\alpha(x_0, \nu)x_0{}^\nu a^{\nu^{\frac{1}{2}}}/\nu^n, \tag{A23II}$$

in which $x_0$, $\alpha$ and $a$ are positive, $n$ need not necessarily be an integer, and $\partial\alpha(x_0, \nu)/\partial\nu$ approaches zero for very large values of $\nu$.

We shall refer to the cases (A23I) and (A23II) as cases I and II, respectively.

Now if

$$\sum_{\nu=1}^{\nu=M} \alpha(x_0, \nu)/\nu^{n-1}>1, \tag{A24I}$$

or

$$\sum_{\nu=1}^{\nu=M} \alpha(x_0, \nu)a^{\nu^{\frac{1}{2}}}/\nu^{n-1}>1, \tag{A24II}$$

respectively, the equation determining $z$, namely

$$G_1=1=\sum_{\nu=1}^{\nu=M} \alpha(x_0, \nu)(x_0z)^\nu/\nu^{n-1}, \tag{A25I}$$

or

$$G_1=1=\sum_{\nu=1}^{\nu=M} \alpha(x_0, \nu)a^{\nu^{\frac{1}{2}}}(x_0z)^\nu/\nu^{n-1}, \tag{A25II}$$

can only be satisfied by $(x_0z)<1$, and the sum $G_1$ as well as all the other sums $G_2$ and $G_3$, etc., will be absolutely convergent; so that if the upper limit of summation, $M$, is sufficiently large, their values, and that of $z$ will be independent of $M$. This case will be referred to as the case of convergent sums.

If, however,

$$\sum_{\nu=1}^{\nu=M} \alpha(x_0, \nu)/\nu^{n-1}<1, \tag{A26I}$$

or

$$\sum_{\nu=1}^{\nu=M} \alpha(x_0, \nu)a^{\nu^{\frac{1}{2}}}/\nu^{n-1}<1, \tag{A26II}$$

which can only be satisfied in case I if $n>2$, and in case II if $a<1$, we find that the solution of (A25) will be $x_0z=1+\epsilon$ where $\epsilon$ is an extremely small quantity. We may estimate the value of $\epsilon$ in the following manner. The order of magnitude of the last term, the term $\nu=M$ in (A25), may be expected to lie between $1/M^2$ and unity (actually it seems probable that it will be of order $1/M \ln M$). Using this inequality, and inserting $e^\epsilon$ for $x_0z$ in the last term of (A25) we obtain

$$1/M^2<\alpha(x_0, M)e^{M\epsilon}/M^{n-1}<1, \tag{A27I}$$

or

$$1/M^2<\alpha(x_0, M)a^{M^{\frac{1}{2}}}e^{M\epsilon}/M^{n-1}<1, \tag{A27II}$$

resulting in

$$(1/M)[(n-3) \ln M-\ln \alpha]<\epsilon<(1/M)[(n-1) \ln M-\ln \alpha], \tag{A28I}$$

$$(1/M)[(n-3) \ln M-\ln \alpha]-(1/M^{\frac{1}{2}}) \ln a<\epsilon<(1/M)[(n-1) \ln M-\ln \alpha]-(1/M^{\frac{1}{2}}) \ln a. \tag{A28II}$$

In case I we see that $\epsilon$ is of the order of magnitude $1/M$, which will be sufficient for the purposes of our investigation. In case II, however, we find that, to within terms of definitely smaller order of magnitude, we may write

$$\epsilon=(-\ln a)/M^{\frac{1}{2}}=\gamma/M^{\frac{1}{2}}, \tag{A29II}$$

where $\gamma=-\ln a$ is positive because the case of divergent sums can occur only if $a$ is less than unity.

The condition of Eq. (A26) will always lead to the equation $z=x_0{}^{-1}$ to within terms of order of magnitude $M^{-1}$ in I, and $M^{-\frac{1}{2}}$ in II. This will be referred to as the case of divergent sums.

If the sums are divergent in the sense discussed in the previous paragraph, the values of the individual terms of the sum $G_1$ will not decrease rapidly with increasing values of $\nu$. It is obvious that the sum $G_0$, the individual terms of which have $1/\nu$ times the value of the terms of $G_1$, must be smaller than $G_1$ and independent of the value of $M$. The terms of $G_2$ and $G_3$, which are $\nu$, and $\nu^2$ fold greater, respectively, than the corresponding terms of $G_1$ will certainly not converge. The values of the sums will be expected to be dependent on the value of $M$. Various methods of estimation lead to the same qualitative result for the order of magnitude of the sums $G_j$, namely

$$G_j \cong M^{j-1}, \quad (j>1). \tag{A30}$$

The equation (A30) is nowhere of great importance to the argument of the article. It is of importance, but fairly obvious, that $G_2$ and $G_3$ are extremely large and dependent on the limit of summation $M$, in the case of divergent sums.

The case that

$$\sum_{\nu=1}^{M} \alpha(x_0, \nu)/\nu^{n-1}=1, \tag{A31I}$$

is used once in the article. In this case the solution of (A25I) is obviously that $x_0z$ is exactly equal to unity. In this case the summation of $G_2$ and $G_3$ offers no difficulties. If $n=5/2$ we obtain

$$G_2 \cong \sum_{\nu=1}^{\nu=M} 1/\nu^{\frac{1}{2}} \cong M^{\frac{1}{2}}, \quad (n=5/2), \tag{A32I}$$

$$G_3 \cong \sum_{\nu=1}^{\nu=M} \nu^{\frac{1}{2}} \cong M^{\frac{1}{2}}, \quad (n=5/2), \tag{A33I}$$

whereas if $n=3$:

$$G_2 \backeq \sum_{\nu=1}^{M} 1/\nu \backeq \ln M, \quad (n=3), \tag{A34I}$$

$$G_3 \backeq \sum_{\nu=1}^{M} 1 \backeq M, \quad (n=3). \tag{A35I}$$

**The function $F_0(Mx)$**

The function $F(M, J, x_1, \cdots, x_\nu, \cdots)$ of the variable $M$, a very large integer, $J$, a parameter, and of the $x_\nu$'s, is defined as

$$F(M, J, x) = \sum_{\substack{\mu_\nu \\ \Sigma \nu \mu_\nu = M}} \prod_{\nu} (Jx_\nu)^{\mu_\nu}/\mu_\nu!, \tag{A36}$$

where, as before, $x$ is taken to represent all the $x_\nu$'s together. If $J$ is set equal to $M$ we shall call

$$F(M, M, x) = F_0(M, x). \tag{A37}$$

Direct differentiation of (A36) with respect to $x_\nu$ leads to

$$\frac{1}{J}\frac{\partial F(M, J, x)}{\partial x_\nu} = F(M-\nu, J, x) = \frac{1}{J^\nu}\frac{\partial^\nu F(M, J, x)}{\partial x_1{}^\nu}, \tag{A38}$$

which, upon setting $J=M$, gives the equation for $F_0$

$$\frac{1}{M}\frac{1}{F_0}\frac{\partial F_0}{\partial x_\nu} = \frac{\partial}{\partial x_\nu}\left(\frac{\ln F_0}{M}\right) = \frac{1}{M^\nu}\frac{1}{F_0}\frac{\partial^\nu F_0}{\partial x_1{}^\nu}. \tag{A39}$$

Since $F_0$ is a homogeneous function of degree $M$ in the variables $y_\nu = x_\nu{}^{1/\nu}$ it follows from Euler's theorem that

$$\sum_\nu y_\nu \frac{1}{M}\frac{1}{F_0}\frac{\partial F_0}{\partial y_\nu} = \sum_\nu \nu x_\nu \frac{\partial}{\partial x_\nu}\left(\frac{\ln F_0}{M}\right) = 1. \tag{A40}$$

We now propose to show that we can write approximately[6]

$$\ln F_0(M, x) = M \ln f(x) + \ln h(x) + \ln g(M), \tag{A41}$$

and that

$$\ln f(x) = G_0(x) - \ln z(x), \tag{A42}$$

$$\ln h(x) = -[\ln G_2(x)]/2, \tag{A43}$$

$$\ln g(M) = -[\ln 2\pi M]/2. \tag{A44}$$

The approximation of Eq. (A42) holds as long as there is a real positive root to Eq. (A4) for $z(x)$, and as long as $z(x)$ is independent of $M$ as discussed in the section under convergence of the auxiliary functions.

The combination of the assumption (A41) with (A40) shows that

$$\sum_\nu \nu x_\nu \partial \ln f(x)/\partial x_\nu = 1, \tag{A45}$$

$$\sum_\nu \nu x_\nu \partial \ln h(x)/\partial x_\nu = 0, \tag{A46}$$

since $f(x)$ and $h(x)$ are assumed to be independent of $M$. We shall use the symbols

$$z(x) = \partial \ln f(x)/\partial x_1, \tag{A47}$$

$$z_1(x) = \partial z(x)/\partial x_1, \tag{A48}$$

$$\sigma(x) = \partial \ln h(x)/\partial x_1, \tag{A49}$$

and later identify $z(x)$ with the $z(x)$ defined by (A4).

Upon using the assumption of (A42) in Eq. (A39), then developing according to powers of $1/M$, and inserting the above symbols, one obtains

$$\begin{aligned}\frac{\partial}{\partial x_\nu}\left(\frac{\ln F_0}{M}\right) &= \frac{\partial \ln f(x)}{\partial x_\nu} + \frac{1}{M}\frac{\partial \ln h(x)}{\partial x_\nu} = \frac{1}{M^\nu}\frac{1}{F_0}\frac{\partial^\nu F_0}{\partial x_1{}^\nu} \\ &= \sum_{\substack{n_k \\ \Sigma k n_k = \nu}} \prod_k \frac{\nu!}{n_k!(k!)^{n_k}} M^{-\sum_k (k-1)n_k} \left[\frac{\partial^k}{\partial x_1{}^k}\frac{\ln F_0}{M}\right]^{n_k} \\ &= z^\nu + \frac{1}{M}\left[\nu z^\nu\left(\frac{\sigma}{z} - \frac{z_1}{2z^2}\right) + \nu^2 z^\nu \frac{z_1}{2z^2}\right] + \cdots. \end{aligned} \tag{A50}$$

Equating powers of $1/M$ leads to

$$\partial \ln f(x)/\partial x_\nu = z^\nu, \tag{A51}$$

$$\partial \ln h(x)/\partial x_\nu = \nu z^\nu(\sigma/z - z_1/2z^2) + \nu^2 z^\nu z_1/2z^2. \tag{A52}$$

The use of (A51) in (A45) gives us Eq. (A4) which identifies $z(x)$ as defined by (A47) with $z(x)$ defined by (A4). Comparison of (A51) with (A10) shows that Eq. (A42) holds to an additive constant which we shall later show to be zero. Having identified $z(x)$ we may now use (A7) to show that $z_1/2z^2 = -1/2G_2$ and inserting this value in (A52), and (A52) in (A46) one obtains

$$\begin{aligned}\sum_\nu \nu^2 x_\nu z^\nu(\sigma/z + 1/2G_2) - \sum_\nu \nu^3 x_\nu z^\nu (1/2G_2) \\ = G_2(\sigma/z + 1/2G_2) - G_3/2G_2 = 0, \end{aligned} \tag{A53}$$

or

$$\sigma/z = (G_3 - G_2)/2G_2{}^2. \tag{A54}$$

Using (A54) and the equation $z_1$ in (A52) finally yields

$$\partial \ln h(x)/\partial x_\nu = \nu z^\nu G_3/2G_2{}^2 - \nu^2 z^\nu (1/2G_2). \tag{A55}$$

Comparison of this equation with (A8) shows that (A43) holds to within a constant of integration, which we shall now show can be taken as zero.

We shall consider the special case that $x_1 > 0$ and $x_\nu = 0$, $\nu \neq 1$. In this case we may evaluate Eq. (A36) with $J=M$ directly by the use of the Stirling approximation obtaining, since only the term $\mu_1 = M$ occurs,

$$\ln F_0(M, x) = M(\ln x_1 + 1) - (\ln 2\pi M)/2, \quad (x_1 > 0;\ x_\nu = 0,\ \nu \neq 1). \tag{A56}$$

In this special case $G_0$ and $G_2$ are both unity and $z = 1/x_1$, so that the equations (A42) and (A44) inclusive lead to the same value for $\ln F_0(M, x)$.[7] This suffices to show that the integration constants properly present in deriving (A42) and (A43) for $\ln f(x)$ and $\ln h(x)$ from (A51) and (A55) are zero and the $\ln g(M)$ of (A44) respectively.

**Validity of the asymptotic expressions for $F$**

Combining equations (A41) to (A44) inclusive we obtain the final asymptotic expression for $F_0(M, x)$ which is

[6] Professor M. Born of Edinburgh has kindly communicated to the authors that this theorem may be proved by using a Cauchy integral and the method of steepest descents.

[7] This special case $x_k > 0$, $x_\nu = 0$ if $\nu \neq k$, may also be readily evaluated by both using (A37) directly and (A42) to (A45). In this case $\ln z = -(\ln k x_k)/k$ and $G_0 = 1/k$, $G_2 = k$. Evaluation by means of (A42) to (A45) leads to $\ln F_0(M, x) = (M/k)(1 - \ln k x_k) - (\ln 2\pi k M)/2$. Direct evaluation of (A37) with $J=M$ using the Stirling approximation for the factorial gives the above expression plus $\ln k$ if $M/k$ is an integer. If $M/k$ is not an integer $F_0(M, x)$ is zero. It is obvious that this extreme case is not covered by Eqs. (A42) to (A45), but it is of interest to note that if the $F_0$ is averaged over a range of $M$'s the above expression is obtained; since only every $k$'th $M$ leads to $F_0$ other than zero, and if this value for $M/k$ an integer is divided by $k$ we obtain agreement with the above.

correct for very large values of $M$,

$$F_0(M, x) = e^{MG_0(x)}/[z(x)]^M(2\pi MG_2(x))^{\frac{1}{2}},$$
$$\ln F_0(M, x) = M[G_0(x) - \ln z(x)] - [\ln 2\pi MG_2(x)]/2. \quad \text{(A57)}$$

If the function $F_1(M, x)$ is defined as

$$F_1(M, x) = F(M-1, M, x) = (1/M)\partial F_0(M, x)/\partial x_1, \quad \text{(A58)}$$

then by direct differentiation

$$F_1(M, x) = e^{MG_0(x)}/[z(x)]^{M-1}(2\pi MG_2(x))^{\frac{1}{2}},$$
$$\ln F_1(M, x) = MG_0(x) - (M-1)\ln z(x) - [\ln 2\pi MG_2(x)]/2. \quad \text{(A59)}$$

The function $F_0(M, x)$ is the same as $Q_T/N!$ if the $x_\nu$'s are the $vb_l$'s of the article and $M$ is $N$, the total number of particles. The function $F_1(M, x)$ is the same as $l^2b_l$ if $l$ replaces $M$ and the $x_\nu$'s are the irreducible integrals $\beta_k$.

The expressions (A57) for $F_0(M, x)$ and (A59) for $F_1(M, x)$ are correct asymptotic expressions for these functions as long as they can be approximated in the general form of (A41). We have already discussed the case that one of the $x_\nu$'s alone is different from zero. Unless $\nu$ is unity, the approximation (A41) is invalid. Even then (A57) and (A59) give correct average values for a range of $M$ values. It appears to be sufficient for the validity of (A57) and (A59) that two $x_\nu$'s alone be different from zero, and that the ratio of the smaller to the greater $x_\nu$ be larger than $\nu/M\nu'$.

One other case that (A57) and (A59) as well as the expression (A41) are invalid is that $G_2(x) < 0$. If all the $x_\nu$'s are positive the equation $G_1 - 1 = 0$ has only one positive root for $z$. If the $x_\nu$'s are all functions of one variable, say the temperature $T$, and are all positive at low values of $T$, it may be that some of them become increasingly negative with increasing $T$'s. Because $G_1 - 1$ is a finite polynomial in $z$ with its zeroth coefficient minus unity, the single positive root of the equation at low $T$'s cannot become zero or infinity, but may, and does, disappear into the complex plane with increasing values of $T$. At this temperature $T = T_c$, $z$ must be a double root, and

$$\partial(G_1 - 1)/\partial \ln z = G_2 = 0. \quad \text{(A60)}$$

At $T = T_c$ the real root $z$ disappears, $G_2$ becomes zero, and the expressions (A41), (A57) and (A59) become invalid. This temperature $T_c$ is shown in the article to be the critical temperature.

**The coefficients of $\Pi\beta_\nu^{n_\nu}$ in $b_l$**

It can be shown that there is a one to one correspondence between the coefficient of the term characterized by the $n_\nu$'s, the powers of the $\nu$'th normalized irreducible integral in a term of $b_l$, ($\sum \nu n_\nu = l-1$), and the answer to the problem discussed in the following paragraph.

Suppose we have $n_1$ identical mechanical frames of type 1, $n_2$ of type 2, $\cdots$, $n_\nu$ of type $\nu$. The frame of type $\nu$ has $\nu+1$ holes into which bolts can be inserted, the frames being so built that every one of the $\nu+1$ holes is exactly equivalently situated with respect to every other one of the holes (a geometrical impossibility in three dimensions for most large values of $\nu$). Suppose we have $l$ numbered bolts with $l = \sum_\nu \nu n_\nu + 1$. The problem is to determine how many ways we can insert the $l$ bolts into the $l - 1 + \sum n_\nu$ holes so that the frames are all singly connected to each other by common bolts.

Each bolted arrangement can be broken down into $l$ different dissociated arrangements consisting of $n$ frames and one free bolt, where each frame has $\nu$ bolts in it and one free hole, and no frames are connected by a common bolt. We can dissociate in exactly $l$ ways because we can choose from the bolted arrangement any one of the bolts as the free bolt, and the dissociation process is then uniquely determined. The number of ways that we can make a dissociated arrangement is

$$l!/\Pi_\nu n_\nu!(\nu!)^{n_\nu}.$$

If $D$ is the number of bolted arrangements we can make make from one dissociated arrangement then the desired answer is $Dl!/\Pi_\nu n_\nu!(\nu!)^{n_\nu} l$.

For the small values of $n = \sum n_\nu$ we know by counting that $D = l^{n-1}$. We now prove that if the equation $D = l^{n-1}$ holds for $n$ it also holds for $n+1$. To do this we add a frame $\nu$ to a system of $n$ frames and bolts and show that the new $D$ becomes $(l+\nu)^n$, (method of complete induction). We consider that the old frames are first bolted together into $\nu+1$ (or fewer) groups, knowing how many ways that can be done, and then these groups are bolted to the new frame. The resulting complicated sum can be shown to be equal to $(l+\nu)^n$. Use must be made of the fact that

$$\sum_{\nu=0}^{\nu=m} \binom{m}{\nu} (-1)^\nu (a+\nu)^P = 0 \quad \text{if } P < m.$$

The final answer then becomes $l!l^n/\Pi_\nu n_\nu!(\nu!)^{n_\nu} l^2$, which is the same as Eq. (19) if it is remembered that $\nu!$ is included in the definition of $\beta_\nu$ as a normalization factor. this proof is primarily due to Dr. M. Goeppert Mayer to whom the authors are greatly indebted. The original equation was deduced by Dr. P. G. Ackermann from a numerical calculation of the first several members. Without this hint as to the correct solution, the proof would have been impossible.

# Statistical Mechanics of Condensing Systems. IV

S. F. HARRISON AND JOSEPH E. MAYER
*Chemical Laboratory, Johns Hopkins University, Baltimore, Maryland*
(Received November 20, 1937)

It is shown that the theoretical equations of the preceding paper lead to the prediction that, in a finite density and temperature range above the temperature of disappearance of the meniscus, a range of microscopic densities are equally stable, and in a sealed bomb different densities may be observed at a given temperature and average density. The densities observed in various parts of the bomb will depend in a predictable way on its previous history. This is in agreement with the published results of O. Maass on systems in the neighborhood of the critical point.

IN the previous paper the authors have deduced certain equations for the thermodynamic properties of a system of chemically saturated molecules. Their deductions were based on general equations and did not involve any special assumptions as to the behavior of the system.

In the neighborhood of the critical point the equations lead to a $P-V$ diagram for the system qualitatively similar to that of Fig. 1. In this figure pressure is plotted as a function of volume, at various temperatures: the heavy solid lines. The curves at two characteristic temperatures $T_m$ and $T_c$ are especially marked. The shaded area enveloped by the dashed line is the region in which the lines are horizontal, that is where $(\partial P/\partial V)_T=0$. The right-hand boundary of this region is called $v_s$, the volume of the saturated vapor, the left-hand boundary $v_f$ is the volume of the condensed phase. The dotted lines inside the shaded area represent the extrapolated pressure of the supersaturated vapor. The dot-dash line on the left-hand side of the shaded area at $T_m$ represents a discontinuous transition in the properties of the condensed phase.*

Below $T_m$ the isothermals show discontinuous changes in slope at $v_s$ and $v_f$. At $T_m$ the surface tension of the condensed phase disappears, and above $T_m$ there will be no visible sharp meniscus between condensed and dispersed phase. The discontinuous transition in the condensed phase shows no heat of transition, at least at the vapor pressure $P_m$. In general the transition temperature will be expected to vary with volume, and it is shown here increasing with decreasing volume (the dot-dashed line lies above the $T_m$ isothermal), but of this there is no certainty. The isothermals go continuously with continuous change of slope through the shaded region between $T_m$ and $T_c$. At $T_c$ the isothermal has a horizontal tangent at only the one point $v_c$, $P_c$. Above $T_c$ the isothermal is never horizontal.

The part of the diagram to the right of $V_c$, and all of it above $T_c$, is deduced strictly from the equations of the previous article. The portion to the left of $V_c$ and below $T_c$ represents a logical guess from the nature of the kinetic picture deduced from these equations. The authors, however, are less certain of the details of this portion of the diagram.

Below $T_m$ and above $T_c$ the diagram corresponds to the usual conception of the diagram

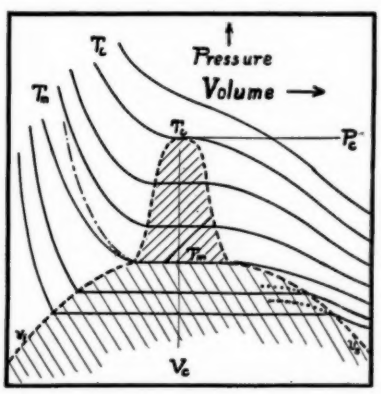


FIG. 1.

below and above the critical point respectively. Between $T_m$ and $T_c$ a system in the shaded area will be expected to have certain unusual properties.

Below $T_m$ compression of the system through the volume region between $v_s$ and $v_f$ will be

* This transition is probably present. It is not a necessary consequence of the equations of the previous article.

accompanied by the separation of two distinct phases of density $1/v_f$ and $1/v_s$. The microscopic density corresponding to a volume between $v_s$ and $v_f$ is unstable. This is indicated on the diagram by the dotted lines showing the higher pressure of the supersaturated vapor. As is well known this phenomenon is associated with the fact that the surface tension increases the vapor pressure of very small droplets of liquid.

Between $T_m$ and $T_c$, however, the denser phase has no surface tension, and corresponding to this, the isothermals pass smoothly through the condensing region, allowing no extrapolation to a higher pressure for the supersaturated vapor. Indeed all microscopic densities in the shaded region between $T_m$ and $T_c$ will correspond to the same pressure (at the same temperature), and to the same Gibb's free energy. Compression of the system at constant temperature $T$ with $T_m<T<T_c$ will be accompanied by a uniform increase in density throughout the whole system, the pressure remaining unchanged between $v_s$ and $v_f$.

It is true that after infinite time, owing to the gravitational gradient in a real system, and the consequent higher pressure at the bottom than at the top, the system should attain an equilibrium state with the density higher at the bottom than at the top of the tube. However, the gravitational pressure gradient amounts to about one part in $10^5$ per cm of height, and it would therefore not be surprising if uniform density could be maintained for weeks or months.

Moreover, should a density difference once be obtained by any means, with higher density at the bottom of the system than at the top, while the temperature was between $T_m$ and $T_c$, and both densities were well within the shaded area between $v_f$ and $v_s$, then uniform compression of the system should result in a uniform logarithmic change in the densities of both portions without a change in their relative abundance. Similarly a change in temperature should result in no change of the two densities, but be accompanied by an increase in the pressure of the system.

If, however, by means of a volume or temperature change, the density in one portion of the tube reached a value corresponding to $v_s$ or $v_f$ on the envelope of the shaded region, then that portion should resist, by increase in relative abundance, any effort to change its density to one outside the shaded region of the diagram. Cooling of such a system should be expected to result in the formation of the meniscus at some temperature lower than $T_m$, a typical supercooling effect. The extent of the supercooling would be expected to be greater the further the densities in various parts of the system were from the values corresponding to the volume $v_{fm}$ and $v_{sm}$ at $T_m$. A system with uniform density $1/v_c$, approximately midway between $1/v_{fm}$ and $1/v_{sm}$, would be expected to show the greatest supercooling.

Experimental evidence for the correctness of these concepts is good. Various experimenters have observed discontinuities in different properties of the condensed phase in the neighborhood of $T_m$, the temperature of disappearance of the meniscus, which is that listed in all existing tables as the critical temperature. These results are summarized in an article by O. Maass.[1] Solubility, dielectric constant and adsorption values have all been found to change discontinuously or rapidly at this temperature. Perhaps the most convincing change is that in the reactivity of HCl with propylene, which shows the usual increase in reaction rate with temperature as long as the HCl is liquid, but the rate drops suddenly to zero as the critical temperature ($T_m$) of HCl is exceeded even though the density of the gaseous HCl is made comparable to that obtaining previously in the liquid. This has been investigated extensively by Maass.[2]

The evidence that the densities of the "liquid" and "gas" are not identical at temperatures considerably above the temperature of the disappearance of the meniscus is extensive and convincing. Again the paper of Maass previously referred to[1] contains a good historical summary. Apparently all investigators who have made measurements just above the critical temperature have found differences of density in the material remaining above the meniscus level and that below. Any contrary evidence would, in addition, have to be regarded extremely critically in view of the experimental results of Maass and

[1] Tapp, Steacie and Maass, Can. J. Research **9**, 217–239 (1933).

[2] Sutherland and Maass, Can. J. Research **5**, 48–63 (1931); Holder and Maass, ibid., **15B**, 345–351 (1937).

the conclusions of the authors that a uniform density, if once attained, would persist almost indefinitely.

Maass[1] has drawn a simple conclusion from a common observation. It is found that the disappearance of the meniscus in a closed tube can be observed with varying total quantities of material in the tube. This can only be true if the density above and below the meniscus is not equal at the time of its disappearance.

Callendar[3] has stated that the dividing line between the material in bottom and top of a quartz tube containing pure water can be seen above 374°C, the temperature at which the meniscus disappears. He reports a difference in density in the ratio 5 to 3 at this temperature for water, and indicates that the true critical point is somewhat over 6°C higher.

The best and most complete experimental evidence is contained in the excellent work of Maass[1, 4, 5] and several co-workers. Densities were measured to about 0.2 percent by means of float suspended on a quartz spiral which could be moved to different parts of the system. Temperature control and the purification of materials were attended to with the greatest care. The density difference observed above the temperature $T_m$ was as much as 100 times the experimental error. The work was done on methyl ether, propylene, and ethylene.

The experimental results which appear to us to be most significant, perhaps under the influence of the fact that they are in perfect agreement with our theory, were as follows. Upon heating a closed bomb containing definite quantities of material through $T_m$, the temperature at which the meniscus was seen to disappear, the densities in top and bottom of the tube followed curves corresponding roughly to the envelope $v_s$ and $v_f$ of the shaded area in our figure. After reaching a temperature between $T_m$ and $T_c$, and subsequent cooling, the density in top and bottom remained constant until a temperature somewhat below $T_m$ was reached. At this temperature the meniscus reappeared and the density difference increased rapidly with falling temperature. Density differences persisted for as long as 6 hours without any tendency to decrease. The density difference was unaffected by mechanical stirring. This appears to be reasonable, since ordinary stirring, although effective in raising macroscopic portions of the high density material into the top of the tube, would not be expected to break up the material into the submicroscopic size droplets which would be prevented from settling by Brownian motion. If the density was once equalized by raising the temperature above $T_c$, or by cooling the top of the tube 1/10°C, a uniform density persisted unchanged. With uniform densities the supercooling phenomenon was most marked. The pressure exerted by the system at any temperature above $T_m$ was the same whether the system was cooling or the temperature was rising. The behavior of any one bomb, with a given filling, was reproducible day after day.

The following observations appear to be at variance with the authors' theory:

The behavior of the different bombs was not in complete numerical agreement. This may possibly be due to a conceivable failure of the float spiral balance to record absolute densities due to an unpredictable reversible variation in constants with pressure and temperature. (The instruments were apparently checked after the operations.) More likely, this lack of agreement between different bombs may be due to the effect of varying amounts of some impurity present in small amounts. For various reasons the influence of a trace of impurity might be expected to be considerable. However, since the total amount of impurity can scarcely exceed 0.1 percent, we believe that the effect is not caused by impurities alone.

The most extreme case of varying behavior of different bombs was that of bomb No. 13[1]. The over-all volume of this bomb corresponded to one exactly midway between $v_{fm}$ and $v_{sm}$ so that the meniscus remained stationary before disappearance. In this case no density differences were observed, but the supercooling was marked. The authors failed to reproduce this later with a different set-up.[4] This is certainly unaccountable, although one may assume that the stationary

[3] Proc. Roy. Soc. **A120**, 460–472 (1928); see also Engineering **126**, 594–5, 625–7, 671–3 (1928).
[4] Winkler and Maass, Can. J. Research **9**, 613–629 (1933).
[5] Maass and Geddes, Phil. Trans. Roy. Soc., London **A236**, 303–332 (1937).

meniscus was peculiarly favorable to superheating.

The curves of density at the top and bottom of the vessel plotted against temperature, on heating, do not show the sharp break in slope predicted by us at $T_m$. Since we cannot, as yet, estimate the magnitude of this change it may not exceed the experimental error. The effect may also be masked in some way by the influence of impurity traces or by other minor effects not considered here. The experimental curves do show a marked curvature at $T_m$.

Certain observations on the effect of varying the total volume of the system[4] are not in numerical agreement with the $v_s$, $v_f$, $T$, curves deduced from the behavior of other bombs. This may, however, be linked with the fact that individual bombs are not in exact numerical agreement with each other.

The $P$–$V$ isothermals of Maass do not show the horizontal portion demanded by us. The experimental points are scarcely sufficiently close together to decide this, and here, certainly, the effect of impurities can be predicted to be considerable, since total and not partial pressures are measured. It is inconceivable that pressure differences can persist in different parts of the same bomb, and this, coupled with the observation that varying density differences (obtained on heating and cooling) lead to the same pressure, appears to us to require the assumption of a horizontal region in the $P$–$V$ diagram.

In short, the authors believe that the observations of Maass and co-workers lead directly to conclusions essentially the same as those deduced from the equations of the preceding paper. The observations, however, show slight deviations from the predictions. Whether these can be accounted for by the influence of impurity traces, or by some unexpected failure of the experimental technique, or whether they indicate additional complications in the theory cannot be easily decided at the present time.

The paper of Verschaffelt[6] who shows that variations in the density in top and bottom of the tube may be due to impurities, and who is quoted as stating that differences as large as 40 percent may be caused by 0.1 mole percent of impurity, must be considered. Verschaffelt shows that, from the known influence of $O_2$ on the critical constants of $CO_2$, we can conclude that if 0.1 percent $O_2$ is in one "phase" and *none* in the other, then just above the critical point the density difference of the two regions would be 36 percent. However, if we assume 0.1 mole percent $O_2$ as impurity in the total $CO_2$, and 10 percent difference in concentration above and below the meniscus, we arrive (using Verschaffelt's figures) at about 6 percent density difference just above the critical point, and only about 1 percent density difference at 1°C above the critical point. Maass' material, especially in the case of dimethyl ether, can scarcely have contained as much as 0.1 percent impurity, and since the impurity must have about the same vapor pressure as the substrate it seems reasonable to assume a concentration difference in liquid and gas of approximately 10 percent. We must compare Verschaffelt's 1 percent predicted density difference with a difference of 15 percent observed by Maass 1° above $T_m$, and of 10 percent some 6°C above $T_m$, where Verschaffelt's predicted difference would be negligible. Although it seems that Verschaffelt showed adequately that work before 1904 could be explained by the influence of impurities, the work of Callendar and especially the careful experiments of Maass indicate that a more fundamental phenomenon is at hand than can be due to impurities alone. Nevertheless, the large effect of impurity traces is regarded by us as lending weight to our supposition that some of the numerical discrepancies of Maass' different bombs are to be explained in this way.

[6] J. E. Verschaffelt, Comm. Phys. Lab., Leiden, Supp. Nr. 10 (1904).

# Note on the Second or Gaussian Approximation in the Heisenberg Theory of Ferromagnetism When $S>\frac{1}{2}$

J. H. Van Vleck
*Harvard University, Cambridge, Massachusetts*
(Received January 12, 1937)

IN the Heisenberg theory, it is customary, except at very low temperatures, to write the expression for the intensity of magnetization in the form

$$M=Ng\beta B_1(g\beta pH+apJ+bp^2J^2+\cdots), \quad (1)$$

where $J$ is the exchange integral, $\beta$ is the Bohr magneton, $H$ is the applied field, and

$$p=1/kT, \quad B_n(\theta)=\sum_{m=-S}^{+S} m^n e^{-m\theta}/\sum e^{-m\theta}. \quad (2)$$

Eq. (1) shows that $(aJ+bpJ^2+\cdots)/g\beta$ plays the role of an internal or "molecular" field. The coefficients $a$, $b$, $\cdots$ are functions of $M$. It is quite easy to prove, as has often been done, that

$$a=2zM/Ng\beta, \quad (3)$$

where $z$ is the number of neighbors. The evaluation of $b$ involves the second or so-called Gaussian approximation, since it can be shown that (1) would be exact, without the unwritten higher order terms, were the energy values for a given spin distributed in accordance with a Gaussian error law. If $S=\frac{1}{2}$, then a calculation made either by means of group theory[1] or the vector model[2] shows that

$$b=-(2zM/Ng\beta)+(4zM^3/N^3g^3\beta^3). \quad (4)$$

The proper formula for $b$ has not previously been given when $S>\frac{1}{2}$, as neither method can be used for this purpose,[3] at least in a simple way, except when $S=\frac{1}{2}$.

A quite different approach has, however, recently been developed by Opechowski.[4] He develops the partition function as a power series in $J$. The constant $b$ in (1) is uniquely fixed by the requirement that the expansion of (1) agree with this series development to $J^2$ inclusive. Opechowski shows that in this way formula (4) can be derived quite easily when $S=\frac{1}{2}$. His work reveals perhaps more clearly than does the ordinary calculation by means of an assumed Gaussian spread,[5] that the practical convergence of the form (1) is very poor at ordinary temperatures. Indeed, better agreement with experiment is usually obtained if one stops with $apJ$ than if one includes $bp^2J^2$, or, as he shows, even $dp^4J^4$.

It is the purpose of the present note to show that the calculation of the partition function which I gave in a previous paper on ferromagnetic anisotropy[6] permits extension of the results to arbitrary $S$. Also it is well to mention that the general mathematical procedure which I used is in many respects similar to that employed by Opechowski, although obtained independently. The essence of both schemes was the development of the partition function in a system of representation in which each atom is separately space quantized in a field $H$. Because of the invariance of the diagonal sum, use of such a system is allowable even with interatomic perturbations. Saturation effects are not overloooked, and so $H$ can be arbitrarily large. In one notable respect, Opechowski's calculations are more general than ours, as he carries the development far enough to include third and fourth powers of the exchange integral, corresponding to unwritten terms $cp^3J^3+dp^4J^4$ in (1). On the other hand, my computation, though carried less far, was made for arbitrary $S$, and allowed the interaction between atoms to be of the dipole-dipole rather than exchange type if desired. The introduction of dipole-dipole coupling is obviously not needed in connection with the present note, but was wanted for other purposes, and somewhat complicates the mathematics, as it makes the perturbing potential cease to commute with the main or Zeeman energy.

[1] W. Heisenberg, Zeits. f. Physik **49**, 619 (1928).
[2] J. H. Van Vleck, *The Theory of Electric and Magnetic Susceptibilities*, Chap. XII.
[3] See especially footnote 16, p. 329 of reference 2.
[4] W. Opechowski, Physica **4**, 181 (1937).
[5] Cf., however, D. Inglis, Phys. Rev. **42**, 442 (1932).
[6] J. H. Van Vleck, Phys. Rev. **52**, 1190 (1937).

For arbitrary $S$, to terms in $J^2$, the formula for the magnetic moment is

$$M/Ng\beta = B_1 + 2zpJB_1(B_2 - B_1^2) + zp^2J^2(B_2 - B_1^2)(-8zB_1^3 + 4zB_1B_2 + 4B_1^3 - 4B_1B_2 - B_1) + zp^2J^2(B_3 - B_1B_2)(2zB_1^2 - 2B_1^2 + B_2 - S^2 - S). \quad (5)$$

Eq. (5) is derived from my previous expression for the partition function in almost exactly the same way as is Eq. (3) of my article on adiabatic demagnetization appearing in the present issue,[7] to which the reader is referred for further detail. The only differences are that in (5) all dipole-dipole terms are omitted, and $S$ is not specialized to the value $S=\frac{1}{2}$. In (5) the argument of the $B$ functions is merely[8] $g\beta pH$. On the other hand, in (1) it is $g\beta pH + apJ + bp^2J^2\cdots$, or to our degree of approximation

$$g\beta pH + 2zpJB_1 + 4z^2p^2J^2B_1(B_2 - B_1^2) + bJ^2,$$

as is seen from (3) and (5). By expanding (1), in essentially the same way as explained more fully on page 192 of Opechowski's paper,[4] it is found that (1) and (5) are the same to $J^2$ provided

$$b = z(4B_1^3 - 4B_1B_2 - B_1) + z(-2B_1^2 + B_2 - S^2 - S) \times (B_3 - B_2B_1)(B_2 - B_1^2)^{-1}. \quad (6)$$

In Eq. (6), $B_1$ may be replaced by $M/Ng\beta$, as in the second-order coefficient $b$ it is unnecessary to distinguish between arguments exclusive and inclusive of the inner field.

In the special case $S=\frac{1}{2}$, one has $B_3=\frac{1}{4}B_1$, $B_2=\frac{1}{4}$ and (6) reduces to the simple expression (4).

If $S=1$, the following formulas apply

$$B_3 = B_1, \quad B_1 = 2\sinh\theta/(1+2\cosh\theta), \quad B_2 = 2\cosh\theta/(1+2\cosh\theta). \quad (7)$$

By elimination of $\theta$ between the last two relations of (7), a quadratic equation is obtained giving $B_2$ in terms of $B_1 = M/Ng\beta$. It is thus possible to reduce (6) to an explicit function of $M$ alone, but the resulting formula for $b$ involves $M$ through radicals and is too cumbersome to be of much value.

When $S>1$, the interrelations between $B_1$, $B_2$, $B_3$ yielded by (2) are more complicated than (7). It is still possible, in principle, to express $B_2$, $B_3$ in terms of $B$ or $M$, but only by solving algebraic equations of high degree, *viz.* $2S$. The practical use of (6) thus appears to be limited to $S=\frac{1}{2}$ and possibly $S=1$, unless the field is weak, as is the case above the Curie point. The limiting general form of (6) for weak fields is tractible, and has been given in a previous paper, as well as discussed in relation to the critical conditions for ferromagnetism.[9] The rather unpleasant result (6) of a calculation of $b$ for $S>\frac{1}{2}$ in arbitrary fields is of interest mainly in connection with the light which it throws on the failure of group theory or the simple vector model to furnish a method of computing $b$ when $S>\frac{1}{2}$. Either of these procedures appear capable of yielding only an answer such as (4) which is a polynomial in $M$ (or at least this is what analogy to the way they work for $S=\frac{1}{2}$ would suggest). Hence they must fail when $S>\frac{1}{2}$, since then the true formula for $b$ is far from a polynomial.

[7] J. H. Van Vleck, J. Chem. Phys. **6**, 81 (1938).

[8] In the application to anisotropy in reference 6, an inner field was included in the argument of the $B$ functions, but is to be omitted in deriving Eq. (5) from our previous calculations, as (5) is obtained by treating the exchange energy as part of the perturbing potential.

[9] J. H. Van Vleck, J. Chem. Phys. **5**, 320 (1937), especially footnote 20.

# LETTERS TO THE EDITOR

*This section will accept reports of new work, provided these are terse and contain few figures, and especially few halftone cuts. The Editorial Board will not hold itself responsible for opinions expressed by the correspondents. Contributions to this section must reach the office of the Managing Editor not later than the 15th of the month preceding that of the issue in which the letter is to appear. No proof will be sent to the authors. The usual publication charge ($3.00 per page) will not be made and no reprints will be furnished free.*

## Bond Force Constants and Vibrations of Tetramethylmethane and Tetramethylsilicon

In order to get information regarding the bond force constants of the molecules tetramethylmethane and tetramethylsilicon, we have treated some of the vibrations of these molecules by the normal coordinate method. These molecules possess a large number of frequencies, but only six for each are considered here. First the totally symmetric nondegenerate frequencies are rigorously treated and second, certain vibrations are calculated assuming that each methyl group behaves like a single atom.

The totally symmetric nondegenerate frequencies of $C(CH_3)_4$ and $Si(CH_3)_4$ can be conveniently treated by considering the symmetric vibrations of a *single* methyl group against a carbon or a silicon atom of infinite mass. This simplifying device can be used because the central atoms are not involved in the motion of those particular vibrations, except insofar as they move with the centers of gravity of the molecules. Assuming valence forces, the secular equations for the totally symmetric nondegenerate frequencies of $C(CH_3)_4$ and $Si(CH_3)_4$ are the same as the equation for the symmetric (Raman active) nondegenerate frequencies of ethane,[1, 2] except that the Hooke's law force constant for the carbon-carbon single bond of ethane is replaced by *one-half* the Hooke's law constant for the carbon-central atom bond of the tetramethyl molecule. The methods employed in arriving at the equation, except as noted, are the same as those described in an earlier paper.[1]

TABLE I. *Tabulation of results.*

| Observed Frequencies[3, 4] | Calculated Frequencies | |
|---|---|---|
| | *A* | *B* |
| **Tetramethylmethane** | | |
| 331 $cm^{-1}$ | | (331) $cm^{-1}$ (2) |
| 415 | | 383 (3) |
| 732 | (732) $cm^{-1}$ | (732) (1) |
| 1248 | | 1264 (3) |
| 1452 | (1452) | |
| 2892 | 2894 | |
| **Tetramethylsilicon** | | |
| 202 | | (202) (2) |
| 239 | | 220 (3) |
| 598 | (598) | (598) (1) |
| 863 | | 793 (3) |
| 1427 | 1427 | |
| 2905 | 2893 | |
| | $k_{C-H}=4.76\times10^5$ dynes/cm | $k_{C-R}=4.71\times10^5$ dynes/cm |
| | $k_\theta=0.468$ | $k_{\theta(CR4)}=0.321$ |
| | $k_{C-C}=5.14$ | $k_{Si-R}=3.14$ |
| | $k_{Si-C}=3.31$ | $k_{\theta(Si-R4)}=0.120$ |

Assuming the methyl groups behave like single atoms of atomic weight 15, four vibrations for each of the molecules $CR_4$ and $SiR_4$ can be calculated. The equations used are the valence force type equations applicable to molecules of the methane type, $XY_4$. Of the four "methane-like" vibrations, one is totally symmetric and nondegenerate and accordingly was also considered by the first method of calculation described above.

The results of the numerical computations are given in Table I. Under column *A* are given frequencies calculated by the first described (rigorous) method and under column *B*, those computed by the second (approximate) method. The figures in parentheses following the numbers in column *B* are the degeneracies of the vibrations. Beneath the columns are given the values of the force constants used. The constant $k_\theta$ refers to bending of angles in the methyl group, and the constants $k_\theta(CR_4)$ and $k_\theta(SiR_4)$ refer to bending of the angles in the molecules indicated for which the central atom forms a vertex. The constant $k_{C-H}$ was taken from reference 1, while the other constants were determined by using those frequencies enclosed in parentheses.

The general agreement between calculated and observed results is good enough to justify the assignment of frequencies. Rank and Bordner,[3] by means of analogies, made different assignments for the higher triply degenerate frequencies here considered. However, our calculations seem to point fairly conclusively to the assignments in the table.

It will be observed that the values for $k_{C-C}$ and $k_{Si-C}$ are, respectively, greater than those for $k_{C-R}$ and $k_{Si-R}$. This would be expected because of the failure to take into account interactions within the methyl groups in obtaining the values for the latter. This result is in accordance with recent observations in connection with ethane and related molecules.[5]

Department of Chemistry,
University of Illinois,
Urbana, Illinois,
January 7, 1938.

F. T. WALL
C. R. EDDY

[1] G. Glockler and F. T. Wall, J. Chem. Phys. **5**, 813 (1937).
[2] J. B. Howard, J. Chem. Phys. **5**, 442 (1937).
[3] Rank and Bordner, J. Chem. Phys. **3**, 248 (1935).
[4] Kohlrausch and Köppl, Zeits. f. physik. Chemie **B26**, 209 (1934); D. H. Rank, J. Chem. Phys. **1**, 572 (1933); Kohlrausch and Barnés, Anales Fisica Y Quimica **30**, 733 (1932).
[5] F. T. Wall, J. Am. Chem. Soc. **60**, 71 (1938).

## Alterations in the Infrared Absorption Spectrum of Water in Gelatin

The absorption spectra in the region 1–2.5$\mu$ have been recorded in the four following instances with a self-registering instrument of slit widths equivalent to 0.003$\mu$: (1) a 0.20 mm specimen of gelatin dried to constant weight at 120°C; (2) a portion of the same specimen after it had absorbed an amount of water equal to 35.7 percent of the total weight and swollen to a thickness of 0.28 mm; (3) a 0.09 mm cell of water at room temperature; (4) a 0.17 mm cell of water. The spectrum of (1), in spite of the complexity of the protein molecules involved, can readily be interpreted in terms of CH and NH vibrations; any absorption by OH groups or by possible residual water is not observable. Although there may be slight changes in the NH bands, the main differences in the percentage transmission curves obtained from the reduction of (1) and (2) and of (3) and (4) can fairly certainly be ascribed to alterations in the water spectrum. Since equal effective thicknesses (0.08 mm) of water were involved, these alterations must arise from differences in the structure or in the environment of the water. The following modifications are observed, and provisional causes are assigned.

(a) The 1.44$\mu$ band ($\nu_\pi+\nu_\sigma$). The maximum absorption is slightly shifted to a longer wave-length in the gelatin specimen, apparently owing to the partial or complete removal of the short wave portion of the band usually associated with the water vapor molecule. This indicates that most or all of the water molecules are bound molecules. Absorption at the maximum is increased but total absorptions in the two instances are comparable owing to a diminution of continuous absorption in the 1.65$\mu$ region.

(b) The 1.96$\mu$ band ($\nu_\pi+\nu_\delta$). The location of the maximum is practically unaltered. This need not be construed as indicating that unbound molecules are present. For, since this band is a combination of the fundamental deformation frequency (6.1$\mu$) and the fundamental asymmetric valence frequency (2.7$\mu$), it should show the characteristics of both fundamentals; and the temperature effects and the hydration studies of Ganz,[1] as well as vapor-liquid band shifts, clearly show opposite behaviors in these two bands. A statement analogous to the last sentence of (a) can also be made in connection with this band.

(c) The 1.79$\mu$ ($\nu_\pi+\nu_\delta+\nu_R$). This band, whose frequency differs from that of 1.96$\mu$ by an amount equal to the frequency of "hindered rotation," $\nu_R$,[2] is stronger and sharper than in pure water. This seems to indicate, first, that at least some of the water molecules are bound in such a way as to permit hindered rotation about the axis of least inertia and, second, that the average field of potential energy is equivalent to that in pure water but that it is more homogeneous.

(d) A new 1.35$\mu$ band ($\nu_\pi+\nu_\sigma+\nu_R$). This band is analogous to the 1.79$\mu$ band and is doubtless observable in the gelatin specimen but not in pure water because of a greater homogeneity in the field.

(e) The 2.4$\mu$ region. The absorption in this broad region, more intense in the gelatin instance, is probably to be interpreted in terms of $\nu_\pi+\nu_R$.

(f) The absorption bands at 4.7$\mu$ ($\nu_\delta+\nu_R$) and 20$\mu$ ($\nu_R$) should, if observed in gelatin, be sharper than in pure water.

It is the authors' opinion that the absorption at 3$\mu$ found by Buswell, Krebs and Rodebush[3] in a gelatin specimen dried for 14 hours at 122°C is caused by protein NH groups rather than by residual water.

JOSEPH W. ELLIS
JEAN BATH

University of California,
Los Angeles, California,
January 13, 1938.

[1] Ganz, Ann. d. Physik. **28**, 445 (1937).
[2] Ellis, Phys. Rev. **38**, 693 (1931); Cartwright, Phys. Rev. **49**, 470 (1936).
[3] Buswell, Krebs and Rodebush, J. Am. Chem. Soc. **59**, 2603 (1937).

---

## Errata: Thermodynamic Functions of the Chloro- and Bromomethanes, Formaldehyde and Phosgene

(J. Chem. Phys. **6**, 25 (1938))

Because of a systematic error the values of $-(F^0-E_0^0)/T$ in Tables VI and VIII are too large by 1.987 cal./°K mole. The value of $\Delta E_0^0$ for the reaction

$$C_{\beta g}+H_2+1/2O_2=H_2CO,$$

as calculated from the work of Newton and Dodge should be −26.0 kcal./mole instead of −27.0 kcal./mole. This leads to a final value of $\Delta E_0^0$ for this reaction of −26.5 kcal./mole in place of −27.2 kcal./mole.

For the free energy of formation of the liquid chloromethanes

$$C_{\beta g}+H_2+Cl_2=CH_2Cl_2(l), \quad \Delta F_{298}^0=-14.7,$$
$$C_{\beta g}+\tfrac{1}{2}H_2+\tfrac{3}{2}Cl_2=CHCl_3(l), \quad \Delta F_{298}^0=-15.9,$$
$$C_{\beta g}+2Cl_2=CCl_4(l), \quad \Delta F_{298}^0=-16.6.$$

The free energies of formation of the gases are given in Table X.

TABLE X. $\Delta F^0$ *of ideal gases.*

| T | $H_2CO$ | $COCl_2$ | $CH_3Cl$ | $CH_2Cl_2$ | $CHCl_3$ | $CCl_4$ |
|---|---|---|---|---|---|---|
| 298.1 | −25.2 | −49.7 | −13.0 | −14.3 | −15.1 | −15.5 |
| 350 | −24.8 | −49.1 | −13.1 | −13.1 | −13.7 | −13.8 |
| 406 | −24.4 | −48.4 | −10.6 | −11.3 | −12.3 | −12.1 |
| 500 | −23.5 | −47.2 | −8.0 | −9.2 | −9.5 | −8.9 |
| 600 | −22.5 | −45.9 | −5.4 | −6.6 | −6.7 | −5.5 |
| 700 | −21.5 | −44.7 | −2.6 | −4.0 | −3.8 | |
| 800 | −20.5 | −43.4 | +0.1 | −1.3 | −0.7 | |
| 900 | −19.4 | −42.0 | +3.0 | | | |
| 1000 | −18.3 | | +5.8 | | | |
| 1100 | −17.2 | | 8.7 | | | |
| 1200 | −16.1 | | 11.5 | | | |
| 1300 | −15.0 | | | | | |
| 1400 | −13.9 | | | | | |
| 1500 | −12.8 | | | | | |

D. P. STEVENSON
J. Y. BEACH

Princeton University,
Princeton, N. J.,
January 14, 1938.

## Photosynthesis*

Photosynthesis has long been known to be composed of two parts, one photochemical and temperature independent and the other thermal. The average life of the thermal reaction has been determined by measurements made in flashing light.[1, 2]

Several explanations of the nature of the thermal (or Blackman) reaction have been advanced, some postulating the return of the plant chlorophyll to its original state after having been involved in the reduction of carbon dioxide. Franck and Herzfeld[3] describe the mechanism of the reaction as the decomposition of per-acids and per-aldehydes to formic and carbonic acids in chain processes started by light. However, the results of Emerson and Arnold[1] show the Blackman reaction to be inhibited by hydrogen cyanide, a characteristic of certain enzyme processes.

The mechanism of photosynthesis here presented is one in which the initial processes result in the formation of an organic compound of the general formula $C_NH_{2N}O_N$ and a peroxide—probably hydrogen peroxide. The formation of hydrogen peroxide is not eliminated by Franck and Herzfeld's[3] calculation of the energy involved in photosynthesis. The Blackman reaction is then the enzymatic decomposition of the peroxide. This latter would be the rate determining process in oxygen evolution at high light intensities and high carbon dioxide concentrations. Conclusions about photosynthesis drawn from measurements made under such conditions are not reliable. Our opinions are the result of experiments, performed in this laboratory, which are described below.

Into a suspension of cells (*chlorella vulgaris*), contained in a Warburg manometer apparatus illuminated by a 150-watt tungsten lamp at a distance of 5 cm, was introduced a small amount of catalase solution and the effect on the production of oxygen was observed. In all cases there was an increase in oxygen pressure beyond the amount due to normal cell activity. Figs. 1 and 2 show the results of two typical experiments. In each case a control run was made parallel to the test. Into the control there was placed, at the same time as the catalase solution was added to the test, an equivalent amount of distilled water. The solid curve in Fig. 1 represents this control. In Fig. 2 we see the results of adding catalase solution first to one cell suspension and later to the other. Attention is called to the fact that, at the end, the difference in oxygen pressures was approximately the same as at the start although there was a large difference before the addition of catalase to the second cell suspension. The experiments were run at $25 \pm 0.02$ degrees centigrade.

Similar experiments we performed with solutions of sodium magnesium chlorophyllin gave like sharp discontinuities in oxygen pressure on the addition of catalase solution and can be interpreted as a duplication of photosynthesis *in vitro* without the intervention of living cells.

Therefore, chlorophyll, in the plant, can be supposed to fill the dual role of light absorber and energy utilizer and,

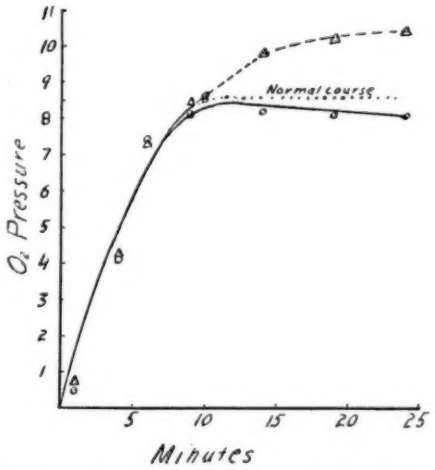


FIG. 1. Effect of catalase on oxygen production during photosynthesis. The broken lines represent oxygen production after the addition of catalase solution.

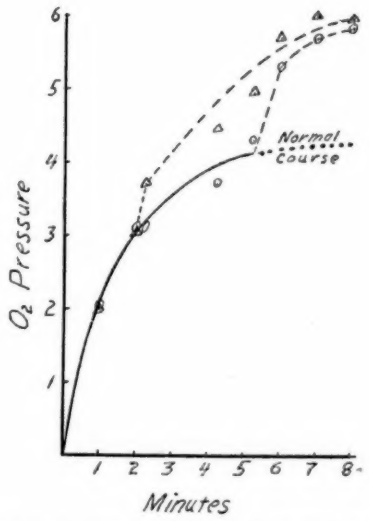


FIG. 2. Effect of catalase on oxygen production during photosynthesis. The broken lines represent oxygen production after the addition of catalase solution. Both systems were opened to and equilibrated with air at the end of two and six minutes in order to add catalase and water. The curves are corrected for the lag.

in conjunction with the fat-protein to which it is connected, as an enzyme which decomposes hydrogen peroxide.

A complete account of the experimental methods and a fuller presentation of the theory will follow in a short time.

ALEXANDER F. KNOLL
FREDERIC L. MATTHEWS, JR.
RAY H. CRIST

Columbia University,
New York, New York,
January 15, 1938.

* Publication assisted by the Ernest Kempton Adams Fund for Physical Research of Columbia University.

[1] Emerson and Arnold, J. Gen. Phys. **15**, 391 (1932).
[2] Emerson and Arnold, J. Gen. Phys. **16**, 191 (1932).
[3] Franck and Herzfeld, J. Chem. Phys. **5**, 237 (1937).

### Infrared Absorption Spectrum of Heavy Acetic Acid

The infrared absorption spectrum of acetic acid-*d* ($CH_3COOD$) vapor has been investigated in the region 1–15.5$\mu$ by means of a rocksalt spectrometer, previously described in the literature.[1] This investigation was undertaken with the aim of bringing out the hydrogen bond frequency by a deuterium substitution. It is well known that acetic acid vapor at room temperature exists mostly as double molecules, the bonding occurring through the mechanism of "hydrogen bridges." According to current ideas,[2] the hydrogen bonded O−H frequency is shifted from 2.75$\mu$ into the region of the C−H valence vibrations at 3.3$\mu$ and cannot be clearly discerned. In heavy acetic acid this frequency will be shifted approximately by a factor of $\sqrt{2}$ and will lie in a region usually unoccupied by absorption bands (4.3$\mu$). That this is so, is clearly brought out by the curves in Fig. 1, and Table I which gives the

TABLE I.

| | | |
|---|---|---|
| 3079±40 cm$^{-1}$ | 1389±10 cm$^{-1}$ | 1000± 5 cm$^{-1}$ |
| 2325±20 | 1317±10 | 840± 5 |
| 2105±15 | 1250±10 | 667±20 |
| 1725±15 | 1056± 5 | |

positions of the band centers. It is of interest to note that the C−H valence frequency appears only weakly. This fact suggests a possible interpretation of the broad and deep absorption at 3.25$\mu$ in light acetic acid as being chiefly due to the hydrogen bond vibration.

Raman spectra of liquid $CH_3COOD$[3, 4] show no lines in the region 1655 to 2940 cm$^{-1}$, thus making impossible a complementary study in the Raman effect.

Our sample of heavy acetic acid was prepared by reacting

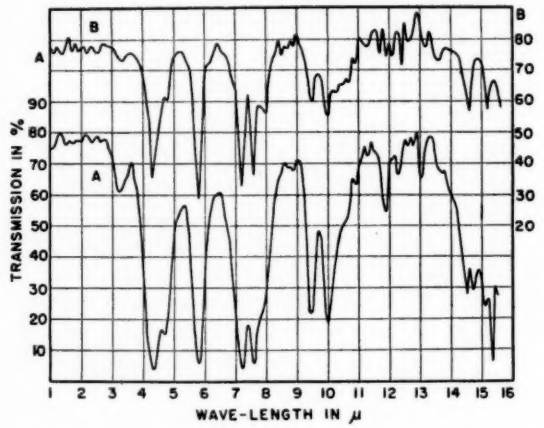


FIG. 1. Absorption spectra of $CH_3COOD$. Curve *A*, pressure 15.5 mm, temperature 24°C; curve *B*, pressure 4 mm, temperature 24°C. Absorption cells 15 cm in length.

pure acetyl chloride with 99.6 percent heavy water by a method previously employed by Engler.[4]

Further experiments are now in progress to determine how association through the deuterium bond is affected by temperature.

We wish to thank Mr. R. R. Brattain for his encouragement and very kind assistance.

Princeton University,
Princeton, New Jersey,
December 17, 1937.

R. C. HERMAN
R. HOFSTADTER

[1] Barnes, Brattain and Seitz, Phys. Rev. **48**, 582 (1935).
[2] Badger and Bauer, J. Chem. Phys. **5**, 839 (1937).
[3] W. R. Angus, A. H. Leckie and C. L. Wilson, Proc. Roy. Soc. **155**, 183 (1936).
[4] W. Engler, Zeits. f. physik. Chemie **B32**, 471 (1936).